

PALEONTOLOGICAL (PLANKTIC FORAMINIFER-OSTRACOD) INVESTIGATION OF EOCENE SEQUENCE OF KARAMAN REGION

Ümit ŞAFAK*

ABSTRACT.- The microfauna of Eocene sequence outcropping around Karaman have been investigated. These planktic foraminifers and ostracods were systematically described; also *Acarinina bullbrooki* planktic foraminifer zone belonging to Lutetian has been determined and this zone was compared with other Eocene planktic foraminifer zones over the world indicating same level. In addition, ostracod species described were stratigraphically and paleogeographically compared with those of other basins.

OSTRACOD AND FORAMINIFER ASSEMBLAGES OF TERTIARY SEDIMENTS AT W. BAKIRKÖY (ISTANBUL)

Ümit ŞAFAK*. Niyazi AVŞAR* and Engin MERİÇ**

ABSTRACT.- The drilling samples taken from the western part of the Bakirköy Basin were investigated, and the microplaeontological data were evaluated. Pliocene, Late Miocene and Late Eocene aged sediments have been observed from top to bottom of drilling, at the results of the laboratory investigation. 14 genera and 25 species from the ostracods and 10 genera and 8 species of benthic foraminifera from the Pliocene sediments: 6 genera and 11 species of ostracods, 9 genera 9 species of benthic foraminifera from the Late Miocene deposits and 11 genera and 11 species of ostracods and 20 genera and 6 species of benthic foraminifera from the Late Eocene sediments were described. The microfauna of Pliocene sediments consists of *Cyprideis seminulum* (Reuss), *C. pannonica* (Mehes), *C. anatolica* Bassiouni, *C. torosa* (Jones), *C. tuberculata* (Mehes), *C. trituberculata* Krstic, *C. pontica* Krstic are rare, and characteristic for Pontic Basin. In addition, *Loxococoncha* sp., *Semicytherura* sp., *Xestoleberis margaritae* Mauller, *X. ventricosa* Mueller, *X. reymenti* Ruggieri, *X. communis* Mueller, *Darwinula stevensoni* (Brady&Robertson), *D. cylindrica* Straub, *Ilyocypris* cf., *bradyi* (Norman), *Candona* (*Candona*) *altoides* Petrovski, *C. (Candona) parallela pannonica* Zalanyi, *C. (Candona) decimal* Freels, *C. (Candona) Candida* (Müller), *C. (Candona) neglecta* Sars, *Heterocypris salina salina* (Brady), *Eucypris dulcifons* Diebel & Pietrzenuik are found in the sequence, and foraminifera consisting of *Siphonaperta aspera* (d'Orbigny), *Quinqueloculina seminula* (Linne), *Eponides concameratus* (Williamson), *Cibicidodites* sp., *Cibicides advenum* (d'Orbigny), *Asterigerina* sp., *Ammonia compacta* Hofker, *A. parkinsoniana* (d'Orbigny), *Challengerella bradyi*, Billman, Hottinger & Oesterle, *Elphidium crispum* (Linne) are of Pliocene age. The following species were identified from the Upper Miocene; these are respectively *Cyprideis seminulum* (Reuss), *C. pannonica* (Mehes), *C. anatolica* Bassiouni, *C. torosa* (Jones), *C. pontica* Krstic, *Tyrrhenocythere triebeli* Krstic, *Xestoleberis ventricosa* Mueller, *X. reymenti* Ruggieri, *Ilyocypris* cf. *gibba* (Ramdohr), *Heterocypris salina salina* (Brady) from the ostracods species and *Quinqueloculina seminula* (Linne), *Q. cf. lamarckiana* d'Orbigny, *Quinqueloculina* sp. 1, *Quinqueloculina* sp. 2, *Cibicidoides* sp., *Eponides concameratus* (Williamson), *Lobatula* (Walker & Jacobs), *Ammonia compacta* Hofker, *A. parkinsoniana* (d'Orbigny), *Porosonion subgranosum* (Egger), *Elphidium crispum* (Linne) from benthic foraminifera. Upper Eocene sediments contain following ostracods; *Cytherella triestina* Kollmann, *Bairdia subdeltoidea* (Muenster), *B. elongata* Lienenklaus, *B. cymbula* Deltel, *B. crebra* Deltel, *Bairdopilata* cf. *gliberti* Keij, *Triebelina punctata* Deltel, *Schizocythere appendiculata appendiculata* Triebel, *S. tessellata tessellata* (Bosquet), *Eucythere* sp. 1, *Eucythere* sp. 2, *Thracella apostolescui* Sönmez, *Krithe rutoti* Keij, *Echinocythereis isabenana* Oertli, *Leguminocythereis genappensis* Keij, *Nucleolina multicostata* (Deltel), *Pokornyella osnabrugensis* (Lienenklaus), *P. ventricosa* (Bosquet), *Hermanites pajenborchiana* Keij, *H. triebeli* Stchepinsky, *Quadracythere vermiculata* (Bosquet), *Q. hulusü* Sönmez-Gökçen, *Cytheretta tenuistriata* (Reuss), *C. bartonica* Sönmez-Gökçen, *Xestoleberis sublobosa* (Bosquet), *X. muelleriana* Lienenklaus, *Uroleberis* sp., *Paracypris contracta* (Jones) Among the foraminifera *Halkyardia minima* (Liebus), *Sphaerogypsina globula* (Reuss), *Asterigerina rotula* (Kaufmann), *Chapmanina gassinensis* (Silvestri), *Nummulites fabianii* (Prever), *N. striatus* (Bruguiere) are characteristic for this level. According to result of the drilling samples taken from the western part of the Bakirköy and Ataköy region, it is indicated that there were the restricted environments, and that salinity reduces depending on the shallowness in Late Miocene and shallow marine in Late Eocene in the region. In addition, it is observed that it changed to lagoonal and shallow marine in the Pliocene.

MORPHOLOGY AND SEDIMENTARY FACIES OF ACTUAL KOCASU AND GÖNEN RİVER DELTAS, MARMARA SEA, NORTHWESTERN ANATOLIA

Nizamettin KAZANCI*, Ömer EMRE**, Tevfik ERKAL**, Özden İLERİ*, Mustafa ERGİN* and Naci GÖRÜR***

ABSTRACT.- In the southern coastal zone of the Sea of Marmara (northwestern Turkey), two important rivers, Kocasu and Gönen, debouch into the sea, with a distance of less than 80 km from each other. The discharge and transport of appreciable amounts of sediment load are due to the prevailing semi-arid climate with wet-winter seasons. The sedimentary input of Kocasu and Gönen rivers have produced two quite morphologically different delta systems. The Gönen river delta is lobate and fluvial-dominated with sediment accumulation having a progradation of 5.5 km and subaerial plain of 28 km² totally. The meandering distributary channels and a number of small lagoonal lakes are the main elements of the delta plain. The input of sediment is abundantly bedload and has resulted in the development of a triangular delta plain, with a slight shifting towards the east. A step-like scarp at 6 m altitude divides the plain into two parts. Two drillings of DSI at apex of the delta show that overall deltaic sequence is 65 m thick, however delta plain sediments are generally 6 m thick. The Kocasu delta is characterized as a highly mud-dominated delta, a specimen of a destructive, curvi-linear delta type. It is a wave-dominated river delta with a 3.5 km of progradation and a subaerial plain of 48 km². The present Kocasu delta has only one straight, major channel. The extensive lateral growth of the delta is provided by wave actions, mostly created by northeasterly winter winds. Fluvial sediments on the delta plain are limited extent. Consequently, actual fluvial sedimentation on the delta plain is low and, two lagoonal lakes, swamps, cheniers, dunes and a long sandy beach are the basic morphological elements of delta plain. A step-like morphology at 4 m altitude, similar to that of Gönen river delta, separates the delta plain to a relatively older and a younger formations. Total thickness of the deltaic sediment body is estimated to be 55-60 m by graphic correlations. Both deltas abound in active right lateral strike-slip faults and their depositional areas were limited by bedrocks on the seashore. Limitation is very typical and sharp in the Kocasu delta due to the presence of fault scarps on the Palaeozoic metamorphics. Geomorphology of drainage areas shows that the modern Kocasu and Gönen river deltas are synchronique deposits and they must have began to develop in early Holocene. The step-like morphology on delta plains may indicate a global sea-level fall to the present level, most probably since the last climatic optimum. Later, local sea-level changes in Kocasu area took place, creating long cheniers in swamp sediments by the activity of the faults on the sea shore. The present-day sea-level has been seen at still-stand period for the last millenia.

INTRODUCTION

Deltas are depositional systems where balance of erosion and transportation between coast and hinterland were established and big amount of sediments were deposited resulting from this balance. Various kinds of deltas are formed by wide range of factors such as climate of drainage area morphology and tectonism, inclination of shoreface and effective energy (Coleman and Roberts, 1988; Orton and Reading, 1993). So, both old and recent deltas give information about the conditions affecting on the coast and hinterland. As the information of recent deltas can be easily observed, they represent geology of actual situation and help the interpretation of old delta facies (Whateley and

Pickering, 1989; Oti and Postma, 1995). Kocasu and Gönen river deltas are good examples of this kind of things. Because these deltas have recently developed at the southern coast of Marmara sea representing at least late Quaternary evolution. In this study actual morphology and sedimentary facies and the process of these deltas will be given.

Physiography of the sea of Marmara that is the depositional area of the Kocasu and Gönen river deltas are almost well-known (Özsoy et al., 1986; Beşiktepe, 1991; Ergin et al. 1991, 1994, 1996), There are many discussion on the opening, formation and Quaternary evolution of the sea of Marmara and they are still disputed (Ardel, 1957; Stanley and Blanpied, 1980; Barka and Kadinsky-

Cade, 1988; Şengör et al., 1985; Emre et al., 1997a. Görür et al., 1997a, b) However there are different opinions on the Neogene and Quaternary evolution of the southern Marmara region (Emre et al., 1997 a, b, 1998). Aspects of this study are deltas with records of at least Quaternary evolution and their three-dimensional interpretation may explain the development of the sea of Marmara.

Kocasu delta (Figs. 1 and 2) is a mud-dominated, lobate type, wave-dominated delta and is approximately 80 km far from Gönen delta, in the E. Latter is also lobate type and fluvial dominated delta (Figs. 1 and 3). Sedimentary facies of both deltas are partly similar to each other. The aim of this study is to discriminate facies distribution in terms of their geometry and to explain their similarity and differences with the processes. In fact, available data about these deltas cover some description of coastal morphology of the sea of Marmara (Ardel, 1957, 1968; Erinç, 1957; Erol, 1969, 1991). However, systematic information has been collected after the studies of National Marine Research Programme (Kazancı et al., 1997 a, b).

Although the drainage areas of the Kocasu and Gönen river deltas are under the effect of tectonism (Şaroğlu et al., 1987; Emre et al., 1997a) the deltas have developed at the margin of active fault scarps (Figs. 2 and 4). By these features Kocasu and Gönen deltas are good examples reflecting direct results of sea-level changes, not only showing sediment supply by tectonic effects. This situation which is frequently seen on fan deltas but not on fluvial deltas, is an important feature discriminating Kocasu and Gönen deltas from others. For this reason, effects of tectonism on the delta plain facies will be explained

INVESTIGATION METHOD

Field studies in the Kocasu and Gönen deltas were carried out in 1996. Firstly, boundaries of facies have mapped by using aerial photographs and samples of each facies have been collected for routine sedimentological analysis. Unexposed areas have been mapped as recent or old swamps based on vegetation. On the other hand, changes in

facies were tried to consider using the correlation of old topographic maps, landsat images and aerial photographs. Interpretation on the delta front and offshore of the delta has been gained from previous studies. Information about bed load transportation onto the delta and annual discharge of rivers has been taken from EİE sources for years of 1993 and 1996. After this, authors have calculated rainy and dry periods, maximum and minimum suspended load, denudation and total load by the comparison available meteorological data (Tables 1 and 2). During the calculations, EİE stations of 210, 317 and 321 have been used (Fig. 1). These stations are 10-25 km back of deltas. As there is not any important tributary, the data collected from these stations have been accepted as real discharge. However the real discharge and suspended load can also be much more than available data (Table 2).

BACKSHORE FEATURES AFFECTING DELTA FORMATION

Southern Marmara region of which is the drainage area of the Kocasu and Gönen deltas is more rainy than the average of Turkey although it has semi-arid climatic conditions (Table 1). Rainy periods extend from December to April, approximately 450 mm/yr., and it is also considerably windy (average 8 m/hr). Average rain in dry period (May to November) is 236 mm/year and it is not windy (average velocity 2-4 m/s). Although the rainy period tends to be summertime in the last decade, it does not affect average value. According to Bandırma and Çanakkale stations it has been understood that intermediate and strong winds trough the year come from 25° NE in 60 percent (Meteorological Bulletin, 1974, 1984). It is thought that wind directions are mostly controlled by regional morphology and particularly Dardanelles and Bosphorus (Özsoy et al., 1986; Beşiktepe, 1991). It can also be assumed that delta progradation is limited in the same period of the winds which they distribute sediments, although the rains supplying sediments into the deltas increase in wintertime.

The Kocasu and Gönen river gain the water of

MORPHOLOGY OF KOCASU AND GÖNEN RIVER DELTAS

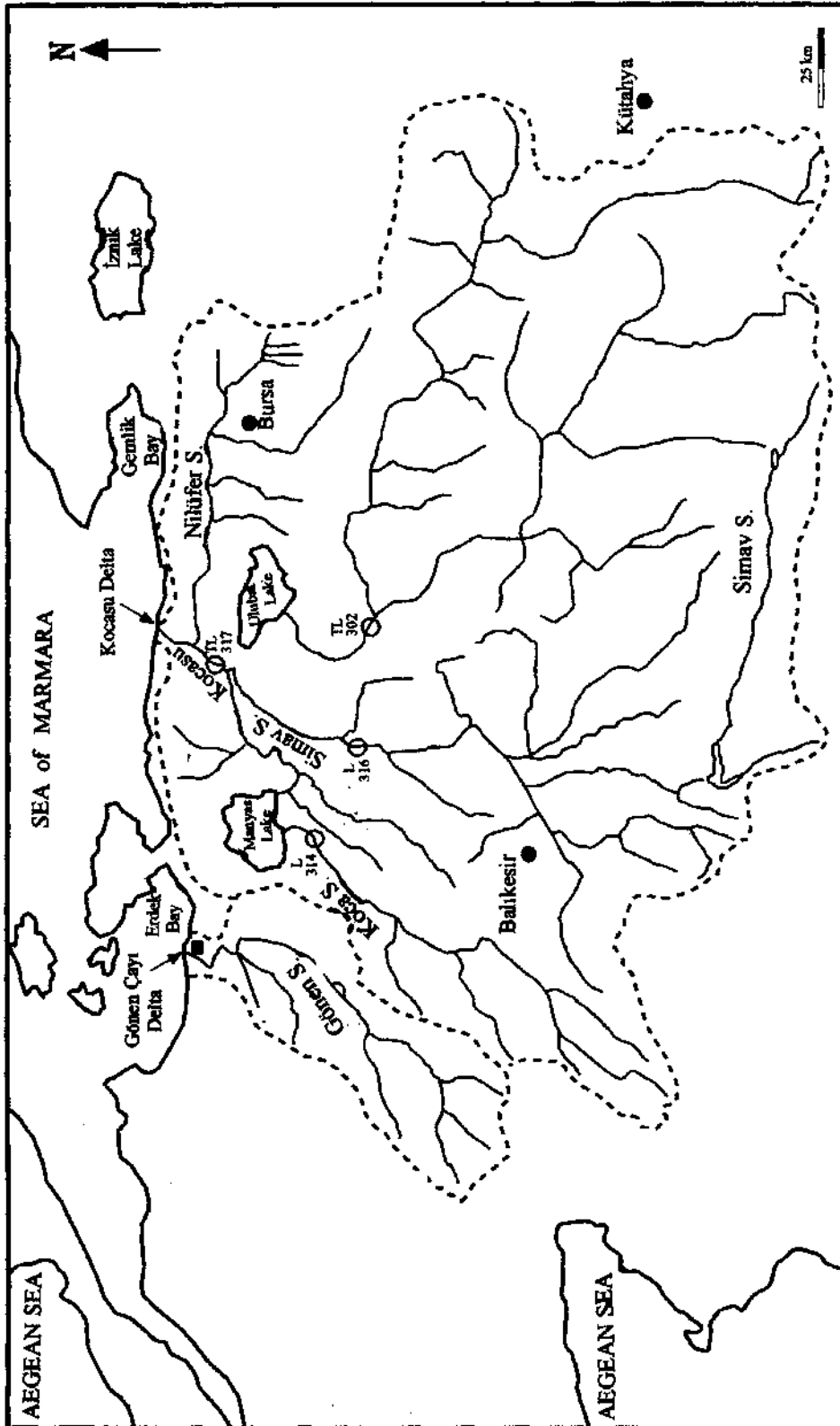


Fig.1- Drainage networks of the southern Marmara deltas. 317 EIE observation station, DSI drilling site.

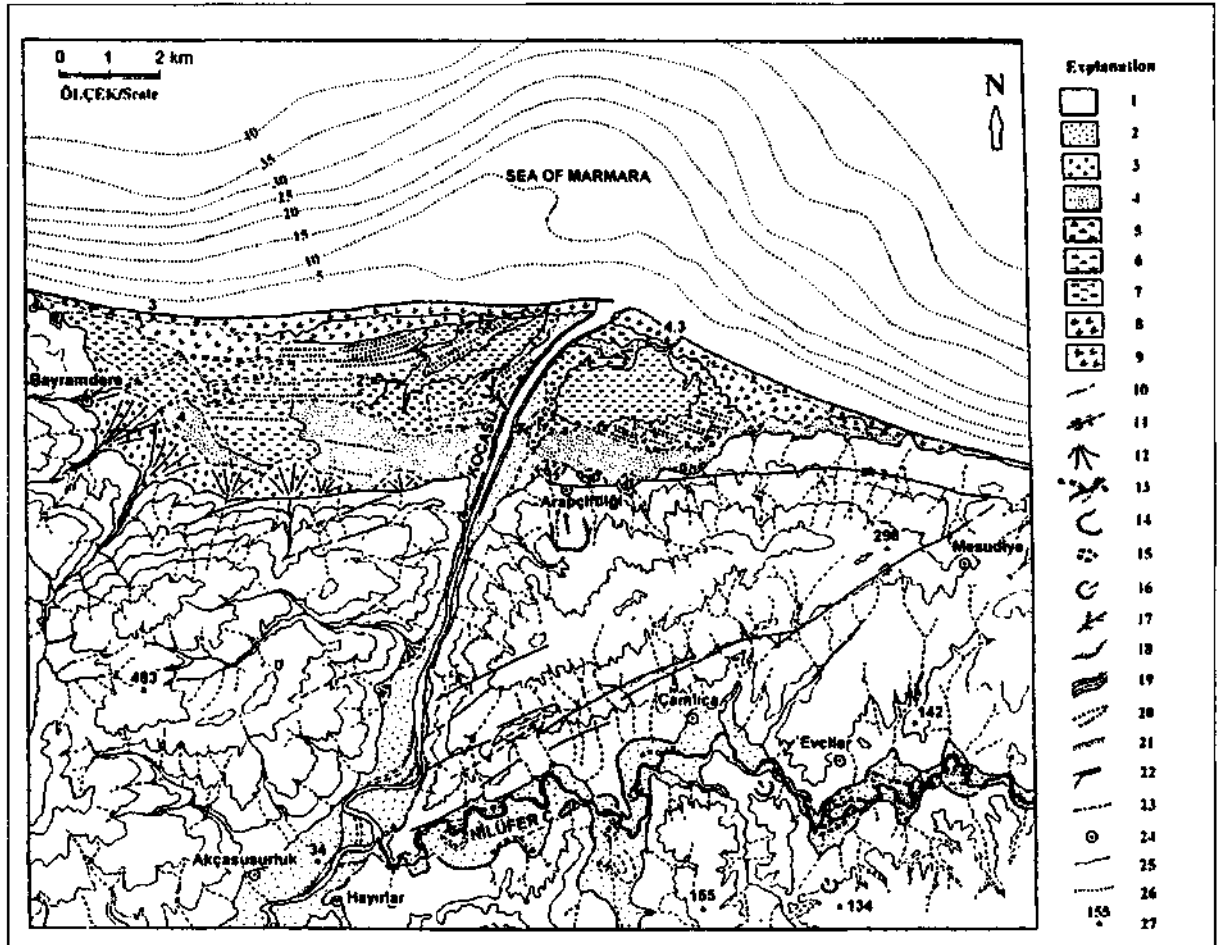


Fig. 2- Quaternary geology and geomorphology map of the Kocasu delta. 1, Denudation area surrounding the delta, 2, Flood plain sediments, 3, Alluvial fan sediments, 4, Sandy delta sediments, 5, New marsh sediments, 6, Old marsh, 7, Lagoon, 8, Actual coastal dune, 9, Old coastal dune, 10, Contact, 11, fault (arrows show the direction of movement, - and + point out downthrown and upthrown sides respectively), 12, Alluvial fan, 13, a) abandoned channel, b) present channel, 14, Old meander scar, 15, cut-off meander, 16, Landslide, 17, crevasse, 18, point-bar deposit, 19, river and its levee, 20, Beach ridges, 21, Beach, 22, Spit, 23, boundary of old and new delta, 24, settlement, 25, isohips (with 100 m interval), 26, isobath, 27, spot height.

2/3 of whole southern Marmara region and some part of northern Aegean region (Fig. 1). Drainage network is mainly rectangular in the E, reflecting tectonic control, and is linear in the W (Fig. 1).

Kocasu

The length of main course of this river is 321 km and its drainage area covers 27600 km². Simav, Orhaneli, Mustafakemalpaşa and Nilüfer creeks and Kocaçay are main tributaries of Kocasu. Ulubat and Manyas lakes are depositional areas on these courses. Beside, there are two water irrigation

ponds on the Simav river which are a kind of sedimentary site.

Mainly Neogene aged sedimentary and volcano-sedimentary units are exposed in the Kocasu drainage basin and soil formation is quite well developed. Drainage network is respectively dense, topography is mature and morphological incision is much. The river follows some fault-lines on pre-Neogene rocks, which are less exposed and topography is quite wild. Valley slopes have high angles except plains.

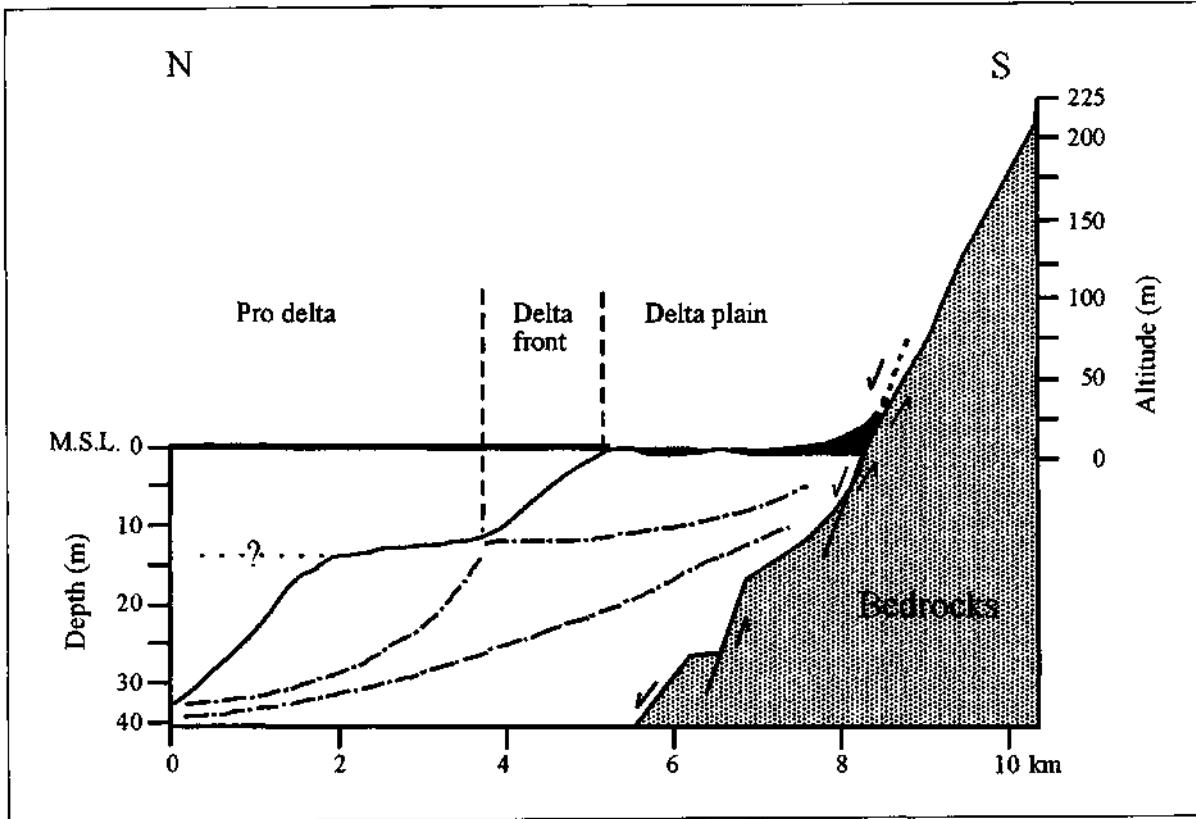


Fig. 3- Subaqueous and aerial part of the Kocasu delta. Notice the platform at the 10-15m deep. ? and dotted truncated line shows probable and deltaic occurrence related to sea level.

Based on long term observation, discharge of Kocasu is $158 \text{ m}^3/\text{sec}$. During the last 28 years, maximum discharge is $1322 \text{ m}^3/\text{sec}$ while the minimum is $7.07 \text{ m}^3/\text{sec}$ (EIE, 1996). This difference reflects semi-arid climate and flood discharge. In the proximal section of the delta, at the EIE station No.317, Kocasu river carries much suspended load, not bed load (Table 2). The main reason of this case is that bed load is hold in meanders and the lakes of Manyas and Ulubat. Very large alluvial fillings in the lower parts of the rivers and the existence of deltas in these lakes give an idea that this situation has started since the late Pleistocene (Emre et al., 1997b).

Kocasu river parses away 8 km length Karacabey gorge before it reaches the sea of Marmara. This gorge has been dissected in mefa morphic rocks in E-W direction. In fact this gorge is

unique passage of southern Marmara region's drainage due to steep coast between Gemlik and Bandirma and it has very important role on local morphology (Erinç, 1957; Emre et al., 1997 a, b). The gorge is 150-1500 m wide and its floor was flattened by alluvium of Kocasu. The course of the river has cut the infillings 1.5-4.5 m depth in a narrow meander. However, to the S., Kocasu river runs at 2 m, near the EIE station 317, some 16 km far from the sea of Marmara. In this distance it runs very quietly. Nilüfer creek, joins the Kocasu river at the entrance of the gorge, has a drainage network reflecting neotectonic effects (Erkal and Emre, 1997). This river carries bed load in rainy period while it is a relict channel of Bursa area in arid time.

Gönen river

This river, forming Gönen delta and reached to Erdek gulf, has a main course and three tributaries

Table 1- Climatological features of the southern Marmara region (Meteoroloji Bülteni, 1984) BUR=Bursa, BAN= Bandırma, ÇAN= Çanakkale Meteorology stations, TEK= Tekirdağ, F= Florya, ORT= Average, F=Florya, Figures in paranteses indicate observation periods for rain and temperature.

Stations and Measurements	M o n t h s												Annual
	J	F	M	A	M	J	J	A	S	O	N	D	
BUR Precipitation (50 years)	92.0	77.6	74.2	61.4	51.8	30.3	24.6	19.9	41.0	58.9	81.0	107.5	720 mm total
BUR Temperature (52 years)	5.1	6.1	8.1	12.6	17.3	21.6	24.1	23.8	19.7	15.4	11.2	7.3	14.4 (°C) av.
BAN Precipitation (31 years)	98.3	84.3	70.6	51.3	33.7	25.0	13.7	15.3	34.2	66.1	91.7	121.3	705.7 mm total
BAN Temperature (31 years)	5.2	6.2	7.5	11.9	16.6	21.0	23.4	23.5	20.1	15.6	11.4	7.6	14.2 (°C) av.
ÇAN Precipitation (50 years)	97.6	71.5	66.5	39.6	28.9	23.3	11.2	8.4	23.7	45.6	85.6	105.0	606.9 mm total
ÇAN Temperature (50 years)	5.9	6.5	8.0	12.3	17.2	21.8	24.6	23.9	19.7	15.6	11.8	81.0	14.6 (°C) av.
ORT Precipitation (mm)	96.0	77.8	70.4	50.8	38.1	26.2	16.5	14.5	33.0	56.9	86.1	111.3	677.6 mm total
ORT Temperature (°C)	5.4	6.3	7.8	12.3	17.0	21.9	24.0	23.7	21.2	14.8	11.4	77.0	14.4 (°C) av.
Wind	Humid period (N+D+J+F+M), total = 441.6 mm/year												
	Dry period (A+M+J+A+S+O), total = 236 mm												
TEK Wind	Annual average wind speed 4 m/s												
F Wind	Strong wind speed 8-25 m/s												
	In Bandırma and Çanakkale 25° NE wind form the 60 % of annual blowns of the region												

(Fig. 1). Its drainage basin covers 2174 km² with main course in 134 km length and the elevation is 850 m at the source. The main channel has been cut into valleys in accordance with the Yenice-Gönen fault while tributaries follow the Sarıköy and Pazarköy faults (Şaroğlu et al., 1992). Gönen river has much step-like profile longitudinally. Its average discharge at the EİE station 210, is 14.2 m³/sec (Table 2). Maximum and minimum water flows are 911 m³/sec and 0.024 m³/sec respectively. Lithological features of its drainage basin are simi-

lar to that of Kocasu river with the difference of more widely Neogene volcanics exposure.

Gönen river passes a wide flood plain around Gönen and Sarıköy and reaches to the sea of Marmara via a gorge forming entrenched meanders (Fig. 4). The thickness of alluvium is about 50 m in this flood plain which is bordered by active faults (Şaroğlu et al., 1992). This thickness is similar to that of the Karacabey plain.

Sediment supply of the Kocasu and Gönen

Table 2- Data for the drainage basin, hydrological regime and delta averages of the Kocasu and Gönen deltas

Characteristics	Kocasu	Gönen River
DRAINAGE BASIN		
area (km ²)	2174	
main course length (km)	321	134
INCLINATION		
Inc. in channel (%)	0.08	0.11
Inc. in delta (%)	0.00113	0.00166
DISCHARGE		
Measurement site	EİE Station No 317, 321	EİE Station No 210
annual average dis. (m ³ /s)	158.5	17
minimum (m ³ /sn)	7.07	0.024
maximum (m ³ /s)	1322	911.0
SEDIMENT TRANSPORT		
Suspended load (%)	90	92
Bed load (%)	10	8
Dry season concentration aver. (ppm)	103.6	67.3
Humid season concentration aver. (ppm)	276.7	122.4
Total sediment transport (ton/ years)	364-486 million	45-53 million
In humid period	5.468	0.841
In dry period	0.423	0.0172
DELTA DIMENSIONS		
Max. coastal length (km)	21	13
Delta plain (km ²)	48	28
Progradation (km)	3.5	5.5
WIND REGIME		
Character	Normal	Normal
Main Direction in summer	Generally SW	Generally SW
Main Direction in winter	NE	NE
Max.-Min. wave length	2-0.5	2-0.5
CURRENT REGIME		
Tidal	?	?
Longshore	?	?
Other	?	?

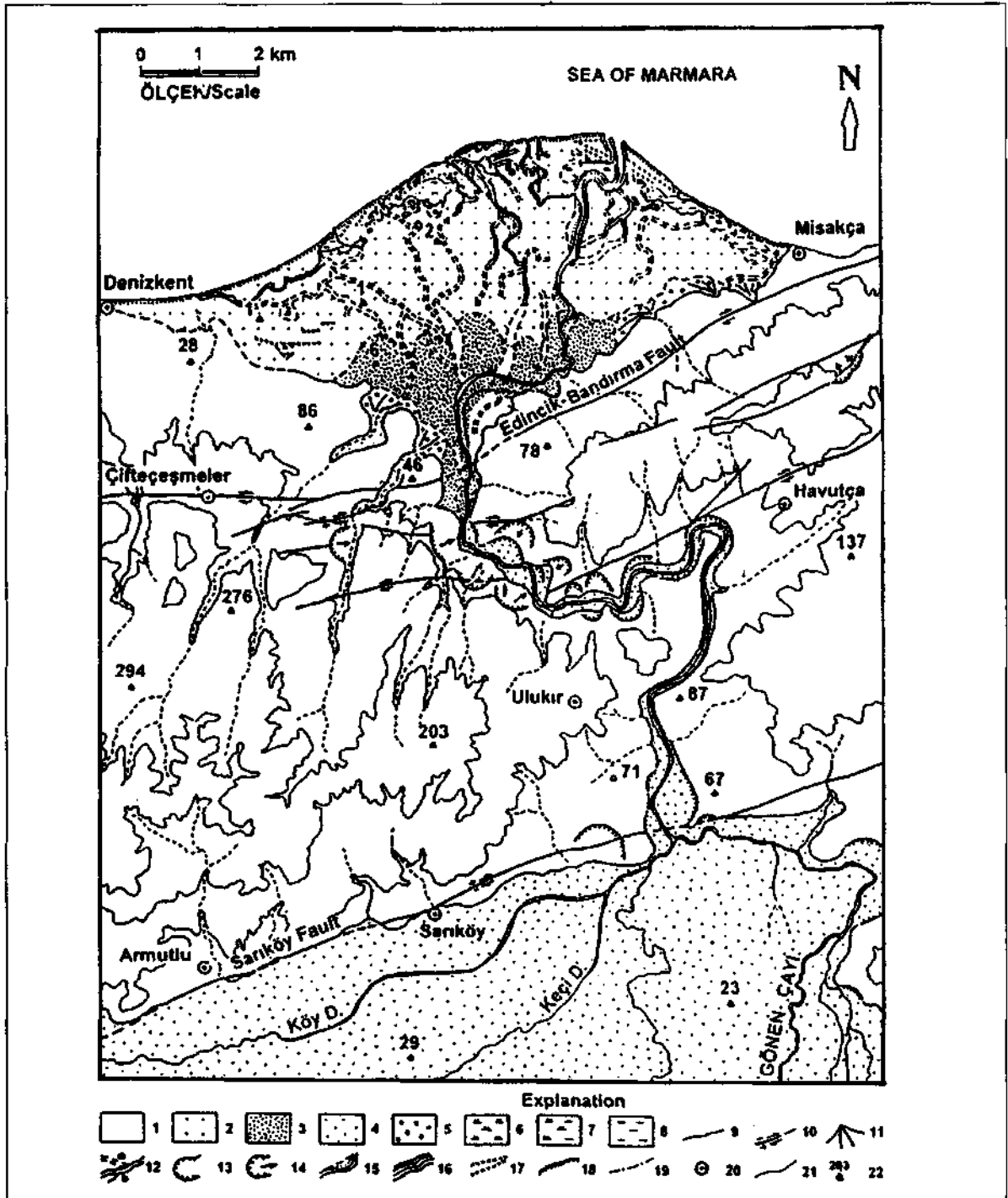


Fig. 4- Quaternary geology and geomorphology map of Gönen delta. 1, Denudation area surrounding the delta, 2, New delta sediments, 3, Old delta sediments, 4, Flood plain sediments, 5, Alluvial fan deposits, 6, New marsh, 7, Old delta, 8, Lagoon, 9, Contact, 10, fault (arrow show the direction of movement, - and + indicate downthrown and upthrown sides respectively), 11, alluvial fan, 12, a) abandoned channel, b) present channel, 13, old meander scar, 14, landslide, 15, point-bar deposit, 16, river and its levee, 17, beach ridge, 18, beach, 19, boundary between old and new delta, 20, settlement, 21, isohips (100 m at interval), 22, spot height.

deltas seem to that it is dependent on rainy/snowy wintertime (Tables 2 and 3). Denudation between rainy and dry seasons in the Kocasu watershed area is 0.072-0.0056 ton/km²/yr while it is 0.141-0.003 ton/km²/yr in the Gönen drainage basin. On the other hand sediment load in dry seasons can be neglected (Table 3). Although they are in the same climatic belt, sediment supply from the denudation is twice in comparison to Kocasu. The reason of this difference is due to that drainage basin of the Gönen river is close to technically active belt and the main channel and tributaries of the river are located in the active fault zone. Although its drainage basin is relatively small, high amount sediment supply of the Gönen delta explains that why the Gönen delta has prograded more than Kocasu delta and has formed a distinctive lobate coast along the sea of Marmara. Additionally hold of bed load by the lakes creates sediment supply against the Kocasu delta.

KOCASU DELTA

Physiography

Actual Kocasu delta has been prograding in front of a fault scarp and in an area surrounded by basement rocks (Fig. 2). It is not clear that how the İmralı island some 20 km in the north, gulfs of Gemlik and Bandırma in the E and W respectively, have changed marine dynamic elements and have affected delta evolution. The river forming the Kocasu delta reaches to the sea of Marmara at a single mouth via 8km length Karacabey gorge that is incised into basement rocks. Its areal deltaic plain is about 48 km²

Coastal length of Kocasu delta is 21 km and its

geometry gets closer in E-W direction, which is 3.5 km through the largest axis. Kocasu river flows in a narrow channel turning to the right and divides the delta into two parts (Fig. 2). Except some seasonal cracks/crevasses, it does not have any recent and/or active distributary channel. The length of Kocasu river on the delta is 4.5 km and the western part is bigger than the other. Maximum delta progradation is near the actual mouth (Fig. 2). There are two irregular shaped lagoons at the two sides of the main channel and their geometry can change from time to time. Aerial part of 0.5-1 m in elevation is widely exposed. Maximum height of the delta is 4 m near Bayramdere village in the W while the maximum height in the E is 2 m where it is juxtaposed a fault (Fig. 2).

Except the active part where there is its main channel, other coastal zone is 2-250 m width beach consisted of fine to medium sand. Grain size of beach sand in this part is homogeneous but it gets coarser towards the W (Sayılı et al., 1997). Kocasu delta does not have a subaqueous platform compared to deltaic plain. Unfortunately its submarine topography could not be understood owing to some technical problems. Bathymetric values of Akbulut and Algan (1985) given in fig.2 are based on some limited measurements. However a step-like morphology can be seen in front of the active delta at 14m depth (Fig. 2 and 3).

Boundary of delta front and delta shore is not clear as depth and topography. It is considered that front of active delta is not large because of being more clayey sediment beyond -6 and -8 metres (Akbulut and Algan, 1985).

**Table 3- Denudation estimation in the drainage basins of the Kocasu and Gönen river deltas
(Data based on EIE sediment observations).**

Streams	Drainage Area (km ²)	Denudation rate ton/km ² /year	Total sediment loss ton/year
Kocasu	27600	0.0723-0.0056	1995.4-154.4
Gönen	2174	0.141-0.003	306.9-6.3

Elements and sediments of delta plain

As is the same in many deltas, surface of the Kocasu delta is partly covered by vegetation, of which some of them are cultural and the others are hydrophilic and "all these are obstacles for transportation. However it is interesting that distribution of vegetation is concordant with deltaic elements and sedimentary facies. Based on this feature and areal photographs the delta plain could be mapped in detail (Fig. 2). It should be reminded that although surface elements of whole deltas are generally similar to each other their dimensions and aerial position could be changeable (Wright, 1985; Reading and Collinson, 1996).

Delta plain elements of the Kocasu delta are main course and its barrier, two crevasses, two lagoonal lakes, active and inactive marshes, N-S directed flood plain, beach ridges and beach (Fig. 2). Although alluvial fans are not included into delta elements in their origin nine alluvial fans have also been mapped. Their dimensions get larger from east to right. However beach ridges (Cheniers) among these deltaic elements are distinctive with their position. These beach ridges are 30-100 cm in height, 150-500 m in length broad ridges with clayey fillings and are parallel to the actual shoreline (Fig. 2). They are old coastal bars and/or old beaches in origin and are located in lagoons or marine marshes due to sea level rise (Elliot, 1978; Reineck and Singh, 1980). As they have not sunk into the swamp deposits and their elongations are still being kept, it reflects a limited sea-level rise and/or very new occurrence. Beach ridges, being kept and mapped are eight in number. So it can be suggested that sea level has been changed recently at least eight stages. Other element of the delta plain is ripples that are in different type and dimension. The orientation of these ripples is 20-30° NE-SW that reflects the concordance with the dominant winds of the region (Table 1).

Sediments of the Kocasu deltaic plain can be divided as old and new/recent deltaic sediments. This is morphologically very clear at 2 m height of the old deltaic sediments. At these heights covered

by cultural vegetation, soil cover in 0-20 cm thick can be seen and Karacabey-Bayramdere highway follows this boundary. There are recent delta plain sediments at 0-2 m height, in front of the 2-4 m height terrace level formed by old delta plain (Fig.2). Although this boundary is not a stratigraphic contact, it shows a delta progradation stage. The surface of new deltaic sediments is bare, underground water-level is considerably high and mostly covered by hydrophilic plants. Towards the east of delta, nowadays cultivation is a human activity.

Most of the sediments subject to this investigation are more or less affected by marine processes. Results of deposition controlled by terrestrial and denudational effects are alluvial fans, river embankments and flood plain sediments and their distribution is relatively limited (Fig. 2), but old marshes; they cover large area, are controlled by marine water inputs. These old marshes have these features especially in rainy stages. Although very large and thick alluvial sediments are characteristics in river dominated deltas (Hoeksta 1989; El-Sohby et al., 1989) alluvial sediments on this delta covering 48 km², are limited amount. In fact in big deltas there is a parallelism between delta drainage basin, delta plain-water discharge and delta cover-delta coast. If delta surface gets larger alluvial sediments also get thicker (Coleman and Roberts, 1989) but the reason of this reverse situation in the Kocasu's both in old and new sediments, is not to be developed distributary channels. It is most likely that the river forming the delta cannot be moved laterally due to very narrow Karacabey gorge and also delta plain is surrounded by active faults and basement rocks.

Sediments of the Kocasu delta plain are not very different in view of textural features. They are generally consisted of silts and there is sorting in beach sediments. In other sedimentary area gravels, sands, silts and clays are mixed. Rate of organic material is very low and it gives dark colour. Sedimentary deposits and/or facies that can be differentiated in the delta are given below.

a) *Sand fades*. - This facies can be seen along

the 5-150 m wide coast except the mouth of active delta. Medium-fine sand is dominant and grain size gets coarser from east to west. Some marine shell fragments can also be seen but heavy mineral concentration is distinctive in fine sediments (Sayılı et al., 1997).

Coastal dunes behind the beach, up to 750 m wide locally, have beach sand features but they have been contaminated by recent disposals. Owing to selection by aeolian effects, grain size of coastal dunes is coarser than beach sediments and they are medium size. Original topography has been demolished in some places resulted from sandy material taken for construction.

Another depositional site where the sandy facies can be observed, are sandy, ridges in marshes. In these deposits fine and very fine sands are dominant and also there is abundant shell fragments. In most cases they are mixed with fine (silt-clay) sediments and they are dark coloured.

Sandy old deltaic sediments are oxidized in some places. They are already covered by vegetation and have shell fragments. Grain size of these sediments is heterogeneous and fine gravels (pebbles) have also been included.

Deltaic elements given in figure 2 are beach, actual and coastal dunes, sandy deltaic sediments and marshy sandy ridges. These sediments are originally bed-load of Kocasu river that they were deposited as mouth bar sediments, and are resulted from the selection of wave and current action and deposition occurred in different places. In fact this is a normal situation in all fluvial dominated deltas and forms architecture of deltaic facies (Scruton 1960; Galloway, 1975; Wright, 1985; Postma, 1990). There is mineralogical similarity in whole facies body having quartz, feldspar, and rock fragments and heavy minerals.

b) Silty clay fades. - This facies is consisted" of fine sediments and silt/clay ratio cannot be discriminated easily. This facies is locally composed of clayey silt, silty clay or clay. The facies has" been mapped as old and actual marshes, lagoonal lakes, flood plain and levee sediments (Fig. 2). These, sed-

iments which are suspended load, can be intruded into lagoons in dry seasons and deposition occurs in rainy seasons. Marsh sediments are blueish-greenish-blackish gray in colour where they are dark gray in flood plain and levee sediments. Unfortunately role of very dense disposals transported by Nilüfer river could not be understood on the effect of facies colour. However it is supposed that blueish colour of the marsh deposits is dependent on this way.

Facies relations and delta progradation

Dominant physiography of the Kocasu delta that waves control deposition is reflected by old and new beach, marsh sand ridges parallel to shoreline. According to classifications (e.g. Galloway, 1975; Elliot, 1978; Orton, 1988) this delta is 'wave dominated river delta'.

Although sand facies covers relatively small area in the delta plain, it seems to be bigger as a volume. Sediment thickness of the actual delta plain is only 4 m above mean sea level and old sandy deltaic sediments are dominant between the heights of 2-4 m (Fig. 2). This position is distinctive in two ways: Deposition is sandy type although actual bedload is not too much and delta progradation is smaller in comparison to having a big watershed area. However in most deltas there is an opposite development (Coleman and Roberts, 1989). Many sea-level changes and wave dominance in the region should cause such a development.

Deltaic section, which was formed by submarine topography and delta plain, depicts that there is 45-55 m thick sequence (Fig. 3). It is supposed that maximum thickness can be observed if it is drilled near the actual active delta. This sequence probably represents delta complex in terms of the data of many sea-level changes. Suddenly happened sea-level rises may cause decrease in sediment thickness resulted from the erosion of some deltaic sediment. For example there are some sea-level rises in the present Caspian Sea since the late Pleistocene, their periods are being getting smaller (e.g. 15 years periods for the last century and they

cause some deltaic recedes in the Reşt delta (Zubakov, 1993; Gülbabazade, 1997).

GÖNEN RIVER DELTA

Gönen river delta has been progradating in the Erdek gulf which is surrounded by Kapıdağ peninsula in the E, and Avşa and Paşalimanı islands in the N (Figs. 1 and 4). Being sheltered by the Erdek gulf is not known well but it may cause a barrier against the NNE directed winds (Table 1). Density currents that are characteristic of the sea of Marmara (Beşiktepe, 1991; Ergin et al., 1994) are undoubtedly affected by these natural barriers.

Physiography

Gönen river delta like Kocasu delta, surrounded by basement rocks but these surrounded rocks do not form a wild topography (Fig. 4). There is right-lateral active Edincik-Bandırma fault and Sarıköy fault to the S (Fig. 4). Drainage network of the Gönen river has been affected by these faults that form a 8 km length antecedent valley with incised meanders as a result of uplift between the faults (Şaroğlu et al, 1987; Emre et al., 1997a). The incised meanders are important data indicating neotectonic activity in the back of the delta (Fig. 4).

Length of Gönen delta coast is 13 km and its progradation amount is 5.5 m. The delta covers 28 km² in aerial extent (Table 1). Gönen delta has a lobate delta form with a diversion slightly towards NE. Activity of the delta progradation is toward the tilting. Main channel of Gönen river is oriented toward the right after the formation of meander. After this meander it turns to N and right before reaching the sea. There are also three active distributary channels. However many abandoned channels form the surface morphology of the delta plain. Lagoons have been formed at the mouths of the old and new distributary channels. The shape of these lakes is changeable and some of these are dry except rainy periods. Hydrophilic plants cover through some lakes.

Gönen delta shows step-like topography with two steps (Fig. 4). Backward part of this delta is 6 m height and covers one fourth of whole delta. But the

other part of the delta forming actual delta plain is dissected by distributary channels up to 1,5 m depth (Fig. 4). Maximum height in this part is 2 m and forms the western part of the delta with abandoned channel forms. These abandoned channels have been shifted from W to E (Fig. 4).

Unfortunately the data about the subaqueous part of the delta have not been gained. Boundaries of the delta front and off the delta are not clear. However bathymetric map prepared by SHOD (Turkish Navy Oceanographic Department) shows the 15-30 m depth few km off the delta. In view of this data it is supposed that subaqueous part of the delta is considerable. On the other hand if the submarine topography of the Erdek gulf is interpreted existence of a submarine valley with its gentle topography can be thought. This topography should have been formed in the last sea-level drop in Marmara sea region and it is most likely to be old Gönen valley developed on the present shelf.

Elements and sediments of delta plain

Grassy plants cover aerial part of the Gönen delta and top of the old deltaic sediments has been transferred to cultural area. Surface of new deltaic sediments close to land, is pasture while the closer site to the sea is covered by reed. Many deltaic plain elements are many distributary channels, and lagoons that are terminals for the distributary channels. Between distributary channels there is flood plain. However parts of flood plain are distinctive if they are close to main channel. Actual delta coast is 1-15 m width with coarse sand, but it is 30 m width near Denizkent. The beach has some sandy patches as distributary channels or lagoonal inlets have cut it.

Gönen river delta plain up to 2 m has an alluvial character except the lagoonal and beach sites. Main and distributary channels transport fine gravel-fine sand while silt-clay size material is transported in the flood plain. Sedimentation on the old delta plain is up to 2-6 m height, forming small size alluvial fans. Old delta sediments have medium-fine sediments with many shell fragments. There is occasionally gravelly and silty/clayey levels.

During the fieldwork it was not possible to collect samples from the lagoons but it is thought that they are similar to marshy and lagoonal sediments of the Kocasu delta. It is noteworthy that beach sediments are gravel-coarse sand size while old beach sediments at the back of the coast are medium to fine sand. Grain composition is heterogeneous. Actual coast with coarse grain is gray-dark colour owing to existence of large amount rock fragments. Not only rock fragments and also feldspar and mafic minerals are abundant in sands. Quartz is quite rare as amount as feldspar. This case is a result of having quite close source area sand total load of Gönen river is transported to the sea of Marmara, except in plains. In fact Gönen delta has been developed rather than Kocasu due to its small watershed area and it has formed a lobe.

Delta progradation

Gönen delta is a fluvial dominated classical delta (Galloway, 1975) because of having lobate geometry and alluvial sediments on the actual delta plain. Much of totally calculated 5.5 km progradation (2/3) seems to be formed in accordance with actual sea level (Fig. 4). It is clear that there are many distributary channels with main channel and this case is thought that right lateral Edincik-Bandırma fault has affected it. Tilting of delta plain and shifted delta mouth to the E, support this idea (Fig. 4). Erdek gulf sheltered against the winds and gently inclined topography in this gulf (maximum depth is 46 m) seem to that rapid delta progradation has been supported by these factors.

Sediment thickness of the Gönen delta is considerably less than its progradation. At two drilling sites (DSI A101168 and A101681) it has been reached to 64 and 42 m depth and reddish Neogene rocks were cut under these depths (Fig. 5). Deltaic sediments are composed of washed up sands and silt-clay interbeddings with shell fragments and gravels (Fig. 5). Sands most likely represent old mouth bars while fine sediments reflect bays and lagoons between distributary channels. These sands are not sorted and it should be result of rapid sedimentation.. The step-like morphology,

which is distinctive for discrimination of old and new deltaic area, shows that there was a sea-level drop during the delta progradation. The same case for the Kocasu delta, indicate that sea-level drop occurred in whole Marmara sea basin, not happened due to local tectonism.

DISCUSSION AND CONCLUSIONS

Although Kocasu and Gönen deltas are different from each other with their dimensions, geometry, basement topography and development processes (Table 2), their position which are developed in basement rocks bounded area and deposited in front of active fault scarps, is similar (Figs. 2 and 4). Thickness of their sedimentary sequences is same (Figs. 3 and 5). Drainage networks and developments at the back of these deltas are also same.

Kocasu delta is a wave-dominated delta with its triangular in shape, 45-55 m thick sedimentary sequence, and maximum 4m height. Marine processes have controlled its delta plain sediments. Tectonic setting of this delta is being on the down-thrown side of an E-W trending right-lateral oblique fault. As the main channel forming this delta is limited with Karacabey gorge, distributary channels on the deltaic plain cannot be developed. However Gönen river delta is a fluvial-dominated, lobate type delta with 55-65 m thick sediments. Fluvial processes control delta plain of this delta and there is many distributary channels on it. This classical fluvial delta is located in an area sheltered by right-lateral fault and close to wave effective zone. Drainage area of the Gönen river delta is small but its progradation is much (Figs. 2 and 4, Table 2). Based on comparison of deltas and their elements some results can be given as follows:

- 1- Main channels and their tributaries forming these deltas form the whole drainage of the southern Marmara region. Reaching to the sea of the drainage network occur these two main channels via the Karacabey gorge. It is known that actual drainage in the region was mainly established in the late Pliocene and developed with some deformations due to tectonism (Emre et al., 1997a; Erkal

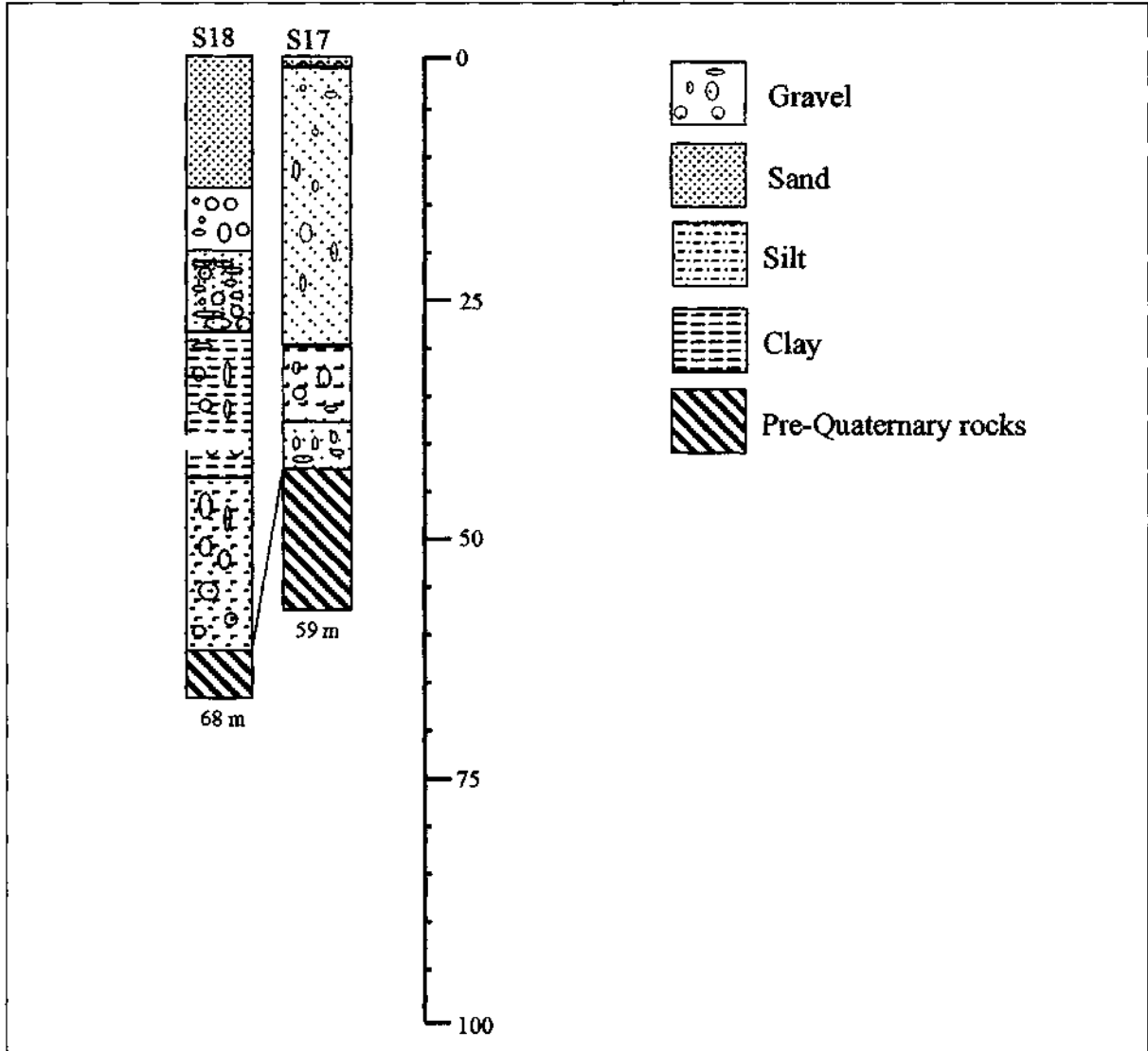


Fig. 5- Sequential features of Gönen river delta (DSI drilling no. A-10, 11680-11681).

and Emre, 1997; Emre et al., 1998). Available data show that Kocasu was flowing into endoreic basin in Karacabey-Mustafakemalpaşa area in early-middle Pleistocene but both Kocasu and Gönen rivers were flowing towards the Sea of Marmara in other times (Emre et al., 1997b). Thickness of this internal basin is less when it is compared to Kocasu drainage basin and sediment influx. It is supposed that there should have been thick sedimentary sequences in these two deltas but thickness of the deltaic sequences are not too much (50-65 m) and

delta lobes are smaller or have not been developed. In case of erosion-sedimentation processes it is understood that these deltas are very young. When they are compared to morphostratigraphy of closer plains, aerial parts of the deltas have been deposited in Holocene.

2- It is supposed that there are Pleistocene aged old deltaic sediments deposited below or off the present deltaic sequences when the sea-level was dropped. Besides, it can be observed that remnants of old deltaic deposits which they have been

formed during the high sea-level periods are seen as terraces along the coast. Unfortunately data on the second alternative and the sea-level between Karabiga and Gemlik reached up to higher than actual mean sea-level could not be gained. This situation covering the delta evolution, supports that the sea of Marmara settled down in the Erdek gulf and Bandırma-Gemlik corridor in the Holocene (Emre et al., 1997a). Because, Kocasu and Gönen deltas are similar to each other in their present position. However the deltas have different palaeogeographic evolution based on the place of their old deltaic systems. This should be owing to different submarine topography.

3- It is observed that there are some step-like morphology at 2-4 and 0-2 meters and 2-6 and 0-2 meters in Kocasu and Gönen deltas respectively. Based on this step-like morphology it is possible to understand the existence old and new deltaic sedimentation stages. Of course, old deltaic sediments indicate higher sea-levels. Additionally more data can be submitted on this subject. Firstly, Kocasu and Gönen rivers were cut into 4.5 m deep in the old deltaic sediments. Secondly, some notches in the basement rocks in the E of Kocasu delta are in the same level with the old deltaic sediments. So it points out that sea-level rise was in global scale as this features have been observed in two deltas with a distance of 80 km from each other (Figs. 2 and 4). It can be said that the sea of Marmara was 4-6 m higher than present sea-level in the beginning of delta evolution.

4- Quite thin delta plain sediments both in Kocasu and Gönen delta show that delta development is young, particularly new delta evolution means that sedimentation has started probably in late Holocene, but it has also been affected by tectonism. The fault behind the Gönen delta has affected deltaic prism oriented to the E rather than sea-level. However dextral fault controlling Kocasu delta is an oblique fault (Fig. 2), caused marine floods and drownings because of drops in the N. Parallel sandy ridges in marsh sediments are evidence of this event. Reason of dominant marine processes in the delta should be tectonism. This event happen-

ing at least eight times formed sand ridges indicating delta progradation, marshes showing marine floodings respectively.

5- Bed load is less but suspended load is much in the Kocasu delta at present. Sandy facies are products of rapid fluvial erosion due to high thalweg following global sea level drop. At present the river transports more suspended load at about the base level along the 30 km from the Ulubat lake. This can be explained that sea-level is increasing.

6- Existence of deltas buttressed by active faults and surrounded by basement rocks are quite rare. Therefore effects of active faults reflect on delta plain elements on the Kocasu and Gönen river deltas. On the other hand strike-slip faults have not affected sea-level. This is quite good example for interpretation of old sequences.

7- Marsh sandy ridges in Kocasu delta plain can be helpful for fault mechanism of oblique faults. They are suitable places for palaeoseismic studies on the North Anatolian fault forming Bandırma-Gemlik corridor where many pull-apart basins have developed. The deltas also have very rare late Holocene deposits for this purpose.

8- It is understood that site for deltaic deposition surrounded by basement rocks has not affected delta progradation too much. Surrounded by basement rocks is clear in the Kocasu delta while it is weak in the Gönen river delta but delta progradation in these two deltas are vice versa. So it can be thought that longshore currents are not important on the bed load transportation of the sea of Marmara.

Kocasu and Gönen river deltas are good examples to understand deltaic sedimentation as much as geological evolution of the sea of Marmara. In point of denudation-transportation-deposition processes view there are many discordance in the drainage evolution of the river, which have formed the deltas. In this study state-of-arts of the deltas has been evaluated in particular attention of regional geology and geomorphology. The interpretation can be made clear if they are correlated with the drillings and submarine geophysical studies

and it may help to understand Quaternary palaeogeographic evolution of the southern Marmara region.

ACKNOWLEDGEMENTS

This study is part of project numbered YDABÇAG 426/G and 598/G, titled "National Marine Geology and Geophysics Programme" carried out by TÜBİTAK, MTA and universities. The editor and referees of this journal kindly improved this paper.

Manuscript received April 20, 1998

REFERENCES

- Akbulut, A.O. and Algan. I.M., 1985, Kocasu Çayı ağız kesiminde denizaltı depoların bazı sedimentolojik özellikleri. İst. Üniv. Deniz Bil. ve Coğr. Enst. Bült., 2, 145-154.
- Ardel, A., 1957, Marmara Denizi'nin tesekkülü ve tekamülü. Türk Coğrafya Dergisi, 17, 1-14
- , 1968, Türkiye Kıyılarının teşekkül ve tekamülüne toplu bir bakış, Türk Coğrafya Dergisi, 24/25, 1-6
- Barka, A.A. and Kadinsky-Cade, K., 1988, Strike-slip fault geometry in Turkey and its influence on earthquake activity. Tectonics, 7, 663-684.
- Beşiktepe, T.T., 1991, Some aspects of the circulation and dynamics of the Sea of Marmara, Ph.D. Thesis, Inst. Marine Sciences. METU, 195 pp., İçel.
- Coleman, J.M. and Roberts, H.H., 1988, Deltaic coastal wetlands. In: Coastal Lowlands Geology and Geotechnology (ed. by W.J.M. Van der Linden, S.A.P.L. Cloeting, J.P.K. Kaasschieter, J. Vanderberghe, W.J.E. Van der Graaf and J.A.M Van der Gun) Kluwer Acad. Pub., 1-24, Dordrecht.
- El Sohby, M.A., Mazen, S.O., Abou-Shook, M. and Bahr, M.A., 1989, Coastal development of Nile Delta. In: Coastal Lowlands Geology and Geotechnology (ed. by W.J.M. Van der Linden, S.A.P.L. Cloeting, J.P.K. Kaasschieter, J.P.K. J. Vanderberghe, W.J.E. Van der Graaf and J.A.M. Van der Gun). Kluwer Acad. Pub., 175-180, Dordrecht
- Elektrik İşleri Etüd İdaresi (EİE), 1993 Türkiye akarsularında sediment gözlemleri ve Sediment taşınım miktarları. EİE Genel Müdürlüğü, Yayl. no. 93-59. Ankara
- , 1996, 1992 Su Yılı Akım Değerleri, EİE Genel Müdürlüğü Yayl No: 95-25, Ankara
- Elliot, T., 1978, Deltas. In: Sedimentary Environments and Facies (ed. by H.G. Reading) Elsevier, 97-142, New York
- Emre, 6., Kazancı, N., Erkal, T., Karabıyıkolu M. and Kuşçu, L., 1997a, Ulubat ve Manyas Gollerinin Oluşumu ve Yerleşim Tarihi. TÜBİTAK YDABÇAG 426/G Raporu (Koord: N. Kazancı ve N. Görür) Ankara, 116-134
- , ——, ——, Görmüş, S., Görür, N., Kuşçu, L., Karabıyıkolu, M. and Keçer, M., 1997b, Ulubat ve Manyas göllerinin oluşumu ve Güney Marmara'nın Kuvaterner evrimi. Marmara Deniz Araştırmaları Workshop-III (2-3 Haz. 1997). TÜBİTAK-MTA-ÜNİVERSİTE Ulusal Deniz Araştırmaları Programı (Koor. N. Görür), Genişletilmiş Bildiri Özetleri, 23-27, Ankara.
- , Erkal, T., Tchepalyga, A., Kazancı, N., Keçer, M. and Ünay, E., 1998, Doğu Marmara'nın Neojen-Kuvaterner'deki Evrimi. MTA Bull., 120, 233-258.
- Ergin, M., Saydam, C., Baştürk, S., Erdem, E. and Yörük, R., 1991, Heavy metal concentration in surface sediments from the two coastal inlets (Golden Horn Estuary and İzmit Bay) of the northeastern Sea of Marmara. Chem. Geology, 91, 269-285.
- , Bodur, M.N., Yıldız M., Ediger, D., Ediger, V., Yemencioğlu, S. and Eryılmaz-Yücesoy, F., 1994, Sedimentation rates in the Sea of Marmara; a comparison of results based on organic carbon-primary productivity and ²¹⁰Pb dating. Continental Shelf Research, 14, 1371-1387.
- , Kazancı N., Varol B., İleri Ö. and Karadenizli L., 1996, Late Quaternary depositional environments on the southern Marmara shelf. Turkish Journal of Marine Sciences, 2, 83-92.
- Eriç, S., 1957, Karacabey Boğazı, İst. Üniv. Coğr. Enst. Derg., 8, 95-99.
- Erkal, T. and Emre, Ö., 1997, Nilüfer Çayı (Bursa) Drenajının Kuruluşu ve Evrimi: Tektonizma-Drenaj İlişkileri Marmara Denizi'nin oluşumu ve Neojen-

- Kuvaterner'deki evrimi. Güney marmara bölgesinin Neojen ve Kuvaterner evrimi. TÜBİTAK YDABÇAG 426/G Raporu (Koord: N. Kazancı ve N. Görür) Ankara 1-22.
- Erol, O., 1969, Çanakkale Boğazı çevresinin jeomorfolojisi hakkında on not. Coğr. Araşt. Derg., 2, 53-71.
- , 1991, Türkiye kıyılarında terkedilmiş tarihi limanlar ve bir gevre sorunu olarak kıyı çizgisi değişimlerinin önemi. İ.Ü. Deniz Bil. ve Coğr. Enst. Bült., 8, 1-44.
- Galloway, W.E., 1975, Process framework for describing the morphologic and stratigraphic evaluation of deltaic depositional systems, In: Deltas, Model for Exploration (ed. by M.L. Broussard). Houston Geol. Soc., 87-98, Houston, Texas, USA
- Görür, N., Çağatay, M.N., Sakınç, M., Sümengen, M., Şentürk, K., Yalıtırak, C. and Tchepalyga, A., 1997a, Origin of the Sea of Marmara as deduced from the Neogene to Quaternary paleogeographic evolution of its frame. Intern. Geology Review, 39, 342-352.
- and ———; 1997b, Marmara Denizi'nin oluşumu ve Neojen-Kuvaterner'deki evrimi. Güney Marmara bölgesinin Neojen ve Kuvaterner evrimi. TÜBİTAK YDABÇAG 426/G Raporu (Koord: N. Kazancı ve N. Görür) Ankara 1-22.
- Gülbabazade, T., 1997, Anzeli Gölü (KD İran) civarındaki Kuvaterner istifinin incelenmesi (Doktora Tezi), A.I). Fen bilimleri Enst., Ankara 121 pp. (Unpubl).
- Hoekstra, P., 1989, The development of two major Indonesian river deltas: morphology and sedimentary aspects of the Solo and Porong deltas, East Java. In: Coastal Lowlands: Geology and Geotechnology (ed. by W.J.M. Van der Linden, S.A.P.L. Cloeting, J.P.K. Kaasschieter, J. Vanderberghe, W.J.E. Van der Graaf and J.A.M. Van der Gun). Kluwer Acad. Pub., 143-160, Dordrecht.
- Kazancı, N., Bayhan, E., Süleyman, N. Şahbaz, A., İleri, Ö., Özdoğan, M., Temel, A. and Ekmekçi, E., 1997a, Manyas Gölü ve güncel tortulları: TÜBİTAK YDABÇAG-426/G no.lu proje raporu (Koord. N. Kazancı ve N. Görür) Ankara, 192-243.
- , N., Emre, 6., Erkal, T., Görür, N., Ergin, M. and İleri, Ö., 1997b. Kocasu ve Gönen deltalarının* Morfolojisi ve Tortul yapısı: TÜBİTAK YDABÇAG-426/G no.lu proje raporu (Koord. N. Kazancı ve N. Görür) Ankara, 140-169.
- Meteoroloji Bülteni, 1974, Ortalama, Ekstrem Sıcaklık ve Yağış Değerleri Bülteni. Devlet Meteoroloji İşleri Genel Müdürlüğü, Başbakanlık Basimevi, Ankara.
- , 1984, Ortalama, Ekstrem Sıcaklık ve Yağış Değerleri Bülteni Devlet Meteoroloji İşleri Genel Müdürlüğü, Başbakanlık Basimevi, Ankara
- Orton, G.J., 1988, A spectrum of Middle Ordovician fan deltas and braid plain delta, North Wales: a consequence of varying flourise clastic input, In: Fan Deltas; Sedimentology and Tectonic Settings (ed. by W. Nemeç and R.J. Stell). Blackie Pub., Glasgow 23-49.
- , and Reading, H.G., 1993, Variability of deltaic processes in terms of sediment supply with particular emphasis on grain size. Sedimentology. 40. 475-512.
- Oti, M.N. and Postma, G. (Eds.), 1995, Geology of Deltas. Balkema Pub. Comp., Rotterdam 480.
- Özsoy, E., Oguz T., Latif, M.A. and Ünlüata, Ü.. 1986. Oceanography of the Turkish Straits. First Annual Report, Inst. Marine Sciences, METU, 1, İçel 269.
- Postma, G., 1990, Depositional architecture and facies of river and fan deltas: a synthesis. In: Coarse-Grained Deltas (ed. by A. Colella and D.B.Prior). IAS. spec. Pub. 10; 13-28.
- Reading, H.G. and Collinson, J.D., 1996, Clastic Coast. (Ed. H.G. Reading), Sedimentary Environments: Processes, Facies and Stratigraphy Blackwell. London; 154-231.
- Reineck, H.E and Singh, I.E., 1980, Depositional Sedimentary Environments (2nd Ed.), Springer Verlag, Berlin, 439.
- Sayılı, İ.S., Ergin, M., Şahbaz, A., Özdoğan, M., Varol, B., İleri, 6., Bayhan, E., Görmüş, S., Turan. S.D. and Soydemir, Ö., 1997, Kocasu deltası plajı kıyı tortullarının sedimantolojik ve mineralojik özellikleri. TÜBİTAK YDABÇAG-426/G -no.lu proje raporu (Koord. N. Kazancı ve N. Görür) Ankara. 170-191.
- Scruton, P.C., 1960, Delta building and the deltaic sequence. In: Recent Sediments. Northwest Gulf of Mexico (ed. by F.P. Shepard, F.B. Phleger and Tj.H. van Andel). AAPG Pub., Tulsa, 82-102.
- Stanley, D.J. and Blanpied, C., 1980. Late Quaternary

- water exchange between the eastern Mediterranean and the Black sea. *Nature*, 285, 537-541.
- Şaroğlu, F., Emre, Ö. and Boray, A., 1987. Türkiye'nin Aktif Fayları ve Depremsellikleri, MTA Rep. no: 8174 (Unpublished). Ankara
- ; ————— and Kuşçu, İ., 1992. Türkiye Diri Fay Haritası, MTA publ., Ankara.
- Şengör, A.M.C., Görür, N. and Şaroğlu, F., 1985, Strike-slip faulting and related basin formation in zones of tectonic escape: Turkey as a case study. In: *Strike-slip deformation, basin formation, and sedimentation* (ed. by K.T. Biddle and N. Christie-Blick). *Soc. Econ. Paleont. Mineral. Spec. Publ.* 37, 227-264.
- Whateley, M.G.K. and Pickering, K.T. (Eds.), 1989, *Deltas; Sites and Traps for Fossil Fuels*. *Geol. Soc. Pub. No: 41*, Blackwell, Oxford.
- Wright, L.D., 1985, *River Deltas*, In: *Coastal Sedimentary Environments 2nd* (ed. by R.A. Davies). Springer Verlag, New York 1-76.
- Zubakov, V.A., 1993, *The Caspian Sea level oscillations in the geological past and its forecast*. *Russian-Meteorology and Hydrology Bull.* 8, 65-70.

AN AUTOCHTHONOUS. RECENT LATERITIC OCCURRENCE IN THE EASTERN TAURUS BELT: BÜYÜKBELLEN
(FARAŞA-YAHYALI) IRON OCCURRENCE

Şuayip KÜPELİ*, İsrail KAYABALI**, Mehmet ARSLAN*** and Hakan-'Aydin SAKA"

ABSTRACT.- In the study area, which is located 28 km southeast of the Yahyalı (Kayseri) village, are cropped out Upper Cretaceous aged pelagic sediments and ophiolitic rocks. These lithologies of the Bozkır unit are studied into the two main groups as Çavdaruşağı olistostrome and Pozantı-Faraşa peridotite nappe. Büyükbelen Laterites are composed of recent, autochthonous lateritic iron crust and red soils derived from pelagic carbonates intercalated with chert of the Upper Cretaceous aged Çavdaruşağı olistostrome. Above mentioned ores were formed by lateritization and partly karstification processes affected after Miocene. Lateritic iron ore is principally composed of goethite, hematite, ferrihydrite, quartz, illite, kaolinite, malahite, azurite and amorphous matter aggregates. Major oxide percentages of the laterites are, in average, 49.71 % Fe₂O₃, 3.12 % Al₂O₃, 30.75 % SiO₂ and 0.09 % CaO. Above mentioned lateritic ore was enriched in Fe, but was depleted in Si and Ca compared to the parent rock. Al component was also removed under poorly acidic-neutral weathering conditions. The red soils including average 4.05 % Fe₂O₃, 7.13 % Al₂O₃, 79.49 % SiO₂ and 1.73 % CaO are made up of quartz, montmorillonite, calcite, illite, opal-CT and amorphous matter. In electron microscopic investigation, it is observed that thin-fibrous goethite and euhedral hematite crystals in the laterite samples are authigenic, and transformations between these two minerals are common. The studied laterites are relatively rich in Cu, Cr, Co, Zn, Ba, Ni but poor in Ce, La, Th and Zr. On the other hand Cr, Cu and Mo concentrations are also high in the parent rock.

LATE MIOCENE ARTIODACTYLES (MAMMALIA) FROM YUKARISAZAK VILLAGE (KALE-DENİZLİ)

Vahdet TUNA****

Amongst the defined Artiodactyla specimen at Kapuşçabaşı locality. Yukarısazak village has been those that Helladotherium duvernoyi Gaudry, Protoryx carolinae Major, Tragoportax amalthea (Roth and Wagner) and Gazella deperdita (Gervais). These paleomammalian species has dated back as early as Late Miocene (Turolian) and implies presence of steppes covered by buch during that era.

EVIDENCES OF DUCTILE DEFORMATION IN EVAPORITES AROUND ZARA AREA (E SİVAS), SİVAS BASIN

Faruk OCAKOĞLU*

ABSTRACT.- A series of ductile deformation evidences and large-scale tectonic lines which remain enigmatic in the light of rigid tectonics principles were observed around Zara and Bolucan areas in the Sivas basin. One group, the evaporite walls which are closely related with the Oligocene-Lower Miocene evaporitic levels, traverses the basin for 30-40 km in an approximate E-W direction. Throughout the contacts, vertical to overturned evaporitic rocks face with the younger sediments as well as with thrusts and folds. Evaporitic diapirs of varying sizes, and basement and cover rock inclusions in the order of several 100's meters to km constitute the smaller scale second set of evidence of this kind of deformation. The available stratigraphic and tectonic data lets us suggest that the ductile deformation occurred subsequent to the N-S compression. Also speculated, that the areal extension of the Oligocene-aged Hafik gypsum is of utmost importance and the basaltic volcanism appeared in late Miocene may well be a factor decreasing the viscosity of evaporites and hence accelerating the phenomenon.

INTRODUCTION

Earth's crust, and especially sedimentary basins which could be appreciated as a memory for the processes operating on it, comprise rock-stratigraphic units of differing Theological properties. Sedimentary rocks within basins become unstable through the ongoing subsidence and some upward moving gravity structures occur mainly due to their different physico-mechanical response to stresses. The most common examples of this group of structures are salt walls and diapirs, serpentinite piercements, granite and gneiss domes and peat diapirs (Talbot, 1977).

One of the most important parameters in the course of development of upward moving gravity structures is the viscosity of source level (i.e. the sedimentary level moving, flowing upward). Low viscosity, as perceived after peat, salt and serpentinite diapirs, makes the process easier. Some other additional factors reducing the viscosity of sedimentary series, for example a volcanic heat source and free water in salt tectonics, can speed up the process (Jenyon, 1991-). A second important parameter is the density differentiation between the

source level (low density) and the cover rocks (high density). In this case, a gravitational reversal comes about, and in conjunction with the viscosity parameter, the process can initiate. On the other hand, some other secondary factors (for instance, existence of regional tectonic stresses, differential loading resulted from the thickness variation of cover rocks, geometry of source layer, lateral density and viscosity changes of cover and source rocks, etc.) do play important roles in triggering the process and also determine the ultimate geometry of the structure (Talbot, 1977).

The most common and satisfactorily studied upward moving gravity structures are the salt structures. Fundamental cause of these structures is the physico-mechanical behaviour of certain salts (such as halite, silvite and carnallite) interbedded with the other evaporitic deposits. Halite, probably the lightest mineral ($d=1.6 \text{ gr/cm}^3$) in nature keeps its low density constant while the surrounding rocks consolidate and get rid of their pore waters and hence become denser. During this early stage, when the sedimentary load over the salt horizon exceeds the values $1.8-2.7 \times 10^5 \text{ kg cm}^{-2}$, it's no more a rigid

body, but becomes ductile and flows (Richter-Bernburg, 1980).

At the early stage of ductile deformation, salt moves towards the gentle anticlines which are developed at the salt-overlying sediment boundary, by means of buoyancy or differential loading, or tectonic forces if the regional context is suitable, and builds the salt pillows. Mean wavelength of the known examples of salt pillows ranges 7 to 15 kms (Jackson and Talbot, 1986). If the main salt level is thick enough, the flowage towards the low-stress fields continues and consequently, salt stocks and walls can develop. As the process still goes on the chimneys feeding the stocks may become narrower and finally cut away resulting in the detached diapirs. Salt stocks and walls may rise as high as 5-10 km from their primary stratigraphic levels, including some rafts (i.e. rigid blocks of surrounding rocks) and they even flow on the earth's surface (Kent, 1979; Talbot, 1993).

Occurrence of extensive evaporitic deposits in Tuz gölü and Sivas basins has been known for a long time. Some geophysical and geological studies revealed the existence of 100 km long salt walls along the SW margin of the Tuz gölü basin (Uygun, 1981; Uğurlutaş, 1975). In the same basin, a borehole was drilled penetrating more than 1300 m within a diapiric salt structure (Turgut, 1978). As for the Sivas basin, ductile deformation generated within the Oligocene-aged evaporitic rocks has caught the researcher's attention since the early times (Nebert, 1956). Later, an oil exploration drill-hole (Celalli-1) performed by MTA in the central part of the basin traversed several thousand meters of evaporitic rocks. A 100 m thick rock salt level was also proved in the hole (Gedik and Özbudak, 1974). In the near past, some geological mapping studies at the south of Sivas city, clearly indicate some domal structures in evaporites (Gökçe, 1989-1990) while Yılmaz (1994) urged a direct relationship of salt tectonics with the end-Miocene regional tectonic framework. In another study, very great apparent thickness and massive appearance of the Oligocene-aged evaporitic Hafik formation was related with diapirism, and some diapiric bodies

were mapped (Poisson et al., 1996). Lastly, a doctoral thesis performed by Çubuk (1994) in the İmranlı area to the east arid Karayün area at the center of the basin indicates the occurrence of very large scale salt structures and these are thought to be connected with the halokinesis driven by extensional regime in the basin.

In the present study, some structures intervening the evaporitic rocks are presented from Zara area. These structures are generally discordant with the compression-related element and are thought unlikely to be explained by means of rigid tectonics principles.

Presentation is arranged so that stratigraphy of the basin summarized at first hand with a special emphasis on the stratigraphic position and expand of evaporitic successions. Secondly, the tectonic style and resultant tectonic elements are briefly explained. Finally, ductile deformation evidences in evaporites and their liaisons with the regional tectonic framework are evaluated.

GEOLOGICAL OUTLINE OF THE SİVAS BASIN

Sivas basin is situated at the eastern part of the central Anatolia where three main tectonic units, namely Pontides, Kırşehir block and Taurid platform converge to each other (Fig. 1). The proposed geotectonic evolution schemes for the basin differ greatly. To Görür et al., 1984 the basin developed on the oceanic lithosphere and evolved as a forearc basin in relation with the closure of the Neo-Tethys. Yılmaz (1994) and Yılmaz et al., 1995 consider the basin, on the other hand, as a postcollisional one following the late Maastrichtian continental collision. Poisson et al., 1996 proposed a foreland setting for the basin, and Cater et al., 1991 supported this interpretation as supposing the occurrence of nap movements from south to north.

The oldest rocks covering unconformably the Taurid platform are of Maastrichtian-Paleocene aged shallow marine to continental deposits (Özgül and Turşucu, 1984; Yılmaz and Özer, 1984). Eocene is represented by olistostromal levels as well as lava-pyroclastics bearing turbidite

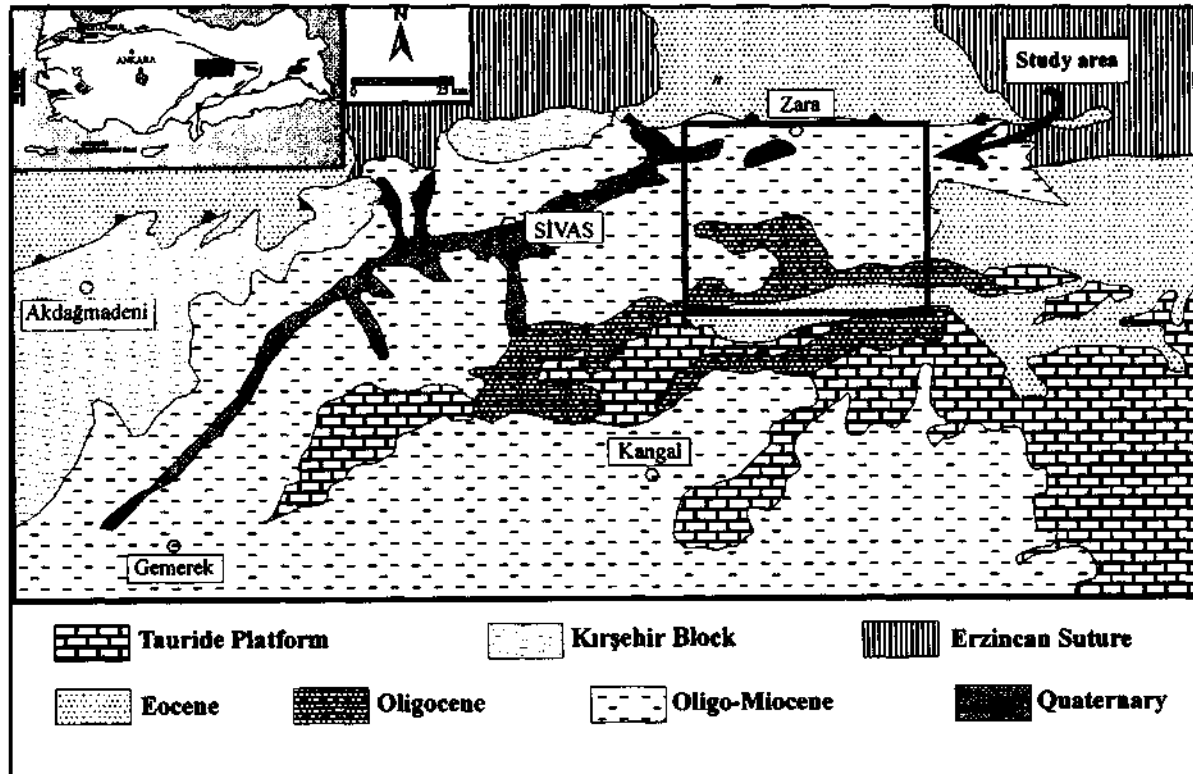


Fig. 1- Location map and main tectonic units of the study area (Simplified after the Geological Map of Turkey of scale 1/2.000.000).

sequences at the south (Kurtman, 1973), whereas the northern area was still dominated by shallow marine carbonate deposition and widespread volcanic activity at that time (Gökten and Kelling, 1991).

A regional marine regression at the end of Eocene resulted in the deposition of evaporites along the southern part of the basin. Oligocene rocks are continental. As a whole at the west (Sümengen et al., 1987) whereas shallow marine to continental at the central areas (Gökçen and Kelling, 1985). Miocene witnessed a transgression developed from east towards west as far as Sivas city. After the early Miocene sea abandoned the region, widespread continental detritics and evaporite deposition developed and just afterwards the whole basin fill was deformed by a tectonic paroxysm (Kurtman, 1973).

STRATIGRAPHY AND POSITION OF EVAPORITIC LEVELS

The Eocene terrigenous sequence makes the oldest sedimentary rocks extending in an E-W direction along the southern part of the study area (Fig. 2). This detrital sequence becomes more and more shallower upward, gradually passing firstly to fan-delta deposits and then gypsum-bearing sediments (Çiner, 1995). Oligocene deposits (i.e. Selimiye formation) were represented by red to green colored detritals and less commonly by evaporites and carbonates at south (Fig. 3). It seems that the thickest (100 m) evaporitic body in Selimiye formation passes laterally northward to main evaporitic unit of the study area, namely Hafik formation. Around the Bolucan at the east, there are salty water sources leaking from the main evaporite level in Selimiye formation. The base of the Miocene, perhaps the uppermost part of Oligocene as sup-

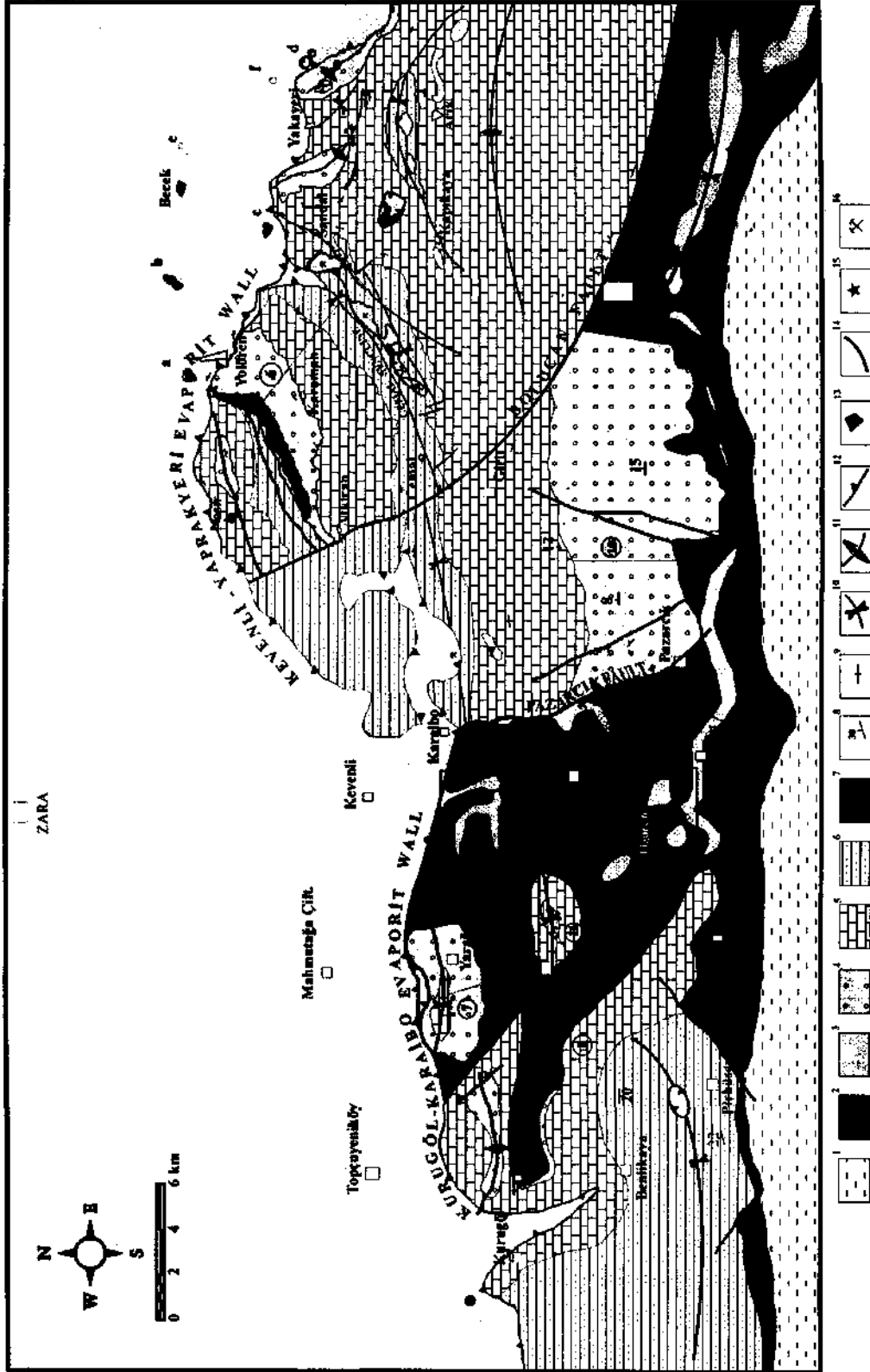


Fig. 2- Simplified geological map of the study area. 1- Eocene detrital sequence, 2- Selimiye fm. (Oligocene), 3- Hatık fm (Oligocene), 4- Karayün fm. (Mio.), 5- Karacaören fm (Mio.), 6- Benikaya fm. 7- Volcanics, 8- Dip and strike of bed, 9- Vertical bed, 10- Syncline, 11- Anticline, 12- Thrust, 13- Village, 14- Fault, 15- Salty water source, 16- Celestite mineralization, for letter a-f refer to the text.

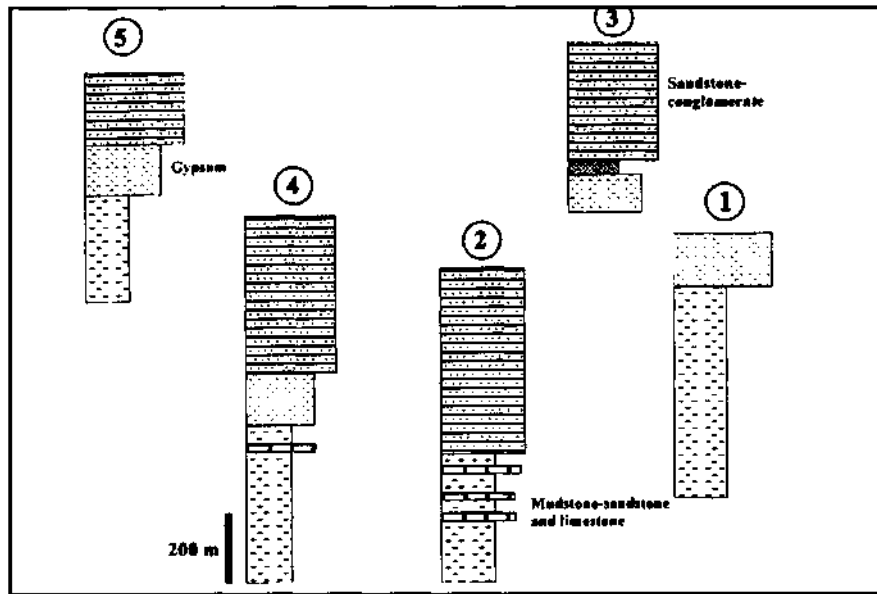


Fig. 3- Columnar stratigraphic sections of the Oligocene deposits in the study area (For section locations refer to figure 2).

posed by Poisson et al., 1996 was occupied by Karayün formation (Fig. 4). This unit is composed of mudstone and gypsum at the SW areas (around Yaragıl and Hidroğlu villages) and is not deposited southwards (around Selimiye and Tuzlagözü vil-

lages), perhaps due to a tectonically controlled uplift (Ocakoğlu, 1977). The uppermost part of the Karayün formation is made up of mudstone and gypsum which were probably deposited in a coastal plain setting.

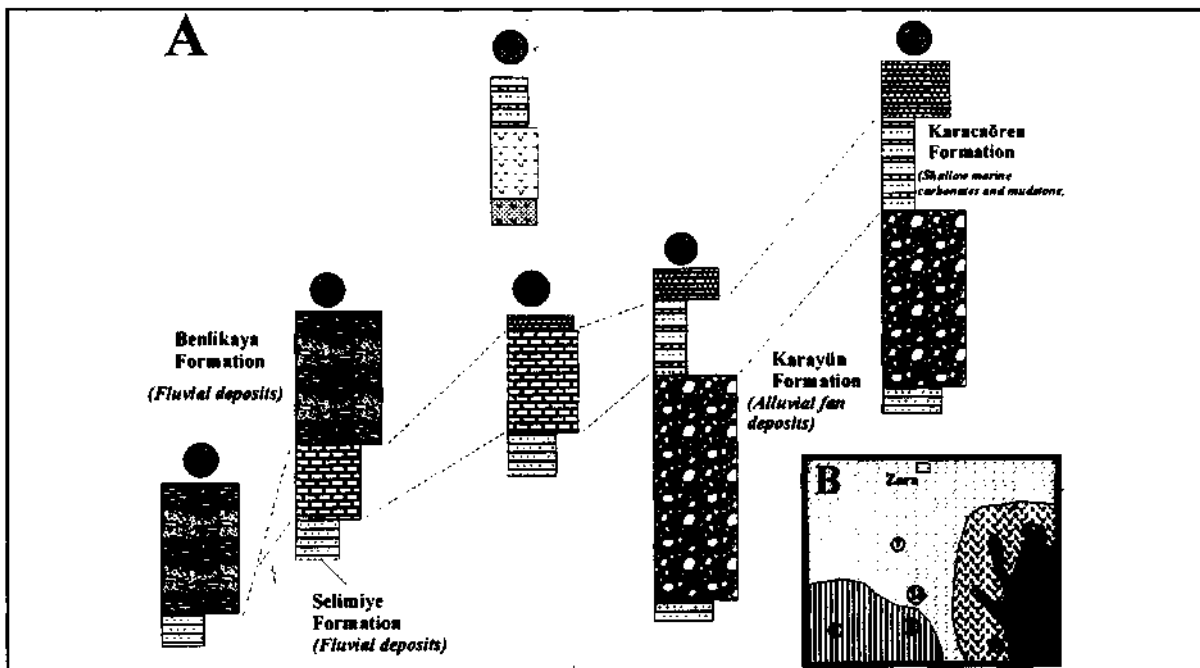


Fig. 4- A-Stratigraphic columnar sections of the Miocene deposits in the study area, B- Paleogeographic reconstruction just before the deposition of the Karacaören formation (for section locations refer to figure 2).

At the beginning of Miocene (Aquitainian), a marine transgression developed and the older continental deposits became submerged. As a result, a stratigraphic record which was deposited in a variety of environments ranging from coastal plains to open shelf has been yielded (Ocakoglu, 1997). Within this mainly marine sequence, 10 gypsum levels with thicknesses of 1-6 m was deposited in coastal sabkhas. The uppermost part of the Miocene record in the study area is again occupied by fluvial deposits and partly by evaporitic rocks (around Pirhuseyin village). Basal relation of these rocks with the underlying marine sediments are low-angle unconformity at the south (Around Keller village), whereas conformable at the central part of the region.

In summary, it can be suggested that there are 4 well determined evaporitic levels in the investigation area. From older to younger, these are;

1. Gypsum, forming the bulk of Hafik formation. These are probably thickening from south to north due to complex depositional transitions.
2. Gypsum occupying the uppermost levels of the Karayün formation.
3. Evaporites, found at the lower section of the marine Karacaören formation, which probably formed in coastal sabkhas.
4. Gypsum, forming the uppermost part of the fluvial Benlikaya formation.

STRUCTURAL GEOLOGY OF THE SOUTHERN ZARA AREA

It would be possible to categorize the structural elements of the study area, following the aim of the study, as the elements observed in the cover rocks of evaporitic Hafik formation (which are the overlying terrigenous and carbonate rocks), and the ones observed in evaporitic rocks (mainly Hafik formation). While the first group was chiefly resulted from the N-S compression, the second group was originated due to ductile behaviour of evaporites within general tectonic framework.

Tectonic elements on the cover rocks

These are E-W trending fold axis and south verging thrust faults, and NE-SW and NW-SE trending strike slip faults, all of them were possibly resulted from regional N-S compressional framework.

E-W trending folds are frequently observed in the Miocene sediments outcropped around Arık and Nasır area to the east and northeast, Tuzlagözü and Benlikaya to the west (Fig. 2). Arık syncline, which is a slightly asymmetric and south verging structure has a convex-to-north geometry. These originally E-W trending structures like Arık syncline to the northeast are rotated by two major faults (Bolucan and Sandal faults) of NE-SW and NW-SE trend respectively (Fig. 2). Two thrust faults which are supposed to be E-W trending before rotation are situated to the south of Yolören village. The Yolören thrust, at the north, corresponds to a detachment surface found at the bottom of the gypsum. From thrust line to the Cemal synclinal axis to the south, Miocene sedimentary sequence shows no tectonic disturbance. Cemal thrust which is 7 km away towards the south is also dipping to the south and surrounded by drag synclines on both sides (Fig. 2).

Tectonic lines cutting the E-W trending fold axis and thrust faults in an oblique manner are especially prominent at the south of the study area. Some of those faults have no appreciable normal slip, some others (such as Bolucan faults and neighbouring NE-SW trending smaller fault) have great vertical offsets. The 600 m thick Karayün formation around Bolucan area is abruptly terminated in front of Selimiye formation due to this structure.

Ductile deformation evidences in evaporites

Kevenli-Yaprakyeri evaporite wall.-It begins around Kevenli village at the center of the study area, and extends towards the east for 30 km in a more or less E-W direction with indented pattern (Fig. 2). Gypsum beds of Hafik formation at the contact are nearly vertical. To the south of Sandal village they even thrust over Miocene sediments by an angle of 30°. Another surprising point related to

this tectonic element is that a several hundred meters sized block belonging to Selimiye formation which is also clearly seen at the base of the thrust fault around Yolören village (Fig. 2 and 3) crops out within the Hafik formation as the prolongation of the mentioned thrust (Fig. 2, a). This situation may be interpreted so that horizontal offset is negligible across the evaporite wall. Another point is that, near the thrust line around Yakayeri village there are two elipsoidal gypsum blocks of several hundred meters in diameter (Fig. 2, d) "floating" in the background Hafik formation.

Kurugöl-Karaibo evaporite wall.- It enters from the western limit of the area and extends at the south of the Atkiran village for about 40 km (Fig. 2). To the east of Karaibo, both limbs of the ancient evaporite ridge are well seen. To the west, around Kurugöl, Hafik gypsum makes an insertion into Miocene sediments towards the south. In this sudden diversion of the evaporite wall, effects of tectonic elements are supposed, but their continuation towards the further south (Benlikaya village) is not

prominent. At the west of Karaibo which also corresponds to the southern evaporite wall (Fig. 2 and 5) an evaporite level of 100 m thick Hafik formation exhibits a complicated folding pattern. Frequent thickening at the fold axis and some isoclinal folds are thought to be several indicators of ductile deformation in these evaporitic bodies. To the east of Karaibo, on the other hand, gypsum bodies belonging to Hafik formation insert into the Miocene sequences (at least 1500 m thick) and reach at the surface and spread out slightly. Two kilometres away from the evaporite wall southward, the evaporite wall extends down there passing over the Cemal syncline (Fig. 2).

Diapiric evaporitic stocks.- Those are ellipsoidal bodies which diapirically emplaced into random levels. Some of them have no clear connection with the faults and folds related with the regional compressional regime. As an example, at the south of Bolucan, 4-5 evaporitic stocks occur 750-1500 m away in the dip direction of 100 m thick evaporitic level of Hafik formation (Fig. 6). At the centre of

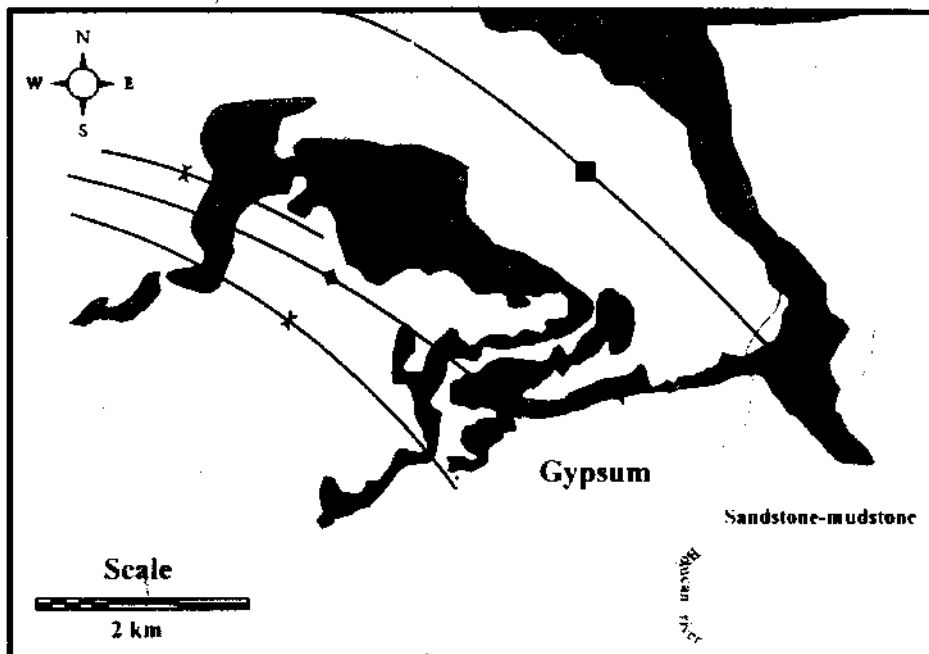


Fig. 5- Ductile deformation structures in evaporites around SW Karaibo (note the isoclinal folds and thickening at synclinal axis).

these stocks some buried salt levels may be found. Additionally, the indentation (about 400 m) on figure 6 (indicated by an arrow) seems likely an evaporite wall inhibited in its initial stage of development. Gypsum bodies outcropped in the synclinal axis at the north of Arık village are two other well-developed examples of evaporitic stocks. These bodies are likely derived from the evaporitic levels found within the marine Karacaören formation. If so, they should be diapirically elevated more than 500-600 metres from their original stratigraphic levels. Lastly, at the west of Pirhuseyin village, the white colored evaporitic body of 1 km in diameter shows clear flowage characteristics on the air photographs (Fig. 2). It is thought to be derived from the lowermost levels of Oligocene sequence.

In addition to the examples given above, 3 gypsum stocks have been observed at the NE of the study area, in relation with the Cemal thrust. Two of them lean on the south-verging thrust line while the largest one spreads over the synclinal axis

southeastwards (Fig. 2).

Inclusions of basement and cover rocks disseminated within the evaporites. - Randomly distributed basement and cover rock blocks within the evaporites make another set of evidence of ductile deformation in the region. At the north of Kevenli-Yakayeri evaporite wall, basement and cover rock blocks of different sizes are found within a wide evaporitic background. Two of them (about 400-600 m in diameter) observed at just north of Yolören village (Fig. 2, a and b) belong to Selimiye and Karacaören formations respectively. These blocks show only small internal deformation. Towards further east, at the north of Sandal and at the east of Yakayeri, is seen ophiolitic blocks this time (Fig. 2, c, f and e). The block at Düden is 20 m in diameter, and includes many fractures in the central part perhaps likely occurred during the previous history (Fig. 7). Close to the periphery, gypsum becomes to fill the fractures. More outward, large ophiolitic blocks become to be separated from the main body,

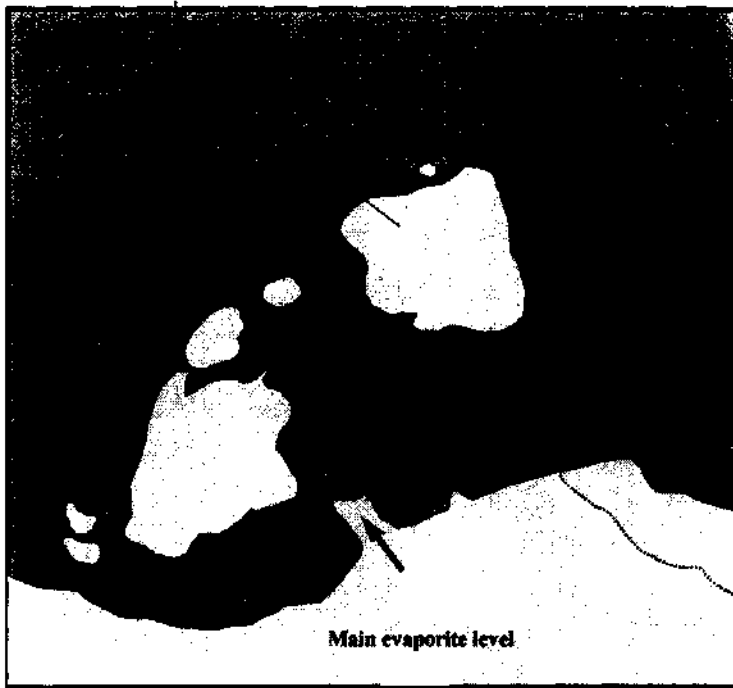


Fig. 6- Diapiric evaporite bodies in the Selimiye formation, south of Bolucan.

and emerge into the evaporitic matrix. Going more outward, rare smaller serpentinite gravels randomly float in evaporites.

All the examples observed in the study area remind us the huge (as big as 5 km) and dense inclusions appeared within the salt and evaporite complex of Hürmüz salt domes, reported by Gansser (1992). Weinberg (1993) indicated by

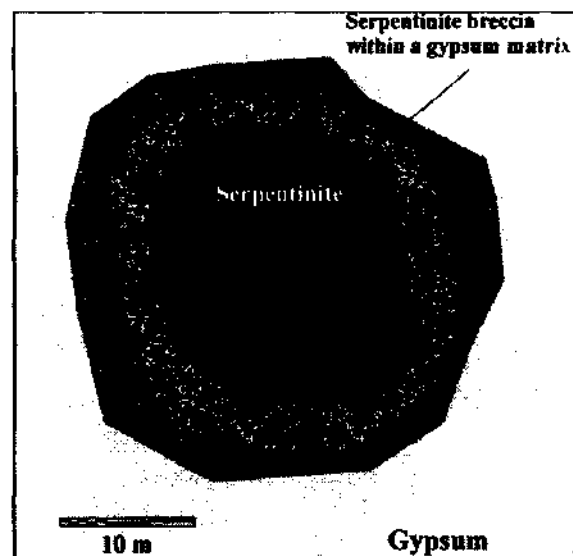


Fig. 7- Serpentinite block within the gypsum background at the east of Yakayeri.

using theoretical calculations, that those inclusions may be transported by diapiric salt movements exceeding the gravity forces of the inclusions. The observations realized in the study area indicate a similar mechanism so that the basement blocks incorporated within the dominantly evaporitic Hafik formation can be elevated upward by a ductile creep in evaporites.

DISCUSSION

Diapiric structures generated within evaporites which are observed in the study area and suggested to be widespread at the eastern part of the Sivas basin seem related with different physico-mechanical behaviour of especially evaporitic rocks and cover strata, as well as the late Miocene regional

tectonic regime and distribution of evaporitic facies within the basin.

The study area which is situated at the east of Sivas basin was affected from heavy tectonic activity occurred in certain periods throughout the Oligo-miocene. Both, structural elements (E-W trending fold axis and thrust fault, NE-SW and NW-S'E trending strike slip faults) and unconformities and great thickness variations observed between the sedimentary series are clues to the tectonic activity. Structural style and depositional distribution, as well as lateral facies relationships in the study area present a close similarity to that of Karayün area investigated by Cater et al., 1991. The authors urged that in Karayün area, Karayün sand bodies were transported towards the north by means of some by-pass zones determined by certain synsedimentary faults. So, they show rapid thickness variations in an E-W direction (Cater et al., 1991). According to these researchers, those N-S trending faults correspond to the lateral ramps of south verging thrust faults. In the study area, it is quite possible that the Miocene paleo-uplift which restricts the Miocene-aged Pazarçık alluvial fan from the west coincides with this kind of lateral ramp of a nappe.

In the study area, existence of a ductile deformation is evident from evaporite walls, numerous evaporite diapirs and floating alien blocks within the evaporites. In order to explain the effect of distribution of evaporitic rocks in the formational mechanism of the evaporite walls, schematic model in figure 8A is proposed for the stratigraphy of the region. The fundamental parameters in the model are thickness variations, density and viscosity of the Hafik, Selimiye and Karayün formations which have lateral transitions with each other and, that of the cover rocks. Although quantitative data obtained from the study area is lacking, it can be suggested from the previous studies that the Hafik formation which is also the source material for the diapirs in the region has lower density and viscosity with respect to neighbouring detrital rocks. It seems still difficult to assess how the model (which is likely unstable one) will behave under these conditions even if the regional tectonic stresses be ignored. Fortunately,

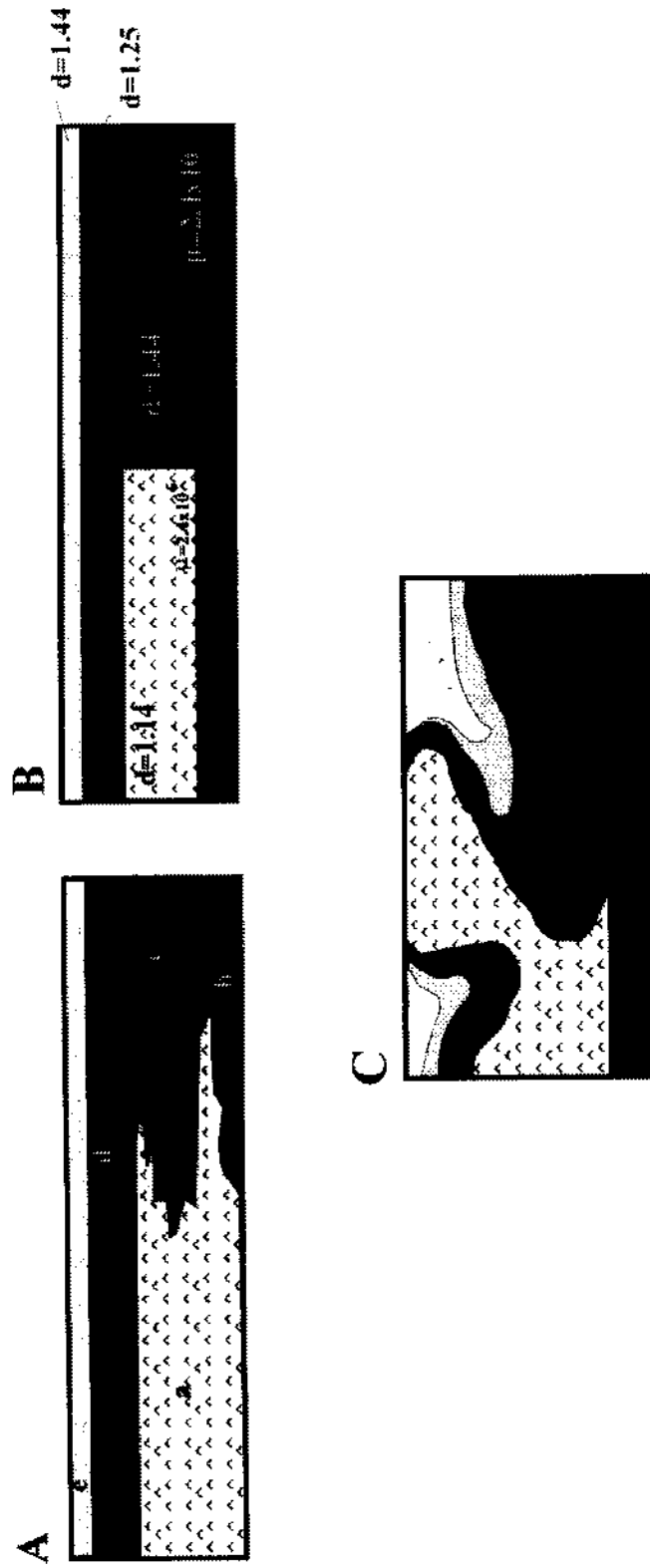


Fig. 8- A) Stratigraphic model developed for the study area. a-Hafik Fm. b-Selimiye Fm. c-Karayün Fm. d-Karacabören Fm. e-Benlikaya Fm.
B) Hypothetical model by Talbot (1977) and C) Deformation of Talbot's model under centrifuging (equal to a force of 2000 gr) for 150 seconds.

the response of a very similar model to the resultant stresses was experienced by Talbot (1977) by using artificial material (Fig. 8B). The result of Talbot's experiment is that low viscosity source rocks flow over the higher density cover elastics which are transient with the former. Meanwhile, the cover rocks are elevated and even truncated and then a dipping asymmetrical upward moving gravity structure (diapir or ridge) results in. This experiment foresees conveniently the position and character of the two great evaporite walls in the study area. At the plan view, on the other hand, northerly situated and convex upward position of the Kevenli-Yaprakyeri evaporite wall, with respect to more or less E-W trending Kurugöl-Karaibo evaporite wall is drawing attention. It seems that the geometry of the Kevenli-Yaprakyeri evaporite wall is determined by the aerial distribution of Pazarçk alluvial fan system (Fig. 4B).

In this context, temperature parameter which was affected the viscosity of the Hafik formation should be seriously taken into account. In salt tectonics studies, a negative correlation has been stressed between temperature and viscosity of salt bodies. In other words, as thermal gradient increases, the flowage capacity of salt increases too (Jenyon, 1991). Jackson and Talbot (1986) indicated that anhydrite shows a similar trend. Under these given examples in the literature, it can be suggested that magmatic activity (mainly olivine sill and dykes cutting Oligo-miocene sediments) occurred at the end of Miocene does increase the flowage capacity of the evaporites. Due to the same magmatism, widespread celestite mineralization is formed within the Oligocene evaporites (Fig. 2). Majority of these mineralizations correspond to the allochthonous evaporitic zones indicated in this study. Fluid inclusion studies on these mineralizations indicate the formational temperatures as high, as 350°C (Tekin et al., 1994). It can be suggested that this high thermal effect of magmatic origin, even be located in limited fracture zones, can reduce the viscosity of the evaporitic masses in the study area.

CONCLUSIONS

Timing of the ductile deformation observed in the evaporitic rocks can be summarized within the context of the structural history of the basin as following: Throughout the Oligo-miocene period, a depositional pattern occurs in the area so that terrigenous sediments situated mostly in the southern area while the evaporite system lies northerly (fig. 8A). At the end of the Miocene times, the whole area was subjected to a strong N-S compression, and as a result, E-W trending south vergent thrusts and asymmetric folds formed. During the early phases of compressional deformation, Hafik gypsums serve as the weak (detachment) zones on which the thrusts were developed. Along these thrust faults, evaporitic rocks originally situated in very different levels in the sequence moved upward in a ductile manner. In this period, a basaltic volcanism expressing itself as sills and dikes inserted in different levels has also occurred and thermal nature of this latter possibly reduced in a certain degree the viscosity of the evaporitic rocks in the sequence. Deformation generated by regional tectonic compressional stresses likely continued by the NW-SE and NE-SW trending conjugate strike slip faults, and as a result, E-W trending previous structural lines have been partly rotated by these latter.

As an ultimate result of the N-S compression, crustal thickness in the basin increases and this thickening likely triggered the main evaporite body (i.e. Hafik formation) to move upward in a ductile manner within the gravitationally unstable evaporite-terrigenous system. This upward movement of the evaporitic mass occurred at the plan view along an E-W line where the terrigenous-evaporite depositional transitions have been realized formerly. Some basement and cover rock blocks incorporated in the evaporitic body are also risen diapirically. Meanwhile, external erosive agents should rapidly truncate the topographically higher cover rocks above the rising diapiric mound, and after this load removal, on the other hand, diapiric uplift should be accelerated. In our opinion, the southern limit of this giant rising evaporite mass corresponds to the Kevenli-Yaprakpınar and Kurugöl-Karaibo evapor-

ite walls in the study area. Towards the west, around SW of Sivas, where the general thrust fault pattern (i.e. south vergent, generally E-W trending faults) resembles very much to that of the study area, three anomalous north vergent thrust faults indicated by Poisson et al., 1996 between the Hafik gypsum and the southern terrigenous area can likely be related with the the rising evaporite body.

Manuscript received, February 27, 1998

REFERENCES

- Cater, J.M.L., Hanna, S.S., Ries, A.C. and Turner, P., 1991, Tertiary evolution of the Sivas Basin, Central Turkey. *Tectonophysics*, 195, 29-46.
- Çiner, A., 1995, Sivas havzasının sedimantolojisi, ekonomik potansiyeli ve çevrimsel sedimantasyona örnekler: Türkiye Bilimsel ve Teknik Araştırma Kurumu, Yer Deniz Atmosfer Bilimleri ve Çevre Araştırma Grubu Araştırma Projesi, No: YBAG-064. 112s.
- Çubuk, Y., 1994, Boğazören (İmranlı) ve Karayün (Hafik) yörelerinde (Sivas doğusu) yüzeyleyen Miyosen yaşlı birimlerin tektonostratigrafisi: Cumhuriyet Üniversitesi, Fen Bilimleri Enstitüsü, Doktora Tezi, 125 s.
- Gansser, A., 1992, The enigma of the Persian dome inclusions. *Eclogae Geol. Helv.*, 85, 825-846.
- Gedik, A. and Özbudak, N., 1974, Sivas Celalli-1 sondajı bitirme raporu. MTA Rep., 5260 (unpublished), Ankara.
- Gökçe, A., 1989-1990, Sivas güneyindeki sölestin yataklarının jeolojisi ve oluşumu: Cumhuriyet Üniversitesi Mühendislik Fakültesi Dergisi, Seri A-Yerbilimleri, 6-7, 1-2, 111-127.
- Gökçen, S.L. and Kelling, G., 1985, Oligocene deposits of the Zara-Hafik Region (Sivas, Central Anatolia): evolution from storm-influenced shelf to evaporite basin: *Geol. Rundsch.*, 74, 139-153.
- Gökten, E. and Kelling, G., 1991, Hafik kuzeyinde Senozoyik stratigrafisi ve tektoniği: Sivas-Refahiye havzası kuzey sınırında tektonik kontrol. In Yetiş, C., ed. Ahmet Acar Jeoloji Simpozyumu, Adana, Çukurova Üniversitesi, Jeoloji Müh., 113-123.
- Görür, N., Oktay, F.Y., Seymen, İ. and Şengör, A.M.C., 1984, Palaeotectonic evolution of the Tuz gölü basin complex, Central Turkey, Sedimentary record of a Neo-Tethyan closure. In: Geological Evolution of the Eastern Mediterranean (eds: Dixon, J.E. ve Robertson, A.H.F.), 464-482.
- Jackson, M.P.A. and Talbot, C.T., 1986, External shapes, strain rates, and dynamics of salt structures. *Geological Society of America Bulletin*, v. 97, 305-323.
- Jenyon, M.K., 1991, Alternatives to halokinesis in salt diapirism. *Journal of Petroleum Geology*, v. 14 (4) (suppl. II), xi-xiv.
- Kent, P.E., 1979, The emergent Hormuz salt plugs of southern Iran. *Journal of Petroleum Geology*, 2, 2, 117-144.
- Kurtman, F., 1973, Sivas-Hafik-Zara ve İmranlı bölgesinin - jeolojik ve tektonik yapısı. *MTA Bull.*, 80, 1-32.
- Nebert, K., 1956, Sivas vilayetinin Zara-İmranlı mıntıkasındaki jips serisinin stratigrafik durumu hakkında. *MTA Bull.*, 48, 76-82.
- Ocakoğlu, F., 1997, Zara (Sivas doğusu) yöresindeki Sivas havzası Oligo-Miyosen dolgusunun stratigrafisi ve ortamsal özellikleri. *Cumhuriyet Üniversitesi Mühendislik Fakültesi Dergisi, Seri A-Yerbilimleri*, 14, 1, 71-88.
- Özgül, N. and Turşucu, A., 1984, Stratigraphy of the Mesozoic carbonate sequence of the Munzur Mountains (Eastern Taurides). In: *Geology of the Taurus belt* (eds: O. Tekeli ve C. Göncüoğlu), 173-180.
- Poisson, A., Guezou, J.C., Öztürk, A., İnan, S., Temiz, H., Gürsoy, H., Kavak, K.S. and Özden, S., 1996, Tectonic setting and evolution of the Sivas Basin, Central Anatolia, Turkey, *International Geology Review*, 38, 838-853.
- Richter-Bernburg, G., 1980, Salt tectonics, interior structure of salt bodies. *Centre de Recherche Exploration Production Elf-Aquitaine Bulletin*, 4, 373-393.
- Sümengen, M., Terlemez, İ., Bilgiç, T., Gürbüz, M., Ünay, E., Ozaner, S. and Tüfekçi, K., 1987, Şarkışla-Gemerek dolaylı Tersiyer havzasının stratigrafisi, sedimantolojisi ve jeomorfolojisi: MTA Rep., 8118, (unpublished), Ankara.
- Talbot, C.T., 1977, Inclined and asymmetric upward-

moving gravity structures: *Tectonophysics*, 42, 159-181.

Talbot, C. T., 1993, Spreading of salt structures in the Gulf of Mexico. *Tectonophysics*, 228, 151-166.

Tekin, E., Ayan, Z. and Varol, B., 1994, Sivas-Ulaş solestin oluşumlarının (Tersiyer) mikrodokusal özellikleri ve sivi kapanım çalışmaları: *Türkiye Jeoloji Bülteni*, 37, 1, 61-76.

Turgut, S., 1978, Tuz Gölü havzasının stratigrafik ve çökelse gelişmesi, *Türkiye 4. Petrol Kongresi Bildirileri*, 115-126.

Uğurlutaş, G., 1975, Tuz Gölü havzasının bir bölümünün jeofizik yorumu: *MTA Bull.*, 85, 38-44.

Uygun, A., 1981, Tuz Gölü havzasının jeolojisi, evaporit oluşumları ve hidrokarbon olanakları: *İç Anadolu'nun Jeolojisi Simpozyumu*, TJK yayl., 66-71.

Weinberg, R.F., 1993, The upward transport of inclusions in Newtonian and power-law salt diapirs. *Tectonophysics*, 228, 141-150.

Yılmaz, A., 1994, An example of a post-collisional trough: Sivas Basin, Turkey: in *Proc., 10 th Petr. Congr.* Turkish Assoc. Petrol. Geol., 21-32.

——— and Özer, S., 1984, Kuzey Anadolu Bindirme Kuşağının Akdağmadeni (Yozgat) ile Karaçayır (Sivas) arasındaki bölümünün temel jeoloji incelemesi ve Tersiyer havzasının yapısal evrimi: *Ketin Simpozyumu*, TJK yayl., 163-174.

——— Uysal, S., Bedi, Y., Yusufoglu, H., Havzaoğlu, T., Ağan, A., Göç, D. and Aydın, N., 1995, Akdağ Masifi ve dolayının Jeolojisi: *MTA Bull.*, 117. 125-138.

AN EXAMPLE TO THE JASPEROIDAL-TYPE EPITHERMAL MINERALIZATION FROM THE WESTERN ANATOLIA:
DEĞİRMENCİLER ANTIMONY MINERALIZATION (SİMAV, KÜTAHYA)

Vedat OYGÜR***** and Ayhan ERLER*****

ABSTRACT.- Değirmencililer antimony mineralization consists of the stibnite-bearing quartz veins emplaced within the marble lenses of the biotite-gneisses which are at the bottom of the stratigraphical sequence of the Simav region. Quartz veins formed both as the replacement of and open-space filling in the limestone cut the schistosity of the host rock and crop out in accordance with it. Limestones were decalcified before the mineralization along the faults and later, transformed to jasperoid as a consequence of the replacement of calcite by silica. Intermediate and advanced argillic alterations consisting of the montmorillonite, smectite, dickite, quartz, opaline-CT and cristobalite developed on the wall rock. Halotrichite which represents the acid leaching zone of the hydrothermal alteration presents as well. Comb, cockade and banded textures as colloform and crustiform are widespread within the silicified rock. Hydrothermal breccias with black silica matrix and partly abundant pyrite are observed at the mineralized parts. Pyrite and graphite accompany the stibnite in the veins. In addition, galena, sphalerite, molybdenite, bismuthinite, gold and silver in lesser amounts are associated with the mineralized veins. Homogenization temperatures measured from the fluid inclusions of the quartz crystals vary 200 to 310° C and signify the deeper parts of an epithermal system. The association of stibnite and molybdenite in the veins points out that the hydrothermal solutions could have gained their metal content from the magmatic emanations. Therefore, it is suggested that the ore-bearing fluids has a genetical relationship with a buried granitoid stock which is represented by the dacite porphyries cropping out near the mineralization. However, graphite, rutile and anatase which are in the content of the vein show an addition to the hydrothermal solutions during their ascension as a leaching from the wall rocks.

PRECIOUS METALS AT SUMADIJA-KOPAONIK-RADAN-NOVA-BRDO ZONE. YUGOSLAVIA

Radule POPOVIC*

That part of the Serbia is characterized by the presence of numerous lead, zinc and at lesser amount copper beds and outcrops accompanying precious metals. Initiating by the Roman times, the mining activities at the area ranges its maximum level at Middle Ages previously and at twentieth century lately, The mentioned metallogenic belt usually is in accordance with the Vardar zone, the predominant tectonic unit and the lead-zinc beds and exposures picture a Avala, Kosmaj, Rudnik. Kotlenik. Tolisnica and Stanca (near Goc), Kopaonik (Sastavci, Kizevak, Plavkovo. Belo Brdo, Crnac. Koporik, Stari Trg and etc), Novo Brdo and Radan Mountains (Lece. Draznja, Tulare, Sijarinska Banja and others) lining up from north to south. Precious metals either go along with lead, zinc and copper and antimony, arsenite and quartz at a lesser degree or in lycvenites and diabase and dacite andesite at a lesser amount in the form of native as well. Mineralization patterns are veins, disseminated bodies and sometimes mesh.

PERIODOTIC XENOLITHS IN ALKALINE BASALTS ATTEKIRDAG REGION (THRACE)

Fahri ESENLİ"

In basaltic volcanics at Tekirdağ region (Thrace), peridotite(xenoliths) such as harzburgite and dunite thought as parts of upper mantle has been found. Petrographically, the basaltic lavas are olivine-basalts showing a primary paragenesis including mainly plagioclase, olivine, augite, magnetite and scarcely hypersthene as well the secondary minerals at important degrees locally. On the other hand, geochemically they correspond to the alkaline basalt, trachybasalt basaltic rock types. Peridotite xenolith-enclosing Hacıköy and Balabanlı and excluding Muratlı basalts also differ in both major and trace element contents. Including olivine (forsterite), enstatite, Cr-spinel and scarcely diopside, the peridotite xenoliths are typically protogranular and partly grading into porphyroclastic in fabric. Magmatic textures are well preserved. Displaying no foliation or lineation, those have coarse-to huge grain sizes. Bandings resembling twinning and deformation lamellas imply the mechanical effect and are characteristic for the olivines and pyroxenes. Whether, the presence of relations depicting partial melting of original mantle, between major elements of the peridotite xenoliths is a fact, the melting point is probably not high. They were unaffected by metasomatism and submit a somewhat consumed composition compared to primitive mantle.

Key words: *Alkaline basalt, xenoliths, peridotite, Thrace-Turkey*

GEOLOGY AND ORIGIN OF SOME CARBONATE-HOSTED HALLOYSITE DEPOSITS IN NW - ANATOLIA (TURKEY)

Ali UYGUN***

ABSTRACT.- Geology and origin of some halloysite deposits in the provinces Çanakkale and Balıkesir (NW-Anatolia-Turkey) are investigated in this study. The deposits of Taban, Ilicaoba, Karasu-Kabakla, Şahbaz and Turplu are mostly located on the contacts of altered Neogene volcanics and Jurassic limestones. Pyrite, manganese, gibbsite and some alunite are the accessory mineralisations. Based on the geological position of the halloysites over the probably karstic topography of the limestones: the absence of halloysite in the volcanics and the correlation of the REE's with the carbonate rocks; the origin of the deposits are suggested to be originated by partial dissolution of the hostrock limestones and formation of halloysite directly from Al and Si-rich acid fluids.

PALAEOGEOGRAPHIC EVOLUTION OF SIVAS TERTIARY BASIN (W-SW SIVAS)

Zeki ATALAY*

ABSTRACT.- Sedimentological studies has been made at the west and the south west of Sivas (Figure 1) and investigated palaeogeographic evolution facies and environmental features of deposit rocks. A1 A2 A3 facies have been recognized at the middle Eocene aged Sahantepe member. A1 facies has deposited at the continental shelf; A2 A3 facies at swamp and coastal sabkha. B1 B2 B3 facies have been recognized at the Oligocene aged Küçüktuzhisar Formation. B facies in lagoon, B1 facies has deposited in barrier island. B2 B3 facies have deposited at continental sabkha and playa lake environment. At the Akören formation C1 C2 C3 C4 C5 C6 C7 facies have been recognized. C1 C2 facies at the meandering river and subenvironments. C3 C4 facies at the playa lake. C5 C6 facies meandering river and C7 facies has deposited at alluvial fan environments. Continental shelf deposits consists of claystone, siltstone and sandstone, has very well (Ta-Tb), (Ta-Tc) and (Ta) structures. These have been deposited by turbidite flows in shallow sea improved. At in the coastal sabkha environment have been deposited gypsum series and they are together with elastics. Meandering river deposits consist of channel fill, point bar and flood plain subfacies fining upward cycles. Playa lake and continental sabkha deposits consist of terrestrial elastics with interlayer gypsum and anhydrite; alluvial fan deposits consist of conglomerates and poorly sorted, pebbly sandstone with muddy matrix and show normal and reverse grading. In the studied area the marine regime has been the dominating agent up to of Eocene- then the marine influence has restrained but continental regime, as a result of this swamp and coastal sabkha environments have improved. During Oligocene period has become more effective. During this period continental sabkha, playa lake, meandering river and alluvial fan environments have been made. At the Sahantepe member palaeocurrent direction is towards from the NE to NW: at the Küçüktuzhisar Formation palaeocurrent directions are towards from the N to S and NW to SE and at the Akören formation palaeocurrent directions are towards from S to N, SW to NE. In Eocene period the formations (Bozbel Formation - Sahantepe Member) was supported by the ophiolites and metamorphic units, situated in the NE of the region and Oligocene period these formations (Küçüktuzhisar and Akören Formations) were supported by the ophiolites and metamorphic units and deep acidic and basic rock as well as volcanics situated in the SW and NW of the region. On the basis of these observations, it can clearly be indicated that the Sivas basin reflects an intraplate basin characteristics following the continent-continent collision.

GEOCHEMICAL CRITERIA FOR THE INVESTIGATION OF FACIES FEATURES OF PONTIAN BASINS IN EASTERN AZERBAIJAN

Saday Azadoğlu, ALİYEV** and Aynur BÜYÜKUTKU*

ABSTRACT.- In this study, distributions and environmental conditions of the mollusc fauna which lived in the evolution of Pontian seas of Azerbaijan were investigated. The research of the environment conditions were based on the determination of conditionuouos geochemical relation which was between the organism and environment. Interpretation of the distribution differences of the Ba, Sr, Mg and Ca in the shell and deposits were indicated the salinity, temperature and paleofacies of the basin at the Ponsien age mentioned above. Detailed investigations indicated that, the reason of the widely appearances of in marine environments depended on the lithofacies properties of deposits, such that in the shallow marine facies deposits contain more barium. In any case the barium content of mollusc species belong to this facies are more than the other ones. Absolute temperatures of fauna and deposits formation environments were determined by Ca/Mg method during the development of the Ponsien seas. These are, in the early Ponsien age the temperature was 21-22° C, in the Middle Ponsien age the temperature was 20.6-21.5 C and in late Ponsien age the temperature was 21.5-22° C and it was determined that the temperatures were constant. In fact, it was proved that there is no balance between the Sr distribution of shell and deposits Sr amount in the deposits is less than the Sr amounts in the shells as a results, it is seen that the main parameter which controls the distribution of the Sr is the salinity rate of the environment. That is why, it is concrete that the lacustrine mollusc Sr amount is poor than the marine mollusc. Hence, Sr is an element which determines the salinity regime of the environment. It can be seen that, in the determination of the environment conditions of biogeochemical methods can also be used together with the other methods.

GEOLOGY OF DOĞANKUZU VE MORTAŞ BAUXITE DEPOSIT AND FEATURES OF SULFUROUS ZONES,
MID-TAURIDES, TURKEY

Hüseyin ÖZTÜRK* and Nurullah HANIÇLI*

Comprising a sulfurous zone made up of marcasite+pyrite+hematite+goethite+boehmite+diasporite+anatase+gypsum minerals at its base, Doğankuzu-Mortaş Bauxite ore bed locates at the discordance zone between Cenomanian and Santonian limestones of Cretaceous. Pisolithic ore bed, including locally calcareous conglomeratic lenticules sits on the sulfurous and lesser one-containing level and where the ore bed is thickening, that conglomeratic zones represent the paleodolines. Toward the upper parts the quality of ore increases and a massive blockage is seen. At uppermost part, a sulfuric zone, that of a few centimeters thick covers the ore and the pyrite-bearing clayey carbonates capping those, grades upward to the Santonian limestones. In these two ore beds, veins, bluish gray and green coloured, including marcasite and pyrite at 15 percent and thickening up to two meters, rich in diasporite, are seen and those are crackfills. These extend into neither underneath nor covering limestones. Petrographical and mineralogical findings show that, especially through internal diagenesis reductive processes were effective and an explanation for the formation of sulfurous zones is that the sulfates in the sea water penetrate into the bauxitic matter and being to the sulfides by the bacteria, synchronously to the deposition of Santonian carbonates.

GEOLOGY, PETROGRAPHY AND PRECIOUS METAL MINERALIZATIONS OF ALTINTEPE AND ÇİLEKTEPE SECTORS OF KARŞIYAKA ORE OCCURRENCES, IZMIR, TURKEY

I. Sönmez SAYILI* and Şener GONCA**

ABSTRACT. - As result of geologic studies on the field and microscopic studies of the samples from Altintepe and Çilektepe areas located southwest of Sancaklı village, Karşıyaka-İzmir, dacitic tuffs and lavas and their silicified types, biotite-hornblend-dacite, andesitic lava, tuff and agglomeras in addition to andesitic dykes are determined and mapped. Investigations indicate two different type of mineralizations, First type is gold and silver mineralizations in quartz veins emplaced in tension fractures of silicified dacitic lavas at Altintepe (Arapdağ) sector. The other kind of mineralizations is related to hydrothermal alterations in dacitic tuffs at Çilektepe (Çerkeskayaş or Pilavtepe) sector. Gold mineralizations are developed as stockworks and disseminations in those kind of rocks because uprising channels are tapped by silica gels. The age of volcanism based on regional geological data is between Late Oligocene and Middle Miocene. Biotite-hornblende-dacites (14.7±0.5 Ma) contain no precious metal mineralizations and are believed to occur after ore mineralizations. According to these findings, the mineralizations should be Middle Miocene in age.

INTRODUCTION

World known gold reserves decreased gradually in recent years. In contrast, gold prices increased sharply between 1980 and 1990. New technologies have been developed for the production of gold and silver from low grade deposits. All these changes increased the exploration efforts for precious metal deposits. Preconditions for the commencement of and an exploration can be summarized as follows: Heat source, faults and fractures on regional and local scale, hydrothermal springs, especially Tertiary volcanics convenient as host rocks. They provide suitable tectonic environments for emplacement of mineralizations. Models developed upon all these conditions brought certain areas of the world and also Turkey as prospect and important areas to search. So, known old gold deposits and occurrences became target areas for new investigations at West Anatolia. Therefore gold bearing quartz veins and its surroundings at Arapdağ-İzmir which is mined at the end of 1900 th's investigated by detail geologic and mineralogic studies and tried to be interpreted for model of formation.

This paper, based on the field studies carried on by MTA General Directorate in 1990, aims presentation of the geological, petrographical and min-

eralogical data collected from surface and drill core samples of gold bearing quartz veins at Altintepe and Çilektepe Sectors close to Altintepe.

Study area is located at southwest of Sancaklı village of Karşıyaka town of İzmir and in İzmir K 18 d3 sheet in 1/25 000 scale. Mineralizations are found around Ilcadere, Kocadere and Eski Sekiköy dere and Altintepe (Arapdağ) and Çilektepe (Çerkestepe or Pilavtepe) 5 to 6 km north of Karşıyaka (Fig. 1).

With the studies carried on volcanics and their relationships in stratigraphic sequence including age data in the study area and its close vicinity are tried to be explained by various authors (Dora, 1964; Borsi et al., 1972; Düzbastılar, 1976; Akyürek and Sosyal, 1978; Kaya and Savaşçın, 1981; Kozan et al., 1982; Ercan et al., 1983; 1984a and 1984b Akdeniz et al., 1986; Ejima et al., 1987; Kissel et al., 1987; Eşder et al., 1991, Turkish-Italian Joint Venture Project, 1991; Ercan et al., 1997; Seyitoğlu et al., 1997; Dönmez et al., 1998; Kaya, 1999). In addition, precious metal mineralizations in Yamanlar volcanics cropping out around Karşıyaka, İzmir have also been the subject of many studies including mineralogical and petrographical investigations, geochemical studies, of

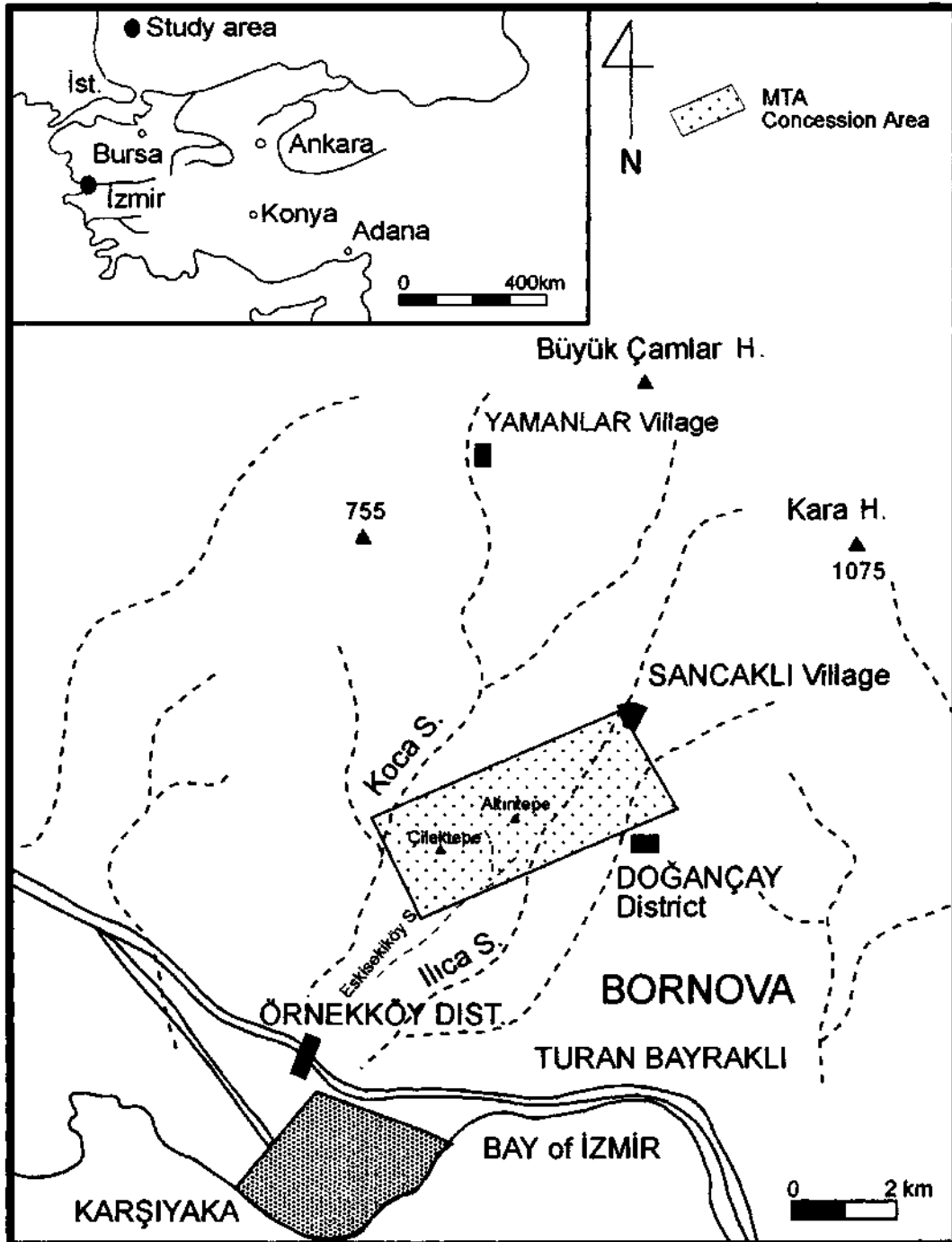


Fig. 1- Location map on the study area.

formation types and for grade/tonnage estimations (Weiss, 1895; Atabek, 1944; Molly, 1956; Vural, 1962; Higgs, 1962; İzdar, 1962; Dora, 1964; Dora, 1970; Çelik and Dayal, 1976; Alpan, 1986; Gonca, 1990; Sayılı et al., 1990 and Turkish-Italian Joint Venture Project; 1991).

REGIONAL GEOLOGY

Study area is regionally located in İzmir-Ankara suture zone (Brinkmann, 1966) lying between Sakarya continent to the north and Menderes massif to the east and southeast.

Volcanic rocks containing mineralizations in the study area divided into three types as dacites, andesites and andesitic dykes by Dora (1964). These volcanics are accepted as "Yamanlar volcanites" by Akdeniz et al. (1986), while the ore bearing volcanites named as "Altintepe volcanites" by Dönmez et al. (1998). Volcanites overlie İzmir flysch (Öngür, 1972) in near vicinity of the study area. İzmir flysch is named for the first time as "Crystalline schists" by Dora (1964) and mapped as phyllite, clay bearing schists and low grade metamorphosed quartzite, greywacke and very low grade metamorphosed arkose alternating with schists and phyllites. The age of crystalline schists is Paleozoic. Lateron, this unit is described as "flysch association" of Upper Cretaceous age according to regional correlations made by Oğuz (1966). This unit is made up of chlorite schists, phyllite, metasandstone, albit-epidote schists, actinolite schists spilite, cherty limestone, meta-conglomerate, bituminous schists and other kind of schists which metamorphosed under greenschist facies. Limestones and serpentinite exotic blocks of Permian, Triassic, Jurassic and Lower Cretaceous age occur in this unit. This unit is called as "Bornova complex" of Maastrichtian-Danien age by Dönmez et al. (1998).

At the east of Bornova, Yamanlar volcanites unconformably overlie Belkahve formation or Dededağ formation which are both described by Akdeniz et al. (1986), Belkahve formation consists of clastic rocks of flysch character in which limestone blocks occur. Clastic sediments contain conglomerate-sandstone, shale-marl, clay bearing lime-

stone alternations and blocks of limestone, radiolarite, greywacke, tuff, spilite and small serpentinites. The age of this unit is Campanian-Paleocene (Akdeniz et al. 1986). At the north of Bornova and near Karaçam region, Yamanlar volcanites horizontally and vertically grade into Vişneli formations. This formation consists of conglomerate, sandstone, claystone and clay bearing limestone and accepted as Middle to Upper Miocene according to its regional counterparts. Vişneli formation is equivalent of "Soma formation" (Akyürek and Sosyal, 1978) at Soma Basin. Near Menemen, upper levels of Soma formation which overlie İzmir flysch contain some sequences of tuff and tuffite of the Yamanlar volcanism (Nebert, 1978). Alluvium and talus of Quaternary age generally unconformably overlie Yamanlar volcanites according to Akdeniz et al. (1986). Dönmez et al. (1998) believe that Altintepe volcanites which are equivalent of Hallaçlar formation at northwest Anatolia, overlie unconformably over Bornova complex. The authors suppose that the age of Altintepe volcanites is Oligocene to Early Miocene. Soma formation (or Group according to Dönmez et al. 1998) overlie Early Miocene aged Aydınlar volcanites with angular unconformity which is overlaid again by Altintepe volcanites. At the northeast of Bornova, partly silicified limnic limestone of Lower Pliocene Yaka formation (Akdeniz et al. 1986) overlie all the rocks mentioned above. This means that silica transporting volcanism is not far from the sedimentation environment.

GEOLOGY AND PETROGRAPHY

Geological map (1/5000) of the study area is prepared by using 1/5000 and 1/2000 topographic maps. The adits of Nr.2, Nr.4 and Nr.6 (G-2, G-4 and G-6) and all others are geologically mapped at 1/500 and 1/200 scales. Thin and polis-hed sections of rock samples collected from surface and adits are investigated.

The stratigraphically lowest unit of the region is a flysch formation called as "İzmir flysch" outcrops outside of our mapping area. Dacitic tuffs and silica gel (hydrothermal breccia) contemporaneous with tuffs overlie the flysch unit. Dacitic lava and their sili-

cified, sericitized, chloritized, actinolitized, turmalinized and brecciated equivalents called as silicified dacitic lava overlies all units. These volcanism becoming more basic created andesitic tuffs and agglomerates and young andesitic dykes with intermediate character (Fig. 2 and 3). This sequence is in very concordance with the sequence given by Dora (1964). Age determinations carried on samples by using whole rock K/Ar method during Turkish-Italian joint venture project revealed that biotite-hornblende dacites and andesites are 14.7 ± 0.5 Ma and young andesitic dykes has the age of 18.9 ± 0.4 Ma. According to the explanations of Italian experts, the reason why the dykes are older than dacites and andesites is related with "argon absorption". Thus, the age of volcanism can be given as Middle Miocene.

Rocks of flysch unit are observed in the channel samples collected from F.VII vein exposed at İlicadere. Rock fragments of bituminous materials bearing quartz-sericite-chlorite schists and bituminous schists are found during microscopic studies. These kind of rock fragments hard to find out at the field because of their small sizes. However, the rock pieces of flysch unit can easily be seen at drill cores.

Dacitic tuff. - The unit (crystalline tuff of Dora, 1964), crops out at Çilektepe sector that takes place at the western part of study area and Eski Sekiköy dere. The color of the unit is dirty white, beige and light yellow because of hydrothermal alterations, however fresh samples are light grey and grey in color. Dacitic tuffs generally comprise fine grained and angular primary quartz crystals, silicified rock fragments, hydrothermal quartz particles, sandstone fragments and phyllosilicate phenocrystals effected from tectonism. The groundmass of rock is composed by very fine grained sericite, biotite, chlorite and clay minerals. Mica minerals are replaced by opaque minerals and the groundmass became darker at the portions where mineralization is affected the rock. In additions, brecciated parts are also observed in tuffs. Fine and medium grained quartz phenocrystals of primary origin and silicified volcanic rock fragments, hydrothermal and recrystal-

lized quartz grains take place in a micro to cryptocrystalline quartz and opaque enriched groundmass.

Dacitic lava and silicified dacitic lava. - These rocks can be observed at the upper levels of Altintepe and Çilektepe sectors of the study area and are light grey and light purple colored. Silica saturated, viscous lavas serve as tapping domes as short and thick lava flows (Dora, 1964 and Gonca, 1990). Hematite, limonite and kaolinized feldspars are generally observed at the cracks of rocks. The rock has an appearance of mixed colors consisting of grey, brown, red, dirty white and purple. Coarse grained quartz, oligoclase-andesine type plagioclase in addition to chloritized, carbonatized biotite and hornblende which are also replaced by opaque minerals. Therefore, the porphyric texture of the rock is easily recognizable. Tectonism creates thin and discontinuous cracks and fractures in phenocrystals and groundmass which are filled by opaque minerals.

As a result of hydrothermal activity, advanced silicification, carbonatization, sericitization, chloritization, actinolitization, prehnitization and turmalinization occurred at Altintepe where the center of dacitic volcanism is. Because of these features of lavas and pervasive silicification observed at macroscopic scale and on hand specimens, the parts of rock which reveal such kind of characteristics are called as silicified dacitic lava. This kind of rock is in grey-green and bluish colors and glassy breakdown feature. In addition to minerals described at other lavas determined by thin section investigations, these rocks comprise the sections of hydrothermal quartz enrichments and very small turmaline needles and suns (Dora, 1964).

Biotite-Hornblende dacite. - This unit crops out to the northeastern and southeastern parts of investigation area and named as biotite-hornblende dacite both by modal analyses executed by Dora (1964) and our microscopic investigations. The final period of dacitic volcanism became more basic at this stage. Fresh parts are generally in greenish brown color. Milky brown colors are developed at

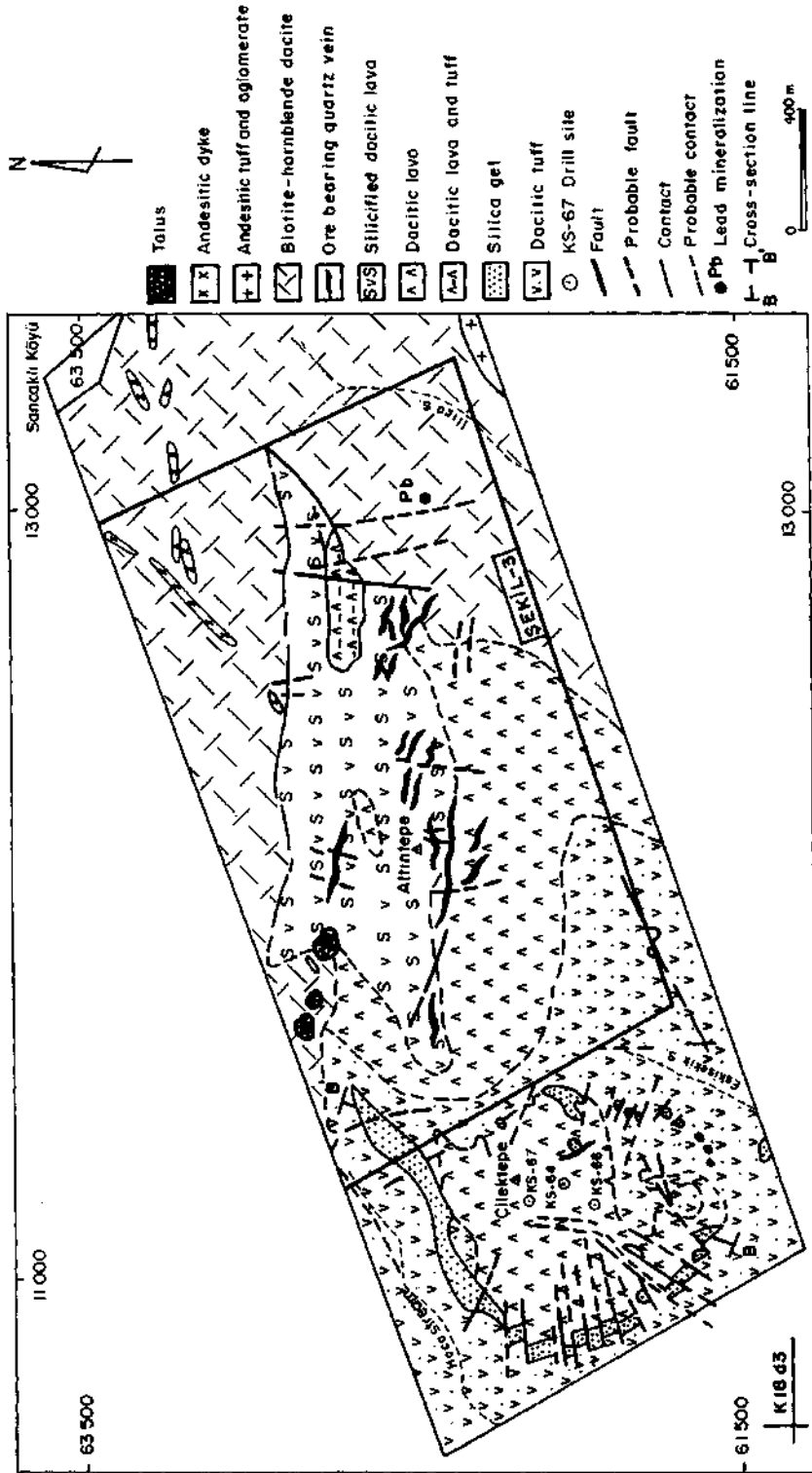


Fig. 2- Geological map and mineralizations of Altıntepe and Çilektepe sectors, Karşıyaka-Izmir (Modified from Gonca, 1990). Ore bearing quartz veins are exaggerated.

the parts where weathering dominantly occurred and gave a soft character to the rock. Porphyric texture can easily be seen. Phenocrystals of quartz, feldspar, biotite and amphibole scattered in glassy and microlitic groundmass at fresh rocks. Plagioclases are generally in andesine composition and exhibit zoned textures. Carbonate fillings are seen at the cracks of rocks. Amphiboles are replaced by quartz, carbonate and opaque minerals, biotites enriched in opaques and chloritized and feldspars are argillized at the altered rocks. Groundmass is kaolinized, chloritized, sericitized and silicified.

Andesitic tuff and agglomerate.- This type of rocks are observed at the eastern part of the study area. Tuffs are banded agglomerates. Lavas generally have vesiculated or scoriaceous forms. Blocky andesites contain sometimes schist and dacite fragments. Andesitic lavas exhibit clearly recognizable flow textures. Coarse and medium grained plagioclase and medium to fine grained pyroxene, biotite and amphibole phenocrystals are dispersed in both microlitic and glassy groundmass. Labradorite and andesine type of plagioclases show zoned textures. Pyroxenes are also observed in the groundmass and replaced by epidotes and amphiboles which are replaced again by epidotes and opaque minerals.

Young andesitic dykes.- These dykes frequently occur at the northeast of the study area. The thickest one is 5 meter and found between the northwest of Sancaklı village and Altintepe. Phenocrystals consisting of coarse grained plagioclases, abundant medium grained pyroxenes and less amount of biotites occur in a groundmass of plagioclases, pyroxenes, biotites and chlorites in addition to opaque minerals. Plagioclases are andesine in composition and are kaolinized and sericitized. Pyroxenes are uralitized and chloritized.

Five fresh samples were taken and analysed by Eşder 1990 (in Gonca 1990), another five samples were collected and analysed during Turkish-Italian Joint Venture project and seven samples were taken and analysed by Dönmez et al., 1998.

Petrological studies carried on all these 17 samples revealed that the rocks are dacites and andesites with high-K calcalkaline character.

E-W trending veins at Altintepe are dipping to north or south with an angle greater than 50°. All the veins occur along the tension fractures, which served channels and open spaces for hydrothermal solutions. These fractures are intersected by young faults with N-S direction. Because of young tectonics, tension fractures are dislocated and therefore fluids ascending along these new open spaces created later on impermeable zones. Solutions circulating beneath these tapped zones caused explosion due to increase at temperature and thus the veins gained brecciated structures.

MINERALIZATION AND MINERALOGICAL INVESTIGATIONS

Lead, antimony and gold-silver mineralizations occur in both sectors of the study area.

Lead mineralization is found at a probable fault with N-S direction near the fountain of Sancaklı village, east of Ilicadere (Fig. 2). Mineralization occurs in biotite-hornblende-dacite and has a strike of N 45-70 E and dip with 50-60° to northwest. Veinlets have 25 m lengths and 3-8 cm thicknesses. Galena, pyrite, anglesite and cerussite are ore minerals while quartz and baryte gangue. Some silver is detected in the samples taken from the veinlets (Dora, 1964 and Gonca, 1990).

Antimony mineralizations take place at around Çilektepe. Antimony veins are 5cm to 2m in thicknesses and arrive up to 50 m length and strike with changing directions, namely NE-SW and NW-SE. Ore minerals such as stibnite, pyrite, cinnabar and senarmontite occur together with gangue minerals of quartz and baryte. The mineralizations are believed to occur related with young tectonism.

Two different types of gold and silver bearing mineralizations are found in the study area. The general features of these types can be summarized as follows:

First type is represented by gold and silver mineralizations and occur in quartz veins which

take place at tension fractures in the silicified dacitic lava (Fig. 2, 3 and 4). Three dimensional studies based on surface and underground geological maps. Drill cores showed that the wall rock alteration of quartz veins are developed as carbonatizations, sericitization, chloritization, actinolitization, prehnitization and tourmalinization in addition to advanced silicification.

Second type is represented by lode type gold and silver mineralizations found in the hydrothermally altered dacitic tuffs at Ilıcadere and Çilektepe. These mineralizations are not well concentrated and therefore can only be regarded as occurrences.

Detailed descriptions for two type of mineralizations are as follows:

Mineralizations at Altıntepe sector

Eleven quartz veins are determined in dacitic lavas and silicified dacitic lavas at Altıntepe. Most of them strike E-W and only a few ones NW-SE (Fig. 2 and 3).

Vein F. I. - The vein occur in silicified, chloritized and tourmalinized dacitic lava at southeast of Altıntepe. It strikes N 80 W and dips with 65° to NE and has a length of 20 m and thicknesses varying between 4 cm and 10 m. Microscopic studies revealed that pyrite, limonite and native gold grains are ore minerals in milky quartz. According to the analyses carried on three samples indicate low grade precious metal contents with less than 0.2 ppm Au and 2 ppm Ag.

Vein F. II. - It trends in E-W direction just below Altıntepe and takes place as two lenses. Silicification, chloritization and argillization represented by quartz, sericite, epidote, chlorite and kaolinite form the alteration pattern in dacitic lavas close to the vein. First lens has a strike of N 85° E with a dip of 50-72° to NW. The thicknesses of this lens change between 2 cm and 3 m with a length of 350 m. Milky quartz, tooth like quartz, limonite, baryte and silicified dacitic lava fragments occur in the lens. An adit (G-2) is driven at the eastern end

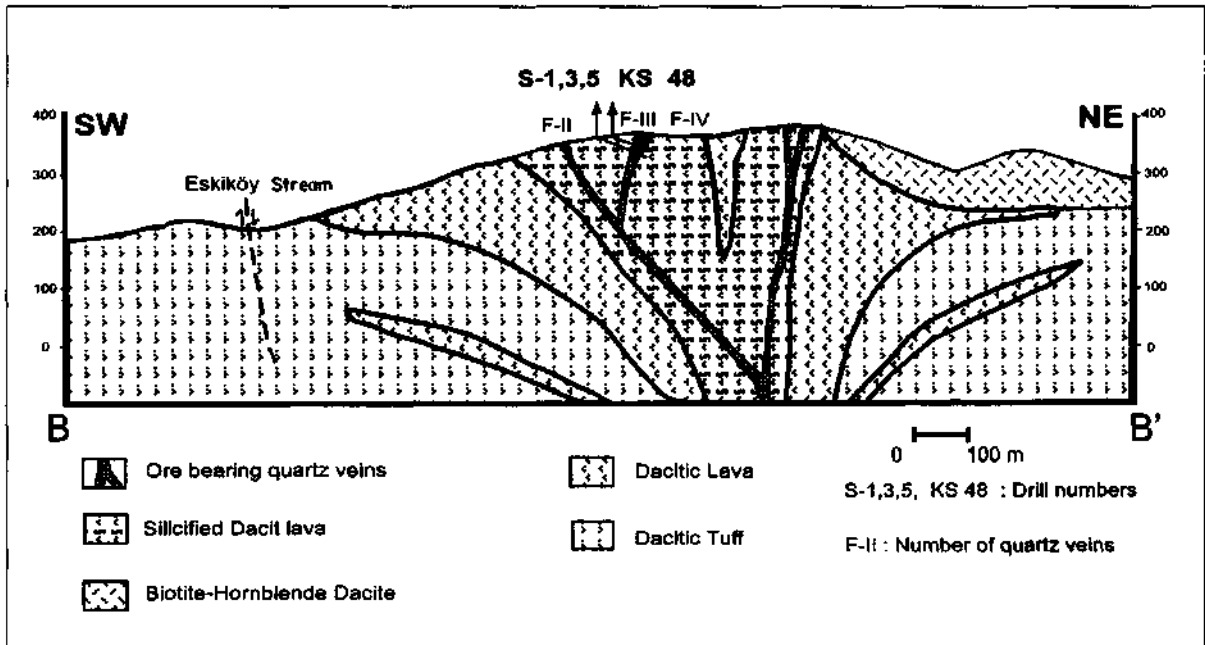


Fig. 4- A cross section from ore bearing quartz veins of Altıntepe.

of it. Due to ore microscopic studies, anglesite, galena, pyrite, chalcocite, covellite goethite, native gold, fahlore, smitsonite and baryte are determined Channel samples taken from the lens and the samples collected from G-2 and G-6 adits and drill cores aimed to intersect this lens indicate that the lens has an average thickness of 1 meter and grades of 4.65 g/t for gold and 60 g/t for silver. Second lens (N 63-84 E, 40-74 NW) takes place at the west to southwest of Altıntepe. It lies in silicified dacitic lava with a length of 150 m and thickness varying between 50-70 cm. Channel samples taken from the lens and samples from drill cores show an average thickness of 70 cm and average grades of 5.4 g/t Au and 70 g/t Ag. Gold and silver values continue to the outside of the vein.

Vein F. III.- The vein strikes N 77-88 E and dips to SE with 60-80° and occurs in silicified dacitic lava at the east to northeast of Altıntepe with a length of 80 m and thicknesses between 5-45 cm (Fig. 4). Mineralization is characterized by milky quartz, toothlike quartz, baryte as ganques and native gold, sphalerite, galena, pyrite, chalcopyrite and limonite. The contact between host rock and veins is not sharp. The vein reaches an average thickness of 140 cm along the drills to the depth (58m). Numerous analyses were carried on the samples taken from G-4 adit, drill cores and the vein as channel samples. The results gave 10.5 g/t Au and 90 g/t Ag grades for an average thickness of 78 cm.

Vein F. IV.- The vein is located ENE of Altıntepe and has a length of 80 m with thicknesses between 20-30 cm. It occurs in silicified dacitic lava and has a strike of N 78-88 E and dips to SE with 72-75° (Fig. 4). The wallrock of the vein is silicified, sericitized and chloritized. Milky quartz, abundant pyrite, limonite, galena, sphalerite, chalcopyrite and a few grains of native gold are observed during microscopic studies. Analyses based on the samples collected from G-4 and G-8 adits, drill cores and as channel samples from the vein revealed a 24 cm average thickness and 13.8 g/t Au and 160 g/t Ag average grades..

Vein F. V.- The vein with a length of 80 m and thicknesses varying between 3-10 cm lies at the east to northeast of Altıntepe and occur in silicified dacitic lavas. It strikes N 88 E and dips with 82° to SE. The vein contains milky quartz, limonite and brecciated fragments of dacitic lava. According to the data from an old drill, the vein reaches a thickness of 67 cm at 64 meter depth. A channel sample from the vein indicate the grades of 14.3 g/t Au and 70 g/t Ag.

Vein F. VI.- This is not an individual vein but a zone of veins lying at E-W direction and dipping to N with 82-87° at the north of Altıntepe. The length of the vein zone is 150 m and the thicknesses vary between 160 and 530 cm. They occur in silicified dacitic lava which is characterized by alterations of sericitization, chloritization, actinolitization, epidotization and pyritization. Ilmenomagnetite and rutile are observed in the host rock, while the veins are rich in pyrite, hematite, limonite and a few grains of native gold with 10-20 micron sizes. Sulphide mineralizations are abundant in some parts of veins. Mineralogical investigations revealed that silicification, actinolitization, chloritization and sericitization together with pyrite, ilmenomagnetite, rutile-anatase and galena crystals occur at these parts. Twelve new trenches are dugged out and G-10 and G-11 adits were driven at this zone. The grades of precious metals are so scarce that 2 g/t Au and up to 10 g/t Ag could be detected at only one trench. The analyses of the samples taken from drill cores indicated even less amount of gold and silver.

Vein F. VII.- The vein is found in a tributary of Ilicadere east of Altıntepe. It lies in silicified dacitic lava. The vein strikes N 60-85 W and dips to SW with 50-82° and is intersected by the vein F.VIII. The length of the vein is around 200 m with thicknesses of 20 to 50 cm. Bituminous schist fragments are also found at this part of the field. These fragments are believed to represent Belkahve formation. Gold grains with 5-30 micron sizes are observed together with pyrite in the schists. The vein consists mainly of quartz but small and thin ankerite veinlets are also found in it. One of the four channel samples taken from the vein gave 19 g/t Au

and 100 g/t Ag in addition to 2.4 % Pb grades.

Vein F. VIII.- The vein (N 37-87 W, 50-73 SW) is located at the tributary of Ilicadere like vein F VII at the east of Altintepe and occur in dacitic and silicified dacitic lava. The length of the vein is 270 m and thicknesses range between 10-50 cm. Grey colored quartz, baryte are gangue minerals and sphalerite, galena, pyrite, hematite and limonite are that of ores. A few gold grains up to 20 micron are also determined. The vein is followed until the depth of 14 meter. Grades of 1.5 g/t Au and 30 g/t Ag are estimated from channel samples of the veins.

Vein F. IX and F. X.- These veins are located to the north of vein F.VIII and stockwork type mineralizations occur in silicified dacitic lava and have E-W, 82 SE strike and dip. Their length are around 40 m and thicknesses vary between 30-40 cm. Quartzs with various sizes and forms seem to represent different generations. Pyrite, sphalerite, galena, covellite, chalcocite, neodigenite, fahlore (tetraedrite), limonite, bournonite, boulangerite, marcasite, native gold (10-20 microns), chalcopyrite, anatase-rutile and hematite in addition to rare amount of ankerite and gypsum are determined. Analyses made on the samples taken from the vein F. IX as channel sample method revealed that an average thickness of vein is estimated as 45 cm and the vein has 12.5 g/t Au and 172 g/t Ag grades. However, surface channel and drill core samples have only trace amount of gold and silver.

Vein F.XI.- This vein (N 56 E, 80 SE) is again in silicified dacitic lava to the north of Vein F.VII. It is rather short and thin one with 5 m length and 25 cm thickness. Ore minerals consist of pyrite, limonite and a few native gold grains between 5 and 20 microns dispersed in a matrix of milky quartz in the vein. A channel sample taken from the vein showed 3.1 g/t Au and 3 g/t Ag.

Although alterations in veins and host rocks close to veins at Altintepe are mentioned, alteration pattern of the whole area will be presented in another publication (Gevrek and Sayılı, in preparation). Therefore, more details will not be given here. Comb structures and crustifications are the main

features that are observed on the veins.

Mineral paragenesis of ore bearing quartz veins

Before starting detailed description of the ore minerals, gangue minerals will be shortly summarized. Main gangue minerals are toothlike quartzs and milky quartzs (Dora, 1964). Initially baryte crystals are replaced by siliceous solutions sometimes leaving some baryte relicts in them are called as toothlike quartzs. Another type of generation occurred from post silica generation which formed dull and pinkish white, white milky quartzs. Limonites accompany to milky quartzs. Gold is found in both type of quartzs, however toothlike ones richer than milky quartzs. Chalcedony occur at the surface while quartz characterize deeper zones at Altintepe. Young and old baryte laths also accompany to the quartzs as gangue minerals. Gold free calcite and siderite minerals are reported by Dora (1964) at the outside of the study area.

Ore microscopic studies on the samples of the study area are in very good concordance with the studies of Dora (1964, 1970) and of Italian mineralogists performed during Turkish-Italian Joint Venture project. The findings of ore microscopic studies and important features of ores from older to younger are mentioned below respectively:

Rutile-Anatase.- They are observed in both host rocks and as transportations to the veins.

Pyrite and Arsenopyrite.- The dominant sulphide mineral is pyrite and some arsenopyrites which are replaced by other sulphide minerals. Thus, they are accepted as the oldest ore minerals. They are especially grown with baryte needles and laths. Electrum grains (around 10 micron sizes) are found at the cracks of pyrites and arsenopyrites. Pyrites are often limonitized. Gel like textured pyrites are contemporaneous with or younger than other sulphide minerals.

Marcasite.- Radial and fibrous marcasites form aggregates. They are subhedral and sometimes very abundant. They sometimes replace pyrites.

Hematite.- As stainings and small and thin needles and laths occur in the cracks of quartzs.

They are also observed as inclusions in pyrites and are grown together with them.

Sphalerite. - Anhedral sphalerites are found as irregular grains up to 2 cm in quartz matrix and are the second abundant sulphide minerals following pyrites. They are associated with galena and chalcopyrites and show cataclastic texture in some grains. Sphalerites are replaced by chalcopyrite, fahlore and galena and by secondary minerals like chalcocite, covelline and neodigenite as well. Gold can be observed at their cracks.

Galena. - Anhedrel galena crystals occur as generally small but sometimes up to 1 cm sized grains at the open spaces or cracks of quartzs together with sphalerite and chalcopyrite. Some grains are dominantly replaced by anglesite. It is the most important mineral for the deposition of electrum.

Chalcopyrite. - Rather small and anhedral grain of chalcopyrites are mainly enveloped by sphalerite, fahlore and galena and fill the cracks of quartzs or as inclusions in them. They are replaced by fahlore especially at rims or cleavages. Chalcopyrite and their oxidation products contain electrum.

Fahlore. - Trace amount of fahlore minerals are found as very small grains in anglesites and are sometimes replaced by covelline and antimony ochers. Chalcopyrites are replaced by fahlore beginning from their rims.

Bournonite - Boulangerite - Zinkenite. - Bournonites and boulangerites are formed as a result of replacement along the rims and cracks of galena. Additionally, these minerals are also found in trace amounts as reaction minerals between galena and fahlore. Very small laths of boulangerites and zinkenites occur in and at the cracks of quartzs.

Electrum. - Electrums occur mainly as isolated grains in quartz crystals or enveloped by sphalerite, galena, chalcopyrite and pyrite or together with limonite and covelline masses and crusts. Grain sizes vary between 5 and 60 microns. Dora (1964) is the first geologist Who reported their silver con-

tents. Later on, by the studies of italians, two samples were analysed by electron microprobe method which gave the results of up to 23.86% Ag content of the old grains. Thus, they can be called as electrum.

Secondary ore minerals. - The most abundant secondary ore mineral is limonit which is formed in two different types. First type can be described as concentric textured limonite fillings in fractures and open spaces and the other types occur as pyrite pseudomorphs. Limonites are sometimes as geotihite in forms and are observed at the cracks and open spaces and also in the outer zones of anglesites. Other secondary minerals are chalcocite, covelline, neodigenite and smitsonite.

Mineralizations at Çilektepe sector

The geological map and cross-section of Çilektepe sector demonstrate (Fig. 2 and 5) that the stratigraphically lower parts are represented by dacitic tuffs and upper parts by dacitic lavas, while tuffs are pervasively silicified. They contain silica gels (hydrothermal breccia), which consist of amorphous and silica oversaturated hydrothermal solutions. Because of tectonic activities, along the main tectonic line represented by N 18 E strike, silica bands are formed from siliceous hydrothermal solutions which were rised along the openings in some levels of tuffs and along the contacts between tuffs and lavas. The thicknesses of silica bands including tuffs arrive up to 20 meter. Flow textures can be recognized in the field and contain metamorphic and silicified volcanic rock fragments. Because of these angular fragments in silica gels, they are also called as hydrothermal breccia.

Argillization, sericitization, chloritization and opaque mineral developments are the alteration types accompanying to silicification at Çilektepe. According to the geological features and antimony adits driven in silicified tuffs, an epithermal type of mineralization can be postulated for this sector (see Henley 1985, 1990). Therefore seven holes were drilled at Çilektepe. Five of them intersected silica gels besides dacitic lavas and dacitic tuffs as expected (Fig. 5). 1 to 23 meter mineralized zones

are cut beneath and sometimes over the silica gel levels which contain gold varying between 40 ppb and 4.37 g/t in every drill holes. Thus, the levels of silica gels should serve as taps for the uprising of weakly ore bearing hydrothermal solutions. At the levels where gold detected, the contents of Cu increase to 1000 ppm, Pb to 700 ppm, Sb to between 70 ppm and 1 % and Ag generally around a few ppm but sometimes up to 200 ppm could not be arranged to any systematic. It has been determined that gold occur in pyrite rich stockworks and thin veinlets.

Antimony mineralizations observed at Çilektepe contain pyrite, cinnabar and senarmontite besides stibnite and quartz and baryte as gangue minerals. Analyses of sample of quartz bearing stibnite veins indicated the contents of 81.29% Si, 7.3% Sb, 2.0% Ba, 0.68% Pb and 617.3 ppm As (Turkish-Italian Joint Venture Project, 1991). Upon all these data, epithermal type of formation model could be

advocated basing on host rock and structures in it, alteration pattern, fluid inclusion studies (details will be published at Sayılı, in preparation).

Mineralization stages

All the data from the field observations and mineralogical investigations of gold bearing quartz veins at Altıntepe demonstrate three mineralization stages. The first stage is characterized by the oldest sulphide minerals of pyrite and arsenopyrite. Hydrothermal solutions at this stage caused silicification, actinolitization, chloritization, argillization and turmalinization alterations at Altıntepe which are typically observed at Vein F.VI. This stage is sterile for gold and silver. Second stage is represented by gold, silver and sulphide mineral associations. Pyrite, sphalerite, galena, chalcopyrite, fahlore, bournonite, boulangerite, zinkenite, marcasite, hematite and according to Dora (1964) proustite, pyrargyrite, polybasite, freibergite ve pet-

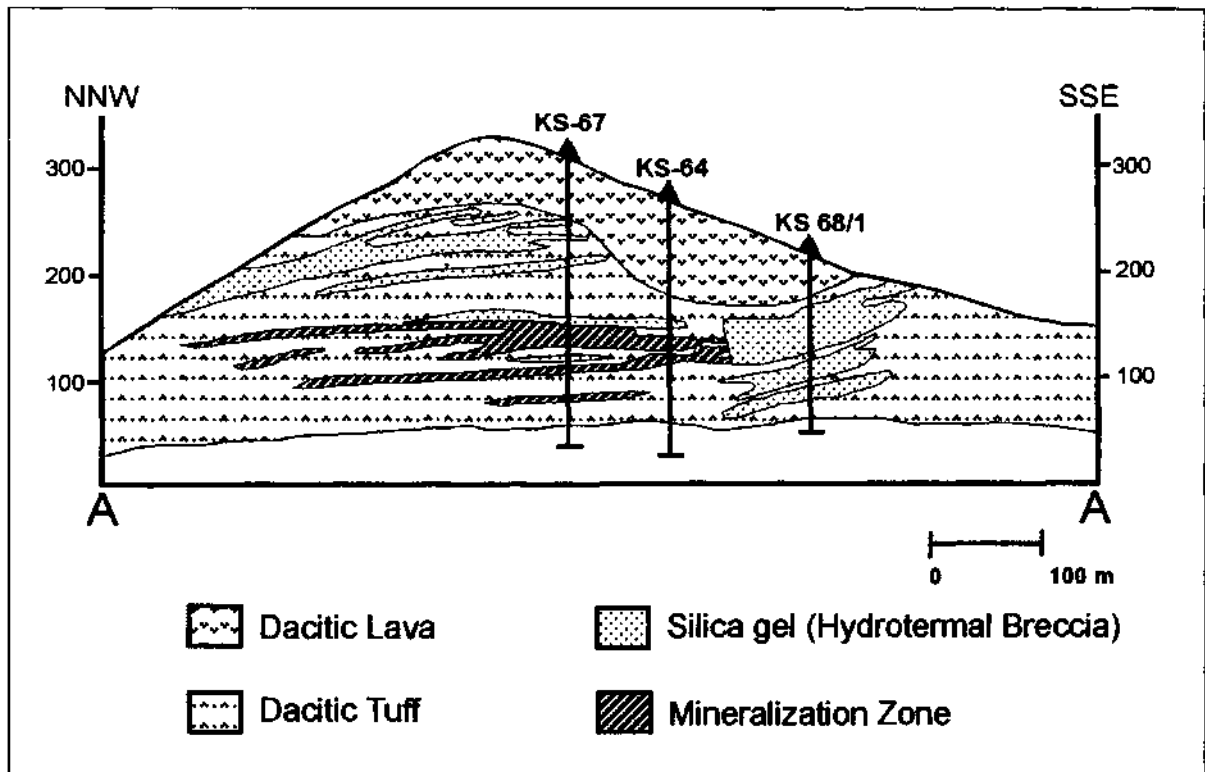


Fig. 5- A cross section showing the mineralizations of Çilektepe sector.

zite(?) as silver bearing minerals occurred at this stage. Dora (1964) pointed out that jamesonite, native silver minerals, sylvanite and electrum minerals are detected. Secondary ore minerals of this stage are limonite, goethite, chalcocite, covellite, anglesite, neodigenite and smithsonite. Gangue mineral are represented by toothlike and milky quartz, baryte, gypsum in addition to some chlorite, actinolite, epidote, sericite and chalcedony. The ore minerals of third stage are galena, pyrite and stibnite (see Mineralization at Çilektepe sector section). In addition to stibnite, cinnabar is found both by us and Dora (1964). Analyses show that gold occurrences as stockwork type and in veinlets developed especially below the silica gel (hydrothermal breccia) levels at Çilektepe have low gold contents. Dora (1964) believe that this stage contains also silver. Anglesite, cerussite and young quartz and barytes from the secondary ore and gangue minerals.

INTERPRETATION AND DISCUSSION

Numerous investigations carried on both host rocks and mineralizations at the study area exhibit different views. At this point, views about host rocks, tectonic lines in which mineralizations emplaced and mineralizations will be discussed and interpreted.

The host rocks around mineralizations are tuffs and lavas which are the products of andesitic volcanism (Dora, 1964, 1970; Gonca, 1990; Sayılı et al., 1990 and Turkish-Italian Joint Venture project, 1991). On the other hand, Dönmez et al: 1998 named the unit of dacitic tuff as Yamanlar tuff. It is believed that Dönmez et al. 1998 could not determine other volcanic products because of detailed lack of knowledge about the mineralized area. Petrological studies carried on 17 rock samples taken from the study area revealed that these rocks are dacite, andesite with high-K calcalkaline character. The age of volcanism is determined by K/Ar method as 14.7 ± 0.5 Ma for biotite-hornblende dacite and andesite and as 18.9 ± 0.4 Ma for young andesitic dykes performed during Turkish-Italian, Joint Venture Project (1991).

At first, some findings should be mentioned in order to make interpretations about the relationships between tectonism and mineralization. These are as follows:

Dora (1964) suggests that the region is affected by Laramian orogenesis. Doming at E-W directions occurred and the center of volcanism used these domes as uprising channels. He also defended the view that giant faults with 1000 to 1500 meter offsets on the characteristic graben zones of West Anatolia caused fractures arriving below to the Moho discontinuity at beginning of Miocene. Magma rising from these fractures which arrive to Sima and spreading into large areas formed recent volcanic rocks. Generally, intermediate to asidic character of volcanic rocks is related with chemical composition of the crustal material which is assimilated during the rising (Dora, 1964; Eşder, 1990 in Gonca 1990).

An interpretation about the age determination of the region indicated that Vişneli formation represented by claystone, clay bearing limestone and tuffs and tuffites alternating with the formers at the upper parts of the sequence overlies Yamanlar volcanites. Due to this stratigraphic relationship, it has been suggested that the region began uprising before the sediments of Vişneli formation of Middle to Upper Miocene age were deposited (Gonca, 1990).

Seyitoğlu et al., (1997, Fig.2) summarise the different views regarding the relationship between tectonic style and volcanic character in western Anatolia. Some studies suggest a close relationship between calcalkaline volcanism and compressional tectonic regime during Oligocene and Early Miocene. However, the other studies proposed that Oligocene-Early Miocene calcalkaline volcanism occurred under extensional regime which continues until Pleistocene.

Dönmez et al., (1998) mapped northern part of İzmir. They divided the main tectonic elements as faults, thrusts and discordances. Faults follow three main lines on NE-SW directions which are observed as big and small faults. The same trends are deter-

mined in the mineralization area around Doğançay-Sancaklı villages.

Kaya (1999) examined the important phases of compressional-extensional tectonics and related trends of faults and fractures during Late Cretaceous to Late Pleistocene in western Turkey. He pointed out that NE-SW trending faults progressively developed from west to east and high-K calcalkaline volcanic centers occurred on the same tectonic lines between latest Oligocene to Early Miocene. During Early Miocene-Middle Miocene period, an E-W trending regional doming is proposed (Kaya, 1999).

Under the light of findings and data given in the Geology and Petrography section, it can be accepted that high-K calcalkaline volcanism in the study area was active at the beginning of latest Oligocene and E-W doming occurred during Early to Middle Miocene.

Views about mineralizations can be summarized as follows: Molly (1956) believed that gold mineralizations at Arapdağ are not directly related with dacites and andesites, but rather with hydrothermal (mesothermal) mineralizations originated from an acidic magma chamber. İzdar (1962) suggested that ore formation is related with quartz rich juvenile hydrothermal solutions which ascended into fault zones. These zones occurred by tectonic activity which is affected dacite, dacite breccia and tuff complex. Dora (1964, 1970) postulated that gold bearing quartz veins at Arapdağ were hydrothermal solutions of gold rich meso- to epithermal character which ascended along the E-W tension fractures and occurred between dacitic and andesitic volcanism. He pointed also out the formation temperatures for quartz veins as 100-200°C. Gonca (1990) suggested that quartz veins filled E-W trending fractures in dacitic lavas at Altintepe and silicified and thus altered the lavas. The mineralizations occurred in these veins. On the other hand, silica gels tapped dacitic tuffs at Çilektepe. Therefore, tapped tuffs caused gold enrichments. Similar findings with Gonca (1990) are expressed at the report written by Turkish-Italian Joint Venture Project (1991). They found the homo-

geneization temperatures of the quartz veins between 130-290°C and low salinities with maximum 1% NaCl equivalent. Homogenization temperatures are in good concordance with Ayan (1990) (in Gonca 1990).

According to the investigations carried on the study area, gold and silver bearing quartz veins associated with sulphide minerals and barytes trend approximately at E-W direction and occur in silicified dacitic lavas at Altintepe. Trace amount of gold and silver contents (Gonca, 1990 vol.2 about the results of analyses) at dacitic lavas highly support that the formation of lavas and quartz veins are contemporaneous. Under these conditions, the age estimations made from Vişneli formation and age determination from the sample of biotite-hornblende dacite as 14.7 ± 0.5 Ma during Turkish-Italian project (1991.) suggests an age of Middle Miocene for the mineralizations.

Because of silica gels (hydrothermal breccia) which crop out at Çilektepe, it is believed that dacitic tuffs and/or dacitic lava gradations are tapped by siliceous solutions. Stibnite and cinnabar mineralizations are recognizable at the surface and thin mineralized zones with low grade gold contents are determined by drills. All these data suggest epithermal type of mineralizations at this sector (Sayılı, in preparation). Mineralizations at this sector contain stibnite and cinnabar type of ore minerals and exhibit some mineralogical differences. Additionally, mineralizations occur beneath the silica gel levels and the trends of faults at Çilektepe sector suggest somewhat different type of mineralizations than Altintepe and they are probably formed at the end of Middle Miocene.

CONCLUSIONS

Acidic volcanic rocks including dacitic tuff and lava, silicified dacitic lava, biotite-hornblende-dacite and andesitic lava, tuff and agglomerate and also andesitic dykes are determined at the study area. During the formation of dacitic tuffs, silica gels occurred arriving up to 23 meter thicknesses which are gained breccia appearances caused by hydrothermal activities.

As result of detailed petrographic, mineralogic and ore microscopic studies, two different types of mineralizations have been determined. First type is as Dora (1964, 1970) mentioned gold and silver mineralizations associated with quartz veins which took place in tension fractures in the silicified dacitic lava at Altıntepe (Arapdağ) sector. Eleven quartz veins not more than 3 meter thicknesses and associations with limonites are determined in the field and their continuations are detected by drill holes. Second type is described for the first time with this study and represented by gold mineralizations of epithermal type (?) related to hydrothermal alterations developed in dacitic tuffs of İlicadere and Çilektepe (Çerkeskayaşı or Pilavtepe). Mineralizations occurred as disseminations and in veinlets representing a stockwork type of formation.

It was reported that Late Oligocene and Middle Miocene high-K calcalkaline volcanism is developed at Western Anatolia. Based on this finding and other data collected, mineralizations should occur in and to the end of Middle Miocene.

ACKNOWLEDGEMENT

The authors are deeply indebted to Nevzat Karabalık, Necmi Yüce, Fahrettin Kayhan, Hasan Durgun, Erden Ağalar, Hüseyin Türkbilek, Tuncay Andıç, Faruk Gültaşlı, Şerif Akyurt and Kemal Kral as staff of MTA General Directorate for their services during the field studies. Special thanks are due Dr. Ahmet Çağatay for ore microscopic investigations and Ahmet Türkecan for the views about volcanism. We are grateful to Nevzat Karabalık and Necmi Yüce for their contributions about the mineralizations.

Manuscript received May 5. 1999

REFERENCES

- Akdeniz, N., Konak, N., Öztürk, Z. and Çakır, M.H., 1986. İzmir-Manisa dolayının jeolojisi: MTA Rep. 7929 (unpublished) Ankara.
- Akyürek, B. and Sosyal, Y., 1978, Kırkağaç-Soma (Manisa)-Savaştepe, Korucu. Ayvalık (Balıkesir)-Bergama (İzmir) civarının jeolojisi: MTA Rep. 6432 (unpublished) Ankara.
- Alpan, T., 1986, İzmir-Karşıyaka-Arapdağ altın prospeksiyon raporu: Bölge Arşiv No: A/21.
- Atabek, S., 1944, İzmir vilayeti dahilinde tetkik edilmiş bazı linyit, antimuan ve bakır madenleri hakkında rapor; MTA Rep. 5813 (unpublished) Ankara.
- Borsi, S., Ferrara, C., Innocenti, F. and Mazzuoli, R., 1972, Geochronology and petrology of recent volcanics of Eastern Aegean Sea: Bull. Vole., 36, 473-496.
- Brinkman, R., 1966, Geotektonische Gliederung von Westanatolien. Neus. Jahrb. Geol. Palaontol. Monatsh., v.10, 603-618.
- Çelik, O. and Dayal, A., 1976, İzmir-Karşıyaka-Arapdağ altın yatağı jeoşimi etüt raporu; Ege Bölgesi ArşivNo:A/3.
- Dora, Ö., 1964. Geologisch-lagerstättenkundliche Untersuchungen im Yamanlar-Gebirge nördlich vom Karşıyaka (Westanatolien): MTA Publ. Nr. 116
- , 1970, Arapdağ (Karşıyaka) kuvars-altın filonlarının mineralojik etüdü; Madencilik Dergisi Cilt. IX, Sayı: 4, 25-41s.
- Dönmez, M., Tükecan, A., Akçay, A.E., Hakyemez, Y. and Sevin, D., 1998, İzmir ve kuzeyinin jeolojisi. Tersiyer volkanizmasının petrografik ve kimyasal özellikleri; MTA Rep.: 10181 (unpublished) Ankara.
- Düzbastılar, M.K., 1976, Yamanlar bölgesi batı kısmının jeolojisi hakkında: Ege Üniv. Fen. Fak. ilmi raporlar serisi. No: 186
- Ejima, Y., Fujina, T., Tagaki, H., Shimada, K., Iwanaga, T., Yoneda, Y. and Murakomi, Y., 1987. The pre-feasibility study on the Dikili-Bergama geothermal development project in the Republic of Turkey-Progress Report II (unpublished).
- Ercan, T., 1983, Batı Anadolu'daki Senozoyik yaşlı volkanik kayalar ve plaka tektoniği açısından kökenselyorumları, MTA Rep.: 7294 (unpublished) Ankara.
- , Türkecan, A., Akyürek, B., Günay, E., Çevikbaş, A., Ateş, M., Can, B. and Erkan.

- M., 1984a, Dikili, Çandarlı, Bergama (İzmir) ve Ayvalık, Edremit, Korucu (Balıkesir) yörelerinin jeolojisi ve magmatik kayaların petrolojisi; MTA Rep.: 7600 (unpublished) Ankara.
- Ercan, T.; Türkecan, A.; Akyürek, B.; Günay, E.; Çevikbaş, A.; Ateş, M.; Can, B.; Erkan, M.C. and Özkirişçi, C., 1984b), Dikili-Bergama-Çandarlı (Batı Anadolu) yöresinin jeolojisi ve magmatik kayaların petrolojisi: *Jeol. Müh Derg.*, 20, 47-60
- , Satır, M., Sevin, D. and Türkecan, A, 1997, Batı Anadolu'daki Tersiyer ve Kuvarterner yaşlı volkanik kayalarda yeni yapılan radyometrik yaş ölçümlerinin yorumu. *MTA Derg*, No, 119, 103-112
- Erdoğan, B., and Güngör, T., 1992, Menderes Masifinin kuzey kanadının stratigrafisi ve tektonik evrimi; *TPDJ Bül.* Cilt. 4, 9-34.
- Eşder, T., Yakabağ, A., Sarıkaya, H., Çiçekli, K., 1991, Aliağa (İzmir) yöresinin jeolojisi ve jeotermal enerji olanakları: MTA Gen. Mud. Ege Bol. Mud. Rep.
- Gonca, Ş., 1990, İzmir-Karşıyaka Arapdağ (Altintepe ve Çilektepe sektörleri) altın cevherleşmeleri maden jeolojisi raporu (iki cilt, II. cilt: analizler cildi); MTA Rep.: 8978 (unpublished) Ankara.
- Henley, R.W., 1985, The geothermal framework of epithermal deposits. In: B.R. Berger and P.M. Bethke (Editors), *Geology and Geochemistry of Epithermal Systems*. Soc. Econ. Geol. Rev. Econ. Geol., 2: 1-24.
- , 1990, Epithermal gold deposits in volcanic terrains. In: R. P.Foster (Editor), *Gold Metallogeny and Exploration*. Blackie, Glaskow.
- Higgs, R., 1962, İzmir (Karşıyaka) Alurca yakınında Arapdağ altın prospeksiyonu için tenör ve tonaj hesabı; *Ege Bölge Arşiv No: 90 A/18*.
- İzdar, K.E., 1962, İzmir-Karşıyaka Alurca K. Arapdağı Au-Ag muhtevi kuvars filonları sahasındaki on günlük arazi müşahadelerini ve son sondaj durumlarını özetleyici ön rapor. *Ege Böl. Arşiv No: A/1994*.
- Kaya, O., 1978, Ege kıyı kuşağı (Dikili-Zeytindağı-Menemen-Yenifoça) neojen stratigrafisi: *Ege Üniv. Fen Fak. Monografiler serisi*, no: 17
- Kaya, O., 1999, Batı Anadolu kırık dizgeleri; petrol ve jeotermal potansiyel yönünden değerlendirme; Baksem'99 1. Batı Anadolu Hammadde Kaynakları Semp. 8-14 Mart 1999, İzmir. *Bildiriler kitapçığı* 1-11
- , and Savaşçın, Y., 1981, Petrologic significance of the Miocene volcanic rocks in Menemen, West Anatolia: *Aegean Earth Sciences*, 1, 45-58
- Kissel, C., Loj, C., Şengör, A.M.C. and Poisson, A., 1987. Paleomagnetic evidence for rotation in opposite senses of adjacent blocks in northeastern Aegean and western Anatolia, *Geophys. Res. Lett.*, Vol. 14, 907-910
- Kozan, T., Ödüm, F., Bozbaş, E. Bircan, A, Keçer, M and Tüfekçi, K., 1982, Burhaniye (Balıkesir)-Menemen (İzmir) arası kıyı bölgesinin jeomorfolojisi; MTA Rep.: 7287 (unpublished) Ankara.
- Molly, E., 1956, İzmir yakınında bir altın madeni zuhuru: Arapdağ; MTA Rep.: 2464 (unpublished) Ankara
- Nebert, K., 1978, Linyit içeren Soma Neojen bölgesi. *Batı Anadolu*, MTA Derg. 90, 20-69.
- Oğuz, M., 1966, Manisa Dağı'nın kuzey ve kuzeybatısının jeolojisi (Geology of the northern and northwestern part of Manisa Dag) *Engl. Summary: Fac. Sci. Ege Üniv., Sci. Rept*, no: 33. 20 p. İzmir,
- Öngür, T., 1972, İzmir Urla jeotermal araştırma sahasına ilişkin jeolojik rapor. MTA Rep.: 4835 (unpublished) Ankara.
- Sayılı, I.S., Gonca, Ş. and Gevrek, A.i, 1990, Gold mineralization at Arapdağ, Karşıyaka, İzmir, *IIESCA 1990, Abstracts*, 29-30.
- Seyitoğlu, G., Anderson, D. Nowell, G, and Scott, B., 1997, The evolution from Miocene potassic to Quaternary sodic magmatism in western Turkey: implication for enrichment processes in the lithospheric mantle. *Jour. Volc, and Geoterm. Res*, 76, 127-147.
- Turkish-Italian Joint Venture Project, 1991, Geological and mining studies in western Turkey with particular reference to production of precious and rare metals using hydrometallurgical.

- processes. Final report, 428p.
- Vural, O., 1962, Karşıyaka Arapdağı zuhurunun 10.5.1961-15.9.1962 tarihlerindeki çalışmalarına ait rapor ve rezerv hesapları; MTA Rep.: 3195 (unpublished) Ankara.
- Weiss, E., 1895, İzmir civarındaki altın yatağı hakkında rapor; MTA Rep.: 1413 (unpublished) Ankara.

A BRAMATHERIUM SKULL (GIRAFFIDAE, MAMMALIA) FROM THE LATE MIOCENE OF KAVAKDERE (CENTRAL TURKEY). BIOGEOGRAPHIC AND PHYLOGENETIC IMPLICATIONS

Denis GERAADS* and Erksin GÜLEÇ**

ABSTRACT.- A sub-adult skull from the Late Miocene of Kavakdere, described and referred to the Indian genus *Bramatherium*. increases the similarity between the Indian sub-continent and the Greco-Iranian province. The contents and subdivisions of the subfamily Sivatheriinae are reviewed, with 2 main groups being recognized, based upon the homologies and position of horns. They are perhaps both of western European origin.

Key words: Giraffidae, Mammalia, Upper Miocene, Turkey.

INTRODUCTION

Kavakdere is one of the many rich upper Miocene Mammal localities of Turkey. It is located close to the famous Sinap hill localities, North of Ankara. While Köhler (1987) doubtfully assigns the locality to zone MN 11, Sickenberg (1975) place it between the middle Vallesian and the early Turolian. The faunal list given by Ozansoy (1965) and Sickenberg (1975:81) includes *Helladotherium* and "Camelopardalis" as Giraffids. Ozansoy did not state, however, what was the basis, for his determinations, nor did he describe any fossil. There are, however, on display in the MTA Museum, several complete Giraffid limb bones and an almost complete skull of unusual interest, since it is one of the very few Sivatheriine skulls known in the late Miocene from any where in the world.

DESCRIPTION

Genus : *Bramatherium* Falconer, 1845
Syn : ? *Helladotherium* Gaudry, 1860
Hydaspathierium Lydekker, 1877

Type species: *B. pehmense*, Perim Island, Dhok Pathan.

Other species: Several other species have been described from the Indian sub-continent.

These are *B. megacephalum* (Lydekker 1876), *B. grande* (Lydekker, 1880), and *B. magnum* (Pilgrim, 1910) (Pilgrim, 1911; Bohlin, 1926; Colbert, 1935). Some may be distinct from the type species, but this has yet to be demonstrated by more complete evidence. The difference in length of the pedicel of the anterior pair of horns, said by Lewis (1939) to distinguish *B. pehmense* from *B. megacephalum* is probably of ontogenic or individual origin; the skull described by this author is that of a very old animal. *Bramatherium suchovi* Godina 1977 from the Turolian of Chimichlia in Moldavia, is not, in our opinion, referable to this genus, as explained below.

The skull from Kavakdere (Fig. 1-2), labelled 1947, is that of a young adult, with all milk premolars in use, M2 but slightly worn, and M3 not erupted yet. Of course, this young ontogenic age should not be overlooked when discussing features of the skull, especially the horns. The skull is complete, except for the premaxillae, tips of nasals and part of the lambdoid crest but only the horn bases are preserved; most of the sutures are indistinct.

The milk-teeth are much worn; the anterior lobe of DP3 is much longer than the posterior one, a primitive character found in all *Sivatheriines*. The permanent molars are only moderately hypsodont; they have a simple occlusal pattern, no entostyle,



Fig. 1- The Kavakdere skull in lateral view. The broken line shows the approximative outline of the anterior horn.
L = lateral posterior horn. Scale = 15 cm.

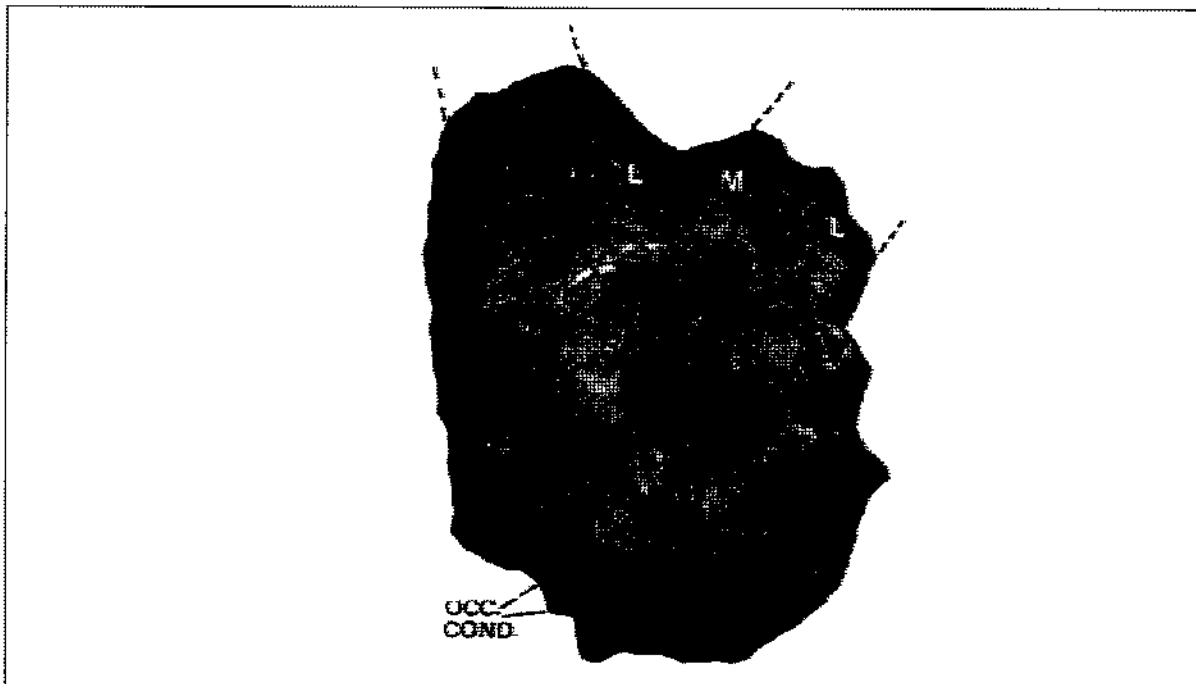


Fig. 2- The Kavakdere skull in posterior view. Occ.cond. = occipital condyles; L = lateral posterior horns;
M = median posterior horn.

weak external pillars but rather strong para-and mesostyles.

The skull can easily be referred to the *Sivatheriinae* by its large size, great height relative to its length and long post-orbital portion. The muzzle is very high above the tooth-row, and the profile of the nasals, whose tips are missing, was certainly slightly concave. A rather large ethmoidal fissure was probably present. The frontal roof was much higher than the orbitae, which look relatively small, with an elongate outline, a large lacrymal foramen inside them, and a rounded lower border (very different from the angular one found in *Palaeotragus* and related genera), which is still thicker than that of the adult *B.perimense* skull figured by Lewis (1939). The anterior border of the orbita is at the level of the middle of M3, and would certainly have been a little more posterior in the fully grown animal. This is again a difference with the skull figured by Lewis, in which the orbit is much more anteriorly placed, but this skull appears to have been partly reconstructed in plaster. The temporal fossae are deep anteriorly, being roofed over by lateral expansions of the frontal, which, however, disappear posteriorly. In other *Sivatheriines*, such as *Bramatherium* (including *Hydaspithehum*) from the late Miocene of India (Colbert, 1935, fig. 174; Lewis, 1939, pl. 2), "Indratharium" and *Sivathehum* from the Plio-Pleistocene of the same area (the skulls of which are in the British Museum of Natural History) and Africa (Harris, 1976; Geraads, 1985) and *Helladotherium* from the Turolian of Pikermi in Greece (Skull PIK 1500 in the Museum National d'Histoire Naturelle, Paris), the whole length of the temporal fossa assumes a groove-like shape, because these lateral expansions of the cranial roof extend backwards as far as the occipital crest: the young ontogenic age of the Kavakdere specimen may well be responsible for this difference. This juvenile condition, and some crushing, may also account for the relatively narrow and rounded outline of the occipital, little expanded laterally. Its central part is deeply hollowed for insertion of extensor muscles and cervical ligament; lateral to this deep pit are strong buttresses diverging from above the foramen magnum, as in other Giraffids.

The occipital condyles are large, with their long axis almost vertical, in contrast to the Recent Giraffids, where they are oblique, allowing the skull to be extended in the same line as the neck; *Bramatherium*, on the contrary, like *Sivatherium* (Geraads, 1985), was certainly unable to lift the muzzle above the horizontal line, and was certainly not a browser.

The cranial basis resemble those of *Bramatherium perimense* (Colbert, 1935, fig. 176) and *Helladotherium* from Pikermi (PIK 1500, MNHNP), but differs from those of *S. Gigonteum* from the upper Siwaliks (BM M15283) and from *S.maurusium* from Africa (Harris, 1976; Geraads, 1985) in that this region is not extremely shortened, with a still tang auditory bulla and an auditory duct slightly inclined backwards, and not quite transversal as in *Sivatherium*.

There are 5 horns: a very large anterior pair, of which only the base is preserved, and 3 much smaller posterior horns, which are little more than swellings. The anterior pair arise in the frontal region, but wholly behind the orbits, their anterior border being at the level of the anterior end of the temporal fossa: they are thus more posterior than the anterior pair of *Sivatherium* or *Decennatherivim* Crusafont, 1952, from the Vallesian of Spain (Morales, 1985) or than the median elevation of the Chimichlia skull (Godina, 1977). Although their bases are close together, the horns do not arise from a common base, but are separated on the skull roof. They are transversely compressed, but not flattened. Their length cannot be estimated, but the fact that they were broken near the base suggests that they were not very short. Their extensive pneumatization was, of course, responsible for their great fragility. Between this main pair of horns and the lambdaoid crest are three transversely aligned bosses: a rounded median one (M in Fig.2), and two antero-posteriorly elongated lateral ones (L in Figs. 1-2). Although not more than 2 cm high, these three bumps are quite distinct. Their surface is as smooth as the rest of the cranial roof, and nothing suggests that they might have been bases upon which true ossicones (i.e. isolated ossifications growing independently from the skull roof; see Geraads, 1991) would have

rested; it seems almost certain, on the contrary, that larger posterior horns would have developed, in the adult, from these incipient outgrowths of the skull roof.

Dimensions:

Height of occipital, from upper border of foramen magnum to lambdoid crest	139mm.
Minimum width across temporal lines	125mm.
Length from anterior border of DP2 to back of condyles	435mm.
Length DP2 - DP4	97.5mm.
Length from anterior border of foramen magnum to level of anterior border of glenoid fossa (in the sagittal plane)	120mm.
Length from anterior border of foramen magnum to back of M3 (id.)	~ 200
Bizygomatic width	2x112
Width from medial border of bulla to lateral border of the skull	84

Limb bones: There are some very large and massive Giraffid limb-bones in the MTA collection from Kavakdere; they certainly belong to *Bramatherium*. The dimensions of two of them are:

Radius:

anterior length	=	640mm
proximal articular breadth	=	147mm

Metatarsal:

length	=	465mm
proximal breadth	=	100mm
breadth of shaft	=	61.5mm
distal breadth	=	105mm

The metatarsal is thus longer than those of all other *Sivatheriines*, but stouter than those of comparable length, such as *Samotherium* (Geraads, 1986, Fig.6).

COMPARISONS

Among the *Sivatheriinae*, two main types may be distinguished. In one, exemplified by *Sivatherium* of the Plio-Pleistocene of Africa and the Indian sub-continent, there is a long pair of recurved posterior horns, arising from the rearmost part of the skull; a much smaller anterior pair of horns arise from above the orbits; they may even be absent in *S.hendeyi* from the early Pliocene of South Africa. Both pairs are laterally inserted, but the skull is not especially wide at the supra-orbital level (in contrast to the middle Miocene *Giraffokeryx* Pilgrim, 1910 and Palaeotragines). To the same type could be referred *Birgerbohlinia* Crusafont, 1952, from the Turolian of Spain, assuming that Montoya and Morales (1991) were correct in determining the position of the horns in this genus.

Another type of horn disposition can be found in *Decennatherium* the Vallesian of Spain, and probably also of Greece (Geraads, 1979, 1989). It has two anterior horns, much closer together (Morales, 1985), which may be homologous with the median hump of "*Bramatherium*" *suchovi*. It is not known whether there was also a posterior pair of horns. *Decennatherium* is certainly not ancestral to *Sivatherium* since its anterior horns are more derived by being larger and less lateral, but it may well be ancestral to *Bramatherium*: the shape and position of the anterior horns of the Kavakdere skull are almost perfectly intermediate between those of the Spanish *Decennatherium*, and those of the Indian *Bramatherium*: they are still separate at the base, as in *Decennatherium*, but already shifted backwards, as in *Bramatherium*. The latter genus has horns of a type completely different from those of *Sivatherium*: the anterior pair, which is post-orbital, is much better developed than the posterior one. The Kavakdere skull shows that the anterior horns also appears earlier in ontogeny, and probably also in phylogeny. *Decennatherium* has no significant derived character in respect to *Bramatherium*. and could be close to its ancestor. *Helladotherium*, whose type-specimen of the type-species, from Pikermi. is evidently the female of some other genus, has more massive limb-bones than *Decennatherium*,

and a long grooved temporal fossa, a synapomorphy with *Bramatherium*, although this character is unknown in *Decennatherium*. It is accordingly provisionally included in the former genus.

The middle Miocene genera *Giraffokeryx* and *Injanatherium* Heintz, Brunet and Sen, 1981 share with the upper miocene *Palaeotragus* and *Samotherium* the following features: long conical supra-orbital horns, widely separated at the base; frontal much broader than the occipital; long and low skull; tendency to molarize P₃. They lack the following features of the *Sivatheriinae*: very large size; skull, and especially muzzle, short and high, with nasals concave in profile; lower border of orbit thickened; very large horns in males; axis of condyles almost vertical; cranial basis shortened, higher than the tooth-row; skull extremely pneumatized; premolars enlarged. These two genera being excluded, the history of the subfamily can be summarized as follows:

No undoubted Sivatheriine is known before the upper Miocene, where they appear in Spain with *Decennatherium*. Towards the end of this Mammalian stage, they are already known by similar or identical genera in Greece (at Ravin de la Pluie and Pentalophos: Geraads, 1979; 1989), perhaps Turkey ("*Samotherium*" *pamiri* Ozansoy, 1965 from Middle Sinap) and the Siwaliks (Flynn et al., 1995).

The Turolian is time of greater diversity, with the subfamily being present in almost all Eurasian sites of this period, south of the Himalaya, and even entering Africa. This expansion could be linked with that of open environments, since they were all mainly grazers. The fact that the earliest African Sivatheriine was found in Tunisia, and the similarity of the posterior horns of *Sivatherium hendeyi*, from the Mio-Pliocene of South Africa with those of *Birgerbohlinia* from the Turolian of Spain strongly suggests that the invasion of Africa followed an occidental route.

As discussed by Montoya and Morales (1991), the group wholly disappears, outside Africa and the Siwaliks, in the latest Miocene. This is also a period of decrease in diversity of Bovids, but of greater di-

versity of Cervids, testifying a return of greater woody cover.

BIOGEOGRAPHY

Although *Sivatheriines* were undoubtedly present in Africa in late Miocene times (in Tunisia at Douaria: Guerin, 1966; Geraads, 1985, and in the lower Oluka formation of Uganda: Geraads, 1994), *Bramatherium* seems absent from this continent, and this genus is known with certainty from Asia only. The Kavakdere skull is its westernmost undoubted representative, as long as *Helladotherium* cannot be demonstrated to be identical. The Kavakdere occurrence increases again the similarities between Indo-Siwalik faunas and those of the Greco-Iranian province, which are rather few: besides the Middle Miocene *Giraffokeryx*, late Miocene ruminants common to both realms include only *Miotragocerus* and *Nisidorcas* among Bovids.

AGE OF THE KAVAKDERE FAUNA

The Indian representatives of *Bramatherium*, with fully united horns, are mainly known in the Dhok Pathan, of late Turolian-equivalent age, while the more primitive *Decennatherium* and "*Bramatherium*" *suchovii* are Vallesian or early-middle Turolian. The Kavakdere skull being intermediate in morphology (and therefore not assigned to any precise species), a middle Turolian age can be suggested on this basis, a conclusion not contradicted by the stratigraphic relations in the area (Ozansoy, 1965); a late Turolian age would perhaps even be more satisfactory, on the basis of the very large size of the limb-bones, but Kavakdere has the Bovid genus *Prostrepsiceros*, which is unknown after the middle Turolian (Bouvrain, 1982).

ACKNOWLEDGEMENTS

We are most grateful to Dr. Ziya Gözler, former General Director of MTA, to Hüseyin Ertuğrul, former head of the MTA Natural History museum, and to Department of Scientific Documentation and Information Boss Sevim Yıldırım, also from MTA, for allowing us to study the Kavakdere material and providing us with all facilities there. D.G. also thanks A.W. Gentry and L. Ginsburg for giving access to the

British Museum (Natural History), London, and Museum National d'Histoire Naturelle, Paris, respectively, and Prof. Y. Coppens, College de France, for constant support.

Manuscript received March 18, 1999

REFERENCES

- Bohlin, B., 1926, Die Familie Giraffidae: *Palaeont.Sin.*, C, 4(1), 1-178.
- Bouvrain, G., 1982, Revision du genre *Prostrepsiceros* MAJOR, 1891 (Mammalia, Bovidae): *Palaont. Zeitschr.*, 56(1/2), 113-124.
- Colbert, E.H., 1935, Siwalik Mammals in the American Museum of Natural History: *Trans.Amer.Phil.Soc.*, N.S. 26, 1-401.
- Crusafont, M., 1952, Los Jirafidos fosiles de Espana: *Mem.Com.Inst.Geol.Dip.Barcelona*, 8, 1-239.
- Flynn, L.J., Barry, J.C., Morgan, M.E., Pilbeam, D., Jacobs, L.J. and Lindsay, E.H., 1995, Neogene Siwalik mammalian lineages: species longevity, rates of change and modes of speciation: *Palaeogeog., Palaeoclim., Palaeoecol.*, 115, 249-264.
- Geraads, D., 1979, Les Giraffinae (Artiodactyla, Mammalia) du Miocene superieur de la region de Thessalonique (Grece): *Bull.Mus.Natl.Hist.Nat.*, Paris, C, 4(1), 377-389.
- , 1985, *Sivatherium maurusium* (POMEL) (Giraffidae, Mammalia) du Pleistocene de la Republique de Djibouti: *Palaont Zeitschr.*, 59(3-4), 311-321.
- , 1986, Remarques sur la sytematique et la phylogenie des Giraffidae: *Geobios*, Lyon, 19(4), 465-477.
- , 1989, Un nouveau Giraffide (Mammalia) du Miocene superieur de Macedoine: *Bull.Mus.Natl.Hist.Nat.*, Paris, C, 11(4), 189-199.
- , 1991, Derived features of Giraffid ossicones: *J.Mamm.*, Baltimore. 72(1), 213-214.
- , 1994, Giraffes fossiles d'Ouganda: *CIFEG occas.Publ.*, 29, 375-381.
- Godina, A.I.A., 1997, On new finds of Sivatherinae on the territory of the USSR: *J.Palaeont. Soc.India*, 20, 21-25.
- Guerin, C., 1966, *Diceros douariensis* nov.sp., un Rhinoceros du Mio-Pliocene de la Tunisie du Nord: *Doc.Lab.Geol.Fac.Sci.Lyon*, 16. 1-50.
- Harris, J.M., 1976, Pleistocene Giraffidae (Mammalia. Artiodactyla) from East Rudolf, Kenya: In: Savage R.J.G. and Coryndon S.C., *Fossil Vertebrates of Africa*, Acad. Press, London, 4, 283-332.
- Heintz, E., Brunet, M. and Sen, S. 1981, Un nouveau Giraffide du Miocene superieur d'Irak: *Injanatherium hazimi* n.g., n.sp. *C.R.Acad.Sc.*, Paris, D, 292. 423-426.
- Köhler, M., 1987, Boviden des türkischen Miozans (Kanozoikum und Braunkohlen der Türkei. 28): *Paleontologia i evolucion*, 21, 133-246.
- Lewis, G.E., 1939, A new *Bramatherium* skull: *Amer.J.Science*, 237, 275-280.
- Montoya, P., and Morales, J., 1991, *Birgerbohlinia schaubi* Crusafont, 1952 (Giraffidae, Mammalia) del Turolinse inferior de Crevillente-2 (Alicante. Espana): *Filogenia e historia biogeografica de la subfamilia Sivatheriinae*: *Bull.Mus.natl.Hist.Nat.* Paris, 4eme ser., C, 13(3-4), 177-200.
- Morales, J., 1985, Nuevos datos sobre *Decennatherium pachecoi* Crusafont, 1952 (Giraffidae, Mammalia): *descripcion del craneo de Matillas*: *Col-Pa*, 40, 51-58.
- Ozansoy, F., 1965, Etude des gisements continentaux et des Mammiferes du Cenozoique de Turquie: *Mem.Soc.Geol.Fr*, N.S., 44(1), 1-92.
- Pilgrim, G.E., 1911, The fossil Giraffidae of India: *Palaeont.Indica*, N.S., 4(1), 1-29.
- Sickenberg, O., 1975, Die Gliederung des höheren Jungtertiars und Altquartars in der Türkei nach Vertebraten und ihre Bedeutung für die Internationale Neogen-Stratigraphie: *Geol.Jb.*, B, 15, 1-167.

GEOLOGY, MINERALOGY AND GEOCHEMISTRY OF SULPHITE MINERALIZATION IN THE ISPENDERE REGION (MALATYA)

Halide DUMANLILAR; Doğan AYDAL** and Özcan DUMANLILAR**

ABSTRACT.- In this study, the geology, mineralogy, petrography, geochemistry, wallrock alteration, ore-wallrock relations, micro structural and textural relations in the copper-pyrite mineralization in Kızmeşmet site (Ispendere-Malatya) and its vicinity were investigated. Ispendere Ophiolite (Jurassic-Lower Cretaceous), Yüksekova complex (Upper Cretaceous) and Kırkgeçit formation (Middle Eocene) crop out in the study area, which is located in Malatya-Elazığ region of the Eastern Taurus orogenic belt. Yüksekova complex is formed by Kuluşığı magmatites, Kapıkaya volcanics, Şişman magmatites and Harabe hill magmatites. Harabe hill magmatites cut all of the mentioned rocks in the complex and caused to form all of alteration types and different mineralizations in the study area. When the mineralogical, petrological and geochemical data are taken into consideration, the ore minerals bearing Harabe hill magmatites and the other type magmatites in Yüksekova complex were determined as product of I-type calcalkaline magmatism. The copper-pyrite mineralization is generally located in the Harabe hill magmatites and its contacts with the surrounding rocks. Four types of alterations related with the mineralization processes were determined in the study area, namely; weak potassic, phyllic, argillic and prophylic. The ore mineralization is generally surrounded by phyllic-prophylic alteration and/or phyllic alteration halos. The ore minerals are found within quartz-carbonate veins, as coatings in joints and faults and as well as disseminated ore minerals in the host rock. The main ore minerals are pyrite, chalcocopyrite and magnetite, while sphalerite, galenite, pyrotite, bornite, rutile-anatase and ilmenite is less amount. Limonite, hematite, marcasite, chalcocite and covellite are found as secondary ore minerals. Porphyry copper-pyrite and/or stockwork type mineralization were detected in the study area according to the studies based on geotectonic environment, ore mineralogy, ore type host rock-ore relation and host rock alteration.

Key words: Granitoid, porphyry, alteration, dacite, Kızmeşmet Site (Malatya).

INTRODUCTION

Study area is located 20 km east of Malatya city and comprises Karakaya dam lake at north and an area of about 70 km² on Malatya-Elazığ highway at south of 1:25.000 scaled Malatya L41-a1 and a4 quadrangles (Fig. 1). Upper Cretaceous Yüksekova

complex within the Eastern Taurus orogenic belt is widely exposed along the belt extending from Hakkari to Elbistan. Kızmeşmet site pyrite-copper mineralization of study interest (Ispendere-Malatya) is found within the Yüksekova complex.

Studies on mineralization within the Yüksekova complex were started in 1991 with general geochemical prospecting works in stream sediments conducted by General Directorate of MTA. In Kızmeşmet site copper-pyrite field, which is one of the anomalies found during these studies, metal concentrations in vertical-horizontal directions and total reserve were determined by drilling works with a total length of 1958 m carried

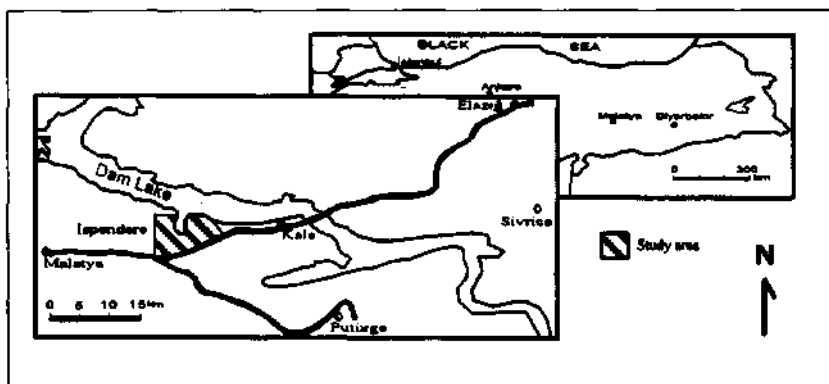


Fig. 1- Location map of study area.

out in 11 different locations (Tüfekçi and Dumanlılar, 1994).

The study area where detailed drilling works were conducted, in the first pyrite-copper mineralization. In the study area, type of mineralization, formation conditions, country rock relations, ore geometry and geotectonics setting were examined in detail to construct a model for the other occurrences within belt.

Several studies were conducted in the study area and its vicinity by means of geology, tectonism, petrography and petrology (Baykal, 1966; Yazgan, 1981; Yazgan and Asutay, 1981; Asutay, 1985, 1986; Yazgan and Chessex, 1991; Turan et al., 1995; Dumanlılar, 1993).

REGIONAL GEOLOGY

Study area located in Malatya-Elazığ section of Eastern Taurus orogenic belt has gained its geological structure through the following stages. During Upper Triassic, an ocean started to open between Eurasia and Arabian platform in the region and it was continued to evolve to the end of Lower Cretaceous (Yazgan et al., 1987). In the region arc magmatism products (Yüksekova complex) were formed in association with a northerly dipping subduction zone which was started to evolve by the beginning of Upper Cretaceous (Cenomanian-Turonian). At the beginning, arc magmatism had an ensimatic character (Hempton and Savcı, 1982) while it gained an ensialic character (in areas where it was developed under the Keban continent) in further stages (Yazgan et al., 1987). During this stage, ophiolitic masses were placed to the passive southern margin (ispendere and Guleman ophiolites). This phase was followed by Upper Maastrichtian transgression which resulted in deposition of Harami limestones. As a result of completely receding of the sea after Upper Maastrichtian, a terrestrial regime was prevailed in the region during Lower Paleocene and, thus, foldings and uplifts were formed (Poyraz, 1988).

At the beginning of Tertiary, a north-west trending compressional stress was dominated in the region and volcanite-bearing Maden complex was

formed in a deep basin (Yazgan et al., 1987; Turan et al., 1995).

In Middle Miocene as a result of compressional stress following a continent-continent collision in the region, formation of tectonic structures such as Southeast Anatolian thrust zone and East Anatolian fault belt had shaped the present structure of the region (Turan et al., 1995).

GENERAL GEOLOGY AND MINERALOGY

In the study area, Yüksekova complex has a tectonic contact with ispendere ophiolite at south, while it is unconformably overlain by Eocene Kirkgeçit formation at north (Fig.2).

ISPENDERE OPHIOLITE

This unit, which is described by Yazgan et al., (1987) at first, is differentiated as nonmetamorphic ispendere and metamorphic Kömürhan units. Jurassic - Lower Cretaceous aged ispendere ophiolite is observed as a tectonic slice, which is northerly dipping between Yüksekova complex at north and Maden complex at south, and exposed in a wide area on Malatya L41-a4 quadrangle.

Ultramafic cumulates consisting of moderately thick dunite and wehrlites are found at the basement of ispendere ophiolite. They are overlain by a zone composing of cumulate gabbros. These two units are transitional and often cut by wehrlitic intrusions. Cumulates are overlain by a transition zone consisting of thinly bedded gabbros followed by isotropic gabbros. Plagiogranites are found between thinly bedded gabbros and isotropic gabbros. Dike complex in the upper part comprises the thickest unit of ispendere ophiolite. Pillow lavas in east of study area make up the upper most part of ispendere ophiolite.

YÜKSEKOVA COMPLEX

This unit is extending from Hakkari city in Eastern Taurus belt to Elbistan town and was first described around Hakkari Yüksekova town by Perinçek (1979). Some workers studied in Eastern Taurus (Perinçek, 1979; Bingöl, 1984; Turan, 1984) use the name of Yüksekova complex for the unit,

while Asutay (1985) who studied in Baskil and Yazgan et al., (1987) who made the geological map of Şişman village named this unit as Baskil magmatites and pointed out that unit is represented with magmatic, volcanic and subvolcanic rocks. Based on K/Ar isotopic determinations the age of these

rocks is 75 my to 86 my (Upper Cretaceous). Calc-alkaline Baskil magmatites are completely defined as I type granitoid and cut the Keban metamorphites thus caused contact metamorphism (Tüfekçi et al., 1979; Asutay, 1985).

In the region, Yüksekova complex is com-

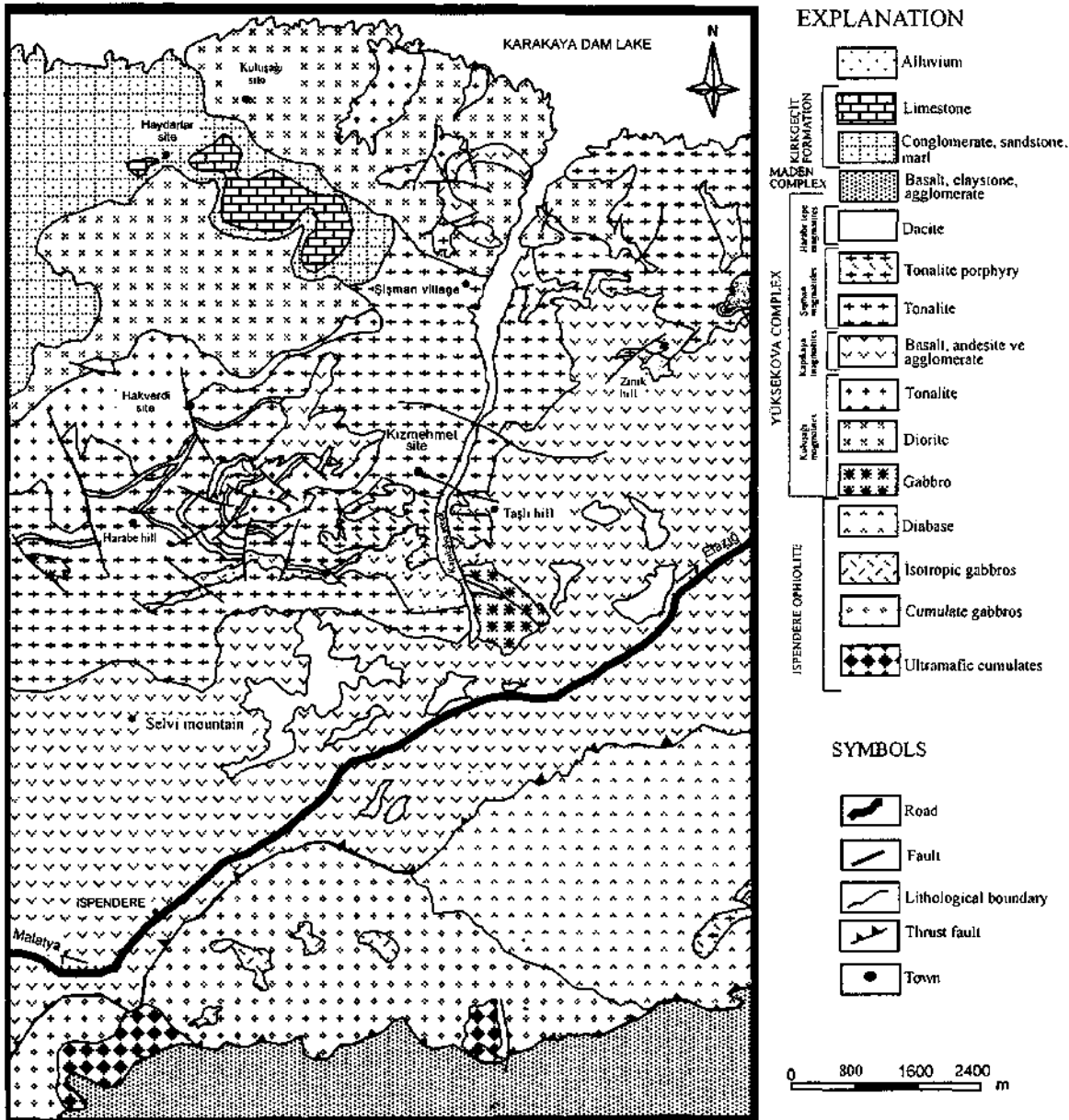


Fig. 2- Generalized geology map of Ispendere (Malatya) region.

posed of Kuluşağı magmatites, overlying Kapıkaya volcاني-tes and Şişman magmatites cutting former two units, and Harabe hill magmatites which have an intrusive contact with all above units and facilitate alteration and mineralization.

Kuluşağı magmatites.- As a result of modal mineralogic analysis and chemical-mineralogical examinations, Kuluşağı magmatites were determined as gabbro, quartz diorite and tonalite (Figs. 3 and 4) (Table 1).

Gabbro: Gabbros those are found in outer zones of batholith, microscopically show two different textures. The Gabbros, where they are exposed in mappable sizes, display holocrystalline grain texture, while they are exposed in small areas in quartz diorites, gabbros show holocrystalline porphyritic texture. Andesine-labradorite type of plagioclase (49.1%) and clinopyroxene (42.1%) are the main constituents of the rock. In addition, some

amount of opaque minerals (7.3%) and quartz(1.5%)are also found in gabbros.

The Pyroxenes are altered to tremolite and actinolite along their edges, while plagioclases do not seem to be subjected to an intense alteration, but are sericitized and argillitized in places.

Quartz diorite and tonalite: Quartz diorite and tonalite have a holocrystalline grain texture. Quartz diorite contains 56.6% plagioclase, 35.1% amphibole, .6.8% quartz and 1.50% orthoclase. Quartz content in tonalite is increased up to 20.8% while amphibole and plagioclase amounts are reduced to 30.2% and 43.1%, respectively. In addition, tonalite contains 3.7% orthoclase and 2.2% opaque minerals.

Plagioclases are of andesine composition and subjected to sericite and lesser amount of epidote alteration.

Table 1- Macro-micro properties of rocks of Şişman and Kuluşağı magmatites.

Rock name	Color	Texture	Modal Mineralogic Composition (%)	Accessory Minerals	Grain size	
K U L U Ş A Ğ I M A G	Gabbro	Dark green-black	Holocrystalline grain texture	Plagioclase (49,1%) Pyroxene (42,1%) Quartz (1,5 %) Opaque Mineral (7,3%)	-	0,5-3 mm.
	Quartz diorite	Dark green-gray	Holocrystalline grain texture	Plagioclase (56,6%) Amphibole (35,1 %) Quartz (6,8%) Alkali Feld. (1,5%)	-	1-2 mm.
	Tonalite	Light green	Holocrystalline grain texture	Plagioclase (43,1%) Amphibole (30,2%) Quartz (20,8%) Alkali Feld. (3,7%) Opaque Mineral (2,2%)	-	1-2 mm.
Ş I Ş M A N M A G	Tonalite	Grayish-white	Holocrystalline grain texture	Plagioclase (49,9%) Quartz (37,2%) Chloritized mafic minerals (11,3%) Alkali Feld. (1,6%)	Sphene. apatite	1-5 mm.
	Tonalite porphyry	Light pink-white	Holocrystalline porphyry texture	Plagioclase, quartz. Orthoclase and chloritized mafic minerals	-	

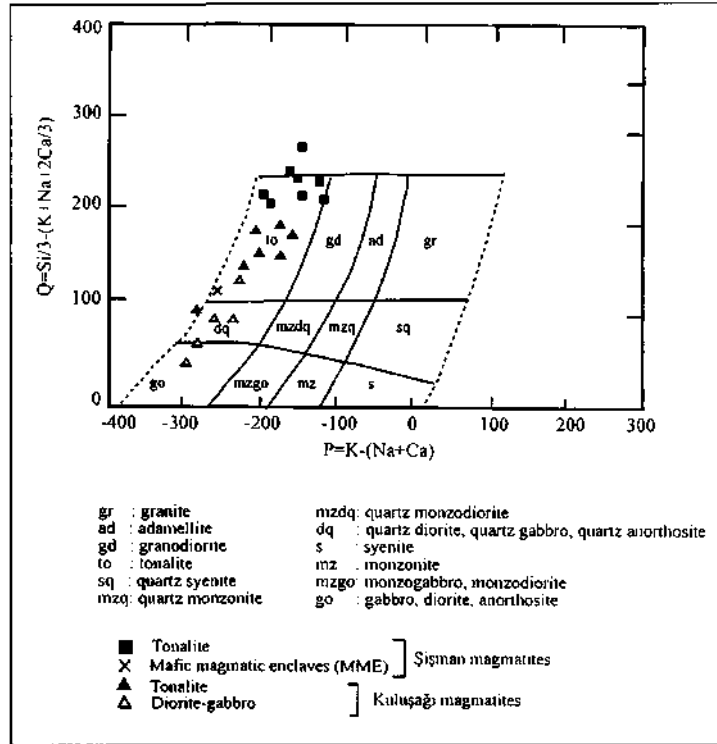


Fig. 3- Position of rock samples from Şişman and Kuluşağı magmatites on Q-P nomenclature diagram, (Debon and Le Ford, 1983).

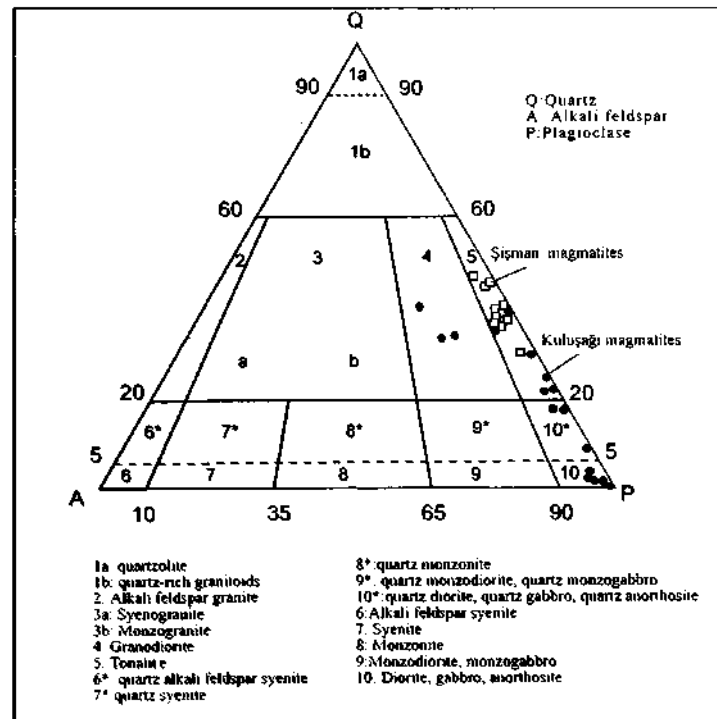


Fig. 4- Distribution of Şişman and Kuluşağı magmatites on QAPF diagram of Streckisen (1976)

Amphiboles of green hornblende type are observed as euhedral or subhedral crystals and, platy and bar-like shapes. Chloritization and opaque minerals are rarely observed in hornblendes. Hornblendes which contain plagioclase inclusions show a poikilitic texture.

Quartz has generally fractures and observed as anhedral crystals.

Quartz diorite and tonalite contains less amount of K-feldspar which is rarely subjected to sericitic alteration. K-feldspar is not detected in some thin sections.

Kapıkaya volcanites.- Kapıkaya volcanites are composed of pyroclastics, and lava flows those compositions change from andesite to basalt.

Lava flows with hyalopilitic and porphyritic texture consist of volcanic glass and pyroxene and plagioclase minerals in phenocrysts and microlite forms. Rarely observed vesicules are filled with calcite and zeolite minerals. Alteration is very common in basalts, and in all thin sections epidotization and Chloritization are encountered. Some carbonatization and opaque minerals are also detected.

Andesitic lava flows have a pilotaxitic texture and composed of intensely altered plagioclase and amphiboles. Amphiboles are observed to have been altered to chlorite and opaque minerals, while plagioclases are subjected to intense argillization and epidotization.

Andesitic pyroclastics consist of agglomerate and volcanic breccia and are composed of grains of 0.5 cm. to 20 cm.

Şişman magmatites.- Şişman magmatites are composed of tonalite and tonalite porphyry. As a result of modal mineralogic and chemical-mineralogic examinations, samples of Şişman magmatites are determined as tonalite (Fig.3 and 4).

Tonalite: Tonalites of Şişman magmatites are distinguished from those of Kuluşağı magmatites with their appearance in the field and mineralogic features in thin sections. Their quartz content and grain size are larger than, but mafic mineral content

is less than those of Kuluşağı magmatites (Table 1).

Main minerals of tonalites are plagioclase (49.9%) and quartz (37.2%) and they contain minor amount of K-feldspar (1.6%) together with mafic minerals (11.3%) that are completely altered to epidote and chlorite. Quartz minerals in tonalites are anhedral and their size changes 1mm. to 5mm. In addition, quartz grains also fill the spaces between other minerals. Symplectite texture is one of the distinct features of quartz and plagioclase grains in tonalites. This texture is an distinctive feature of tonalites of Kuluşağı and Şişman magmatites. The size of subhedral and platy plagioclases ranges from 1 mm. to 1.5mm. Although plagioclases display typical albite twinning, some of them are observed to have a zoning structure. Needle-like apatite inclusions are rarely found in plagioclases.

Besides argillization, epidotization is also common in plagioclases. The fact that, epidotization is formed in inner part of the zoned plagioclases, which indicates that anorthite content of inner zones is higher than that of outer zones.

Tonalite porphyry: Tonalite porphyries are determined to be a sub-intrusive rock and have a porphyry texture. Microscopic examinations reveal that rock is composed of plagioclase, quartz, orthoclase and chlorite. In general, plagioclases show polysynthetic twinings and are detected as euhedral phenocrysts or anhedral grains in the matrix. They are extremely argillaceous and carbonaceous and rarely altered to epidote and opaque minerals. In comparison to plagioclases, quartz phenocrysts show little amount of anhedral forms. In addition to quartz and plagioclases, some amount of orthoclase are also observed as the rockforming mineral. Orthoclases are commonly subjected to sericitization and argillization. Mafic minerals are completely chloritized. The matrix contains micro crystalline quartz and orthoclase minerals.

Mafic magmatic enclaves (MME): Mafic magmatic enclaves are observed in tonalite and porphyries of Şişman magmatites. They generally have and ellipsoidal shape with a diameter of 2 to 20 cm, but some cases, they may also show irregular

shapes.

Mafic magmatic enclaves have a fine-grained texture and are composed of plagioclase, quartz, hornblende, chlorite, apatite, sphene and opaque minerals. Oligoclase-andesine type of plagioclases are observed as microlites and in general, quartz minerals are detected as microcrystals. Hornblends partly are chloritized. Opaque minerals besides needle-like apatites and sphenes are also seen in the rock.

Harabe hill magmatites.- Harabe hill magmatites comprising the last stage of Yüsekova complex, that hosts mineralization and alteration, is composed of dacite and granodiorite porphyrites which were cut by drill holes.

Dacite: Thickness of the dacite around Germik stream changes from 10m. to 70m. On the other hand, the thickness of the dacite were found changing from 20cm. to 6m. in drill holes. Strike and dips of units in the study area are N80E/35°NW and EW/35°N to a lesser extent. They easily recognized with their pink colored alteration. In hand specimens, it could be easily distinguished by quartz crystals scattered in a pink matrix. They are irregularly, but widely exposed around Selvi mountain. Microscopically, rock has a holocrystalline hypidiomorphic porphyritic texture. Plagioclase and quartz are the main components of the rock. Plagioclase phenocrysts have euhedral and subhedral forms and on the basis of extinction angles, they are of oligoclase and andesine composition. Plagioclases are intensely subjected to carbonation and sericitization besides lesser clay alterations. Quartz phenocryst are corroded by the matrix along their edges.

Dacites contain vast amount of enclaves of the units which they cut, along the boundaries.

Granodiorite porphyry: They are typical with their pink colored alteration on the surface and their grain size is increased with increasing depth. Therefore, rock is named as granodiorite porphyry.

Examinations on thin sections reveal that rock is completely undergone to sericite and carbonate

alteration. For this reason, it is difficult to get information on primary texture and composition of the rock.

ALTERATION

BIOTITE+QUARTZ ALTERATION (POTASSIC ALTERATION)

An alteration assemblage composing of biotite and quartz was encountered at depths 0-45 m. in well no KS-5. This alteration was observed only in andesites. Biotite, quartz and opaque minerals are detected as veinlets and matrix material.

In addition, it was also determined that hornblendes are altered to an aggregate consisting of biotite and quartz. There are also little amount of sericite and chlorite. This type of alteration as observed together with andesites in well no KS-5 and described as quartz-biotite alteration, resembles to potassic alteration which consists of biotite, K-feldspar, sericite, and albite minerals and described by Lowell and Guilbert (1970).

CHLORITE+CARBONATE+EPIDOTE ALTERATION (PROPYLITIC ALTERATION)

Alteration consisting of chlorite, carbonate and epidote minerals is widely, exposed in the field. Propylitic alteration, observed on the surface and in drill holes together with all rocks belonging to Yüsekova complex, is characteristic with its gray-green color in hand specimens and on the exposures.

Under microscope, except for quartz, all other minerals are observed to alter to chlorite+carbonate+epidote+sericite+clay. Intense propylitic alteration are observed around Germik stream and cut by pyrite-chalcopyrite bearing carbonate and quartz veinlets. Based on the results of XRD analysis, type of carbonatization was determined to be dolomite, calcite and aragonite.

The plagioclases were subjected to completely carbonate, clay, partially epidote and a lesser degree of sericite alteration. Based on the XRD data clay type was found to be kaolinite. In general, mafic minerals are intensely altered to an aggregate

consisting of chlorite and opaque minerals.

Chlorite-epidote-carbonate-sericite-kaolinite alteration described in the field is similar to propylitic alteration that is characterized by chlorite-calcite-epidote-adularia-albite mineral paragenesis and described by Lowell and Guilbert (1970).

QUARTZ+SERICITE+PYRITE ALTERATION (PHYLITIC ALTERATION)

In the study area, quartz + sericite + pyrite consisting phyllitic alteration is found around Germik stream as surrounded by propylitic alteration. Additionally, this alteration is also observed as narrow zones around dacites of Harabe hill magmatites. Phyllitic alteration exposing in a wide area is surrounded by propylitic zone around Kara stream and Selvi mountain in south of the region.

In the intensely altered areas, all minerals except quartz were altered to sericite, thus primary texture of the rock is completely destroyed and primary quartz minerals are recrystallized and enlarged. Based on the results of XRD analysis, in intensely altered areas (quartz + sericite + pyrite alteration), pyrophyllite also participates into the alteration paragenesis. Quartz + sericite alteration in the area is similar to phyllitic alteration described by Lowell and Guilbert (1970).

In sericitic alteration, carbonatization also appears with the participation of chlorite into the paragenesis (weak sericitic zone). In this zone, feldspar minerals are completely sericitized, while mafic minerals are partly sericitized and altered to opaque minerals and partly to chlorite-opaque mineral. With the existence of chlorite, carbonatization and carbonate veins are also increased. Due to chloritization of primary mafic minerals (biotite), sagenitic structures are often observed that are formed by lattice-shaped rutile needles. Ashley et al., (1978) state that sagenitic structures are formed in chlorite-carbonate zone.

In the study area, weak phyllitic alteration consisting of sericite + carbonate + clay + chlorite minerals are observed in dacites and granodiorite porphyries encountered in drill holes. Primary quartzs

are corroded and grown. It was determined that matrix is completely transformed to sericite, carbonate and clay, feldspars are commonly changed to sericite + carbonate while mafic minerals are transformed to chlorite and sericite.

XRD analysis revealed that clay type is kaolinite. Argillization is observed in feldspars and matrix. Dominant carbonate minerals in this alteration type are dolomite and calcite in lesser amount.

CLAY + CHLORITE + QUARTZ ALTERATION (ARGILLIC ALTERATION)

Argillization observed within tonalitic rocks around Delav hill at north of Kizmehmet site and between Deve stream and Kavak stream gives a yellowish color to these areas.

During the clay alteration, plagioclases are completely altered to clay and sericite while mafic minerals are altered to chlorite. XRD analysis yield that clay mineral in this alteration is kaolinite. Partly limonitized, disseminated or veinlet type pyrite is the ore mineral.

The mineral paragenesis of this alteration is similar to argillic alteration belt of Lowell and Guilbert (1970), that is composed of quartz, kaolinite, montmorillonite, and lesser amounts of sericite and leucosene minerals.

PETROGENETIC AND TECTONOGENETIC EXAMINATIONS

In order to determine tectonic setting of Şişman and Kuluşağı magmatites, Y-SiO₂, Yb-SiO₂, Nb-Y, Rb-SiO₂, and Rb-(Y+Nb) diagrams (Pearce et al., 1984) were used. In Y-SiO₂ and Yb-SiO₂ diagrams (Pearce et al., 1984), rock samples plot in volcanic arc granitoids (VAG)+collision granitoids (COLG) + ocean ridge granitoids (ORG) fields (Fig. 5).

On Nb-Y stable elements diagram (Pearce et al., 1984), all the samples plot in (VAG)+syn-COLG fields (Fig.6). Exact tectonic position of Şişman and Kuluşağı magmatites were determined with the use of Rb-(Y+Nb) and Rb-SiO₂ diagrams, and this magmatites are found to represent a set of volcanic arc granitoids (VAG) (Fig. 7).

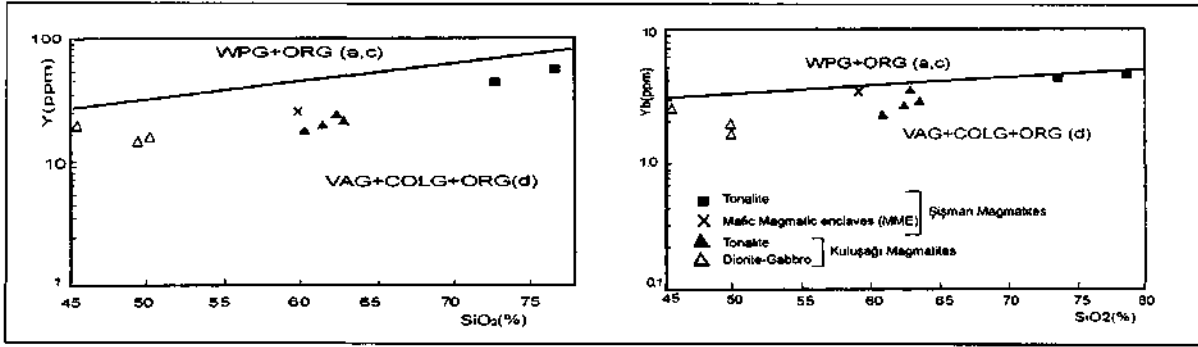


Fig. 5- Position of rock samples from Şişman and Kuluşağı magmatites on Y-SiO₂ and Yb-SiO₂ diagrams (Pearce et al., 1984). WPG: Within plate granitoids, ORG: Ocean ridge granitoids, VAG: Volcanic arc granitoids, syn-COLG: Syn-collision granitoids.

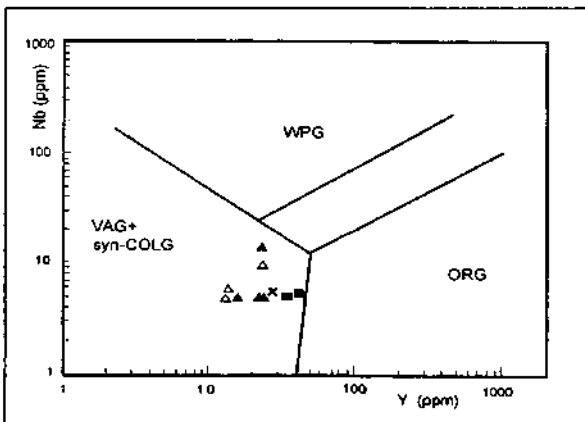


Fig. 6- Position of rock samples from Şişman and Kuluşağı magmatites on Nb-Y diagram (Pearce et al., 1984) (See Fig. 5 for other explanations).

GEOCHEMISTRY OF KULUŞAĞI AND ŞİŞMAN MAGMATITES

Major and trace element contents of 21 samples collected from intrusive rocks of Yüksekova complex were determined with ICP method while their rare earth element contents were found with ICP-MS method.

Results of chemical analysis of major and trace elements and CIPW norms and some ratios are given in Table 2 and 3.

Examination of changes of major oxides with respect to SiO₂ contents reveals that CaO, Fe₂O₃, Al₂O₃, MgO and TiO₂ values are decreased, with respect to the increasing in SiO₂ content, and there is a weak positive correlation in Na₂O values. K₂O concentration in Kuluşağı magmatites increases

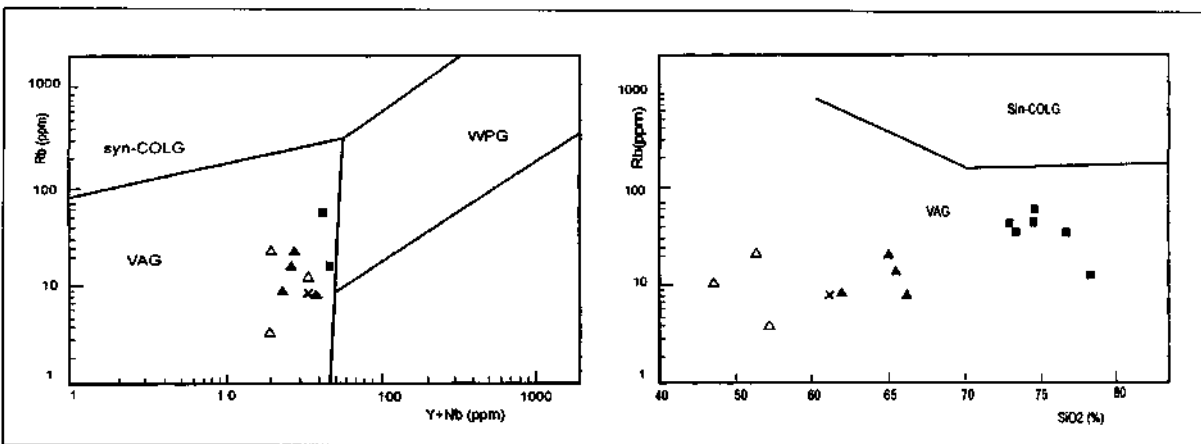


Fig. 7- Position of rock samples from Şişman and Kuluşağı magmatites on Rb-(Y+Nb) and Rb-SiO₂ diagrams (Pearce et al., 1984) (See Fig. 5 for other explanations).

Table 2- Major element percents (%), trace element concentration (ppm), A/CNK= $Al_2O_3/CaO+Na_2O+K_2O$ molecular ratios and CIPW norms of Kuluşağı magmatites.

Sample No	KS1-P3	KS1-P28	KS2-P18	HD-24	ÖD-K4	ÖD-K6	ÖD-K9	HD-27	HD-50	HD-51	ÖD-K7	ÖD-K11
Symbol	▲	▲	▲	▲	▲	▲	▲	▲	▲	▲	▲	▲
Results of major element analysis												
SiO ₂	63,01	60,49	63,5	62,81	63	63,5	64,48	44,16	49,88	49,63	54,06	47,35
TiO ₂	0,65	0,54	0,74	0,41	0,4	0,7	0,6	0,78	0,61	0,65	0,7	0,5
Al ₂ O ₃	13,9	14,62	14,43	17,09	14,5	15,6	14,6	16,04	13,85	14,5	10,47	11,72
Fe ₂ O ₃	8,00	7,48	7,77	2,41	7,2	6,6	6	12,54	9,55	11,87	11,18	11,98
MnO	0,15	0,13	0,12	0,04	0,1	0,1	0,1	0,21	0,21	0,28	0,1	0,1
MgO	3,39	5,09	3,02	0,94	3,6	1,9	2,34	4,78	9,55	8,02	10,38	13,41
CaO	4,66	6,44	4,68	4,86	4,2	5,6	3,55	10,69	9,31	11,03	10,35	13,55
Na ₂ O	3,11	3,04	3,26	6,06	3,9	3,4	5,2	2,72	3,29	1,55	1,5	0,6
K ₂ O	1,12	0,49	0,57	0,42	1,19	0,21	0,56	0,38	0,22	0,69	0,31	0,12
P ₂ O ₅	0,09	0,07	0,1	0,12	0,1	0,1	0,1	0,12	0,14	0,12	0,1	0,1
Cr ₂ O ₃	0,048	0,075	0,051	0,35				0,018	0,092	0,078		
L.O.I.	1,9	1,5	1,7	4,8	1,45	0,81		7,4	3,2	1,6		
Total	100,02	99,96	99,94	100,3	99,64	98,53	97,53	99,83	99,90	100,02	99,15	99,43
Results of trace element analysis												
Rb	20,05	8,6	15	8,06				10,43	4,28	21,23		
Sr	131,6	166,2	130,6	414,0				452,5	167,5	189,7		
Nb	<10	<10	<10	13				10	<10	<10		
Zr	74	55	70	157				64	44	67		
Y	26,3	18,6	25	23,4				22,7	16,5	16,4		
Hf	3,44	2,27	3,31	5,26				2,42	1,79	1,75		
Ta	<,1	<,1	<,1	1,0				2,9	0,2	0,4		
Th	3,25	1,12	1,13	20,85				7,06	3,43	2,47		
U	0,4	0,2	0,4	3,6				1,2	0,6	0,5		
Ba	118	58	64	55				45	33	143		
Ni	176	258	195	141				82	254	215		
Sc	21	25	21	<10				18	26	26		
CIPW - Norms												
Q	21,13	16,19	23,27	17,74	17,26	24,67	18,14	0	0	0	5,34	0
Or	6,81	2,97	3,46	2,62	7,22	1,28	3,41	2,47	1,36	4,21	1,87	0,72
Ab	27,05	26,34	28,32	54,02	33,85	26,94	45,39	21,73	29,1	13,5	12,95	5,17
An	21,25	25,41	23,23	19,19	19,03	27,5	15,32	33,41	23,4	31,48	21,34	29,49
C	0	0	0,17	0	0	0	0	0	0	0	0	0
Di	1,67	5,72	0	4,66	1,4	0,38	1,83	20,29	19,58	19,96	24,81	31,72
Ap	0,22	0,17	0,24	0,30	0,24	0,24	0,24	0,31	0,35	0,29	0,24	0
Il	1,27	1,05	1,44	0,82	0,78	1,37	1,18	1,62	1,21	1,27	1,36	0,97
OI	0	0	0	0	0	0	0	18,34	16,54	2,76	0	16,49
Hpr	20,65	22,21	19,92	3,73	20,22	14,92	14,49	0	8,52	26,6	32,09	15,44
A / CNK = $Al_2O_3 / CaO + Na_2O + K_2O$ Molecular ratios												
A/CNK	0,95	0,86	0,99	0,89	0,94	0,97	0,82	0,46	0,62	0,43	0,48	0,45

Table 3- Major element percents (%), trace element concentrations (ppm), A/CNK= $Al_2O_3/CaO+Na_2O+K_2O$ molecular ratios and CIPW norms of Şişman magmatites.

Sample No	KS4-24	HD-106	HD-180	ÖD-K1	ÖD-K2	ÖD-K3	ÖD-K5	ÖD-K8	ÖD-K10
Symbol	■	■		■	■	■	■	■	■
Results of major element analysis									
SiO ₂	73.07	77.28	58.3	74.9	71	72.27	70.5	71.69	71.92
TiO ₂	0.53	0.22	0.76	0.3	0.5	0.3	0.3	0.5	0.35
Al ₂ O ₃	13.05	12.14	15.21	12.5	13.5	13.6	13.7	13.66	12.95
Fe ₂ O ₃	2.37	1.78	8.29	2	2.9	2.8	3.2	4.79	4
MnO	0.06	0.03	0.11	0.1	0.1	0.1	0.1	0.1	0.1
MgO	1.59	0.44	2.15	0.6	1.2	0.5	1	1.52	0.72
CaO	2.3	0.98	6.58	1.56	2.8	1.8	2.33	1.8	2.2
Na ₂ O	3.57	5.07	3.83	5.5	4.6	4.4	3.6	4.2	3.4
K ₂ O	1.5	0.65	0.37	0.32	0.4	1.16	1.8	0.3	1.5
P ₂ O ₅	0.09	0.03	0.11	0.1	0.1	0.1	0.1	0.1	0.1
Cr ₂ O ₃	0.041	0.062	0.023						
L.O.I.	1.8	1.5	4.2	1.81	1.81	1.1	2.7		
Total	99.97	100.18	99.9	99.69	98.92	98.13	99.34	98.67	97.24
Results of trace element analysis									
Rb	52.59	14.19	8.7	40	40	70	50		
Sr	61.9	51.9	154.8						
Nb	<10	<10	<10						
Zr	126	139	125						
Y	37	42.9	28.6						
Hf	5.38	6.06	4.51						
Ta	<.1	<.1	<.1						
Th	2.71	1.44	1.11						
U	0.8	0.7	0.2						
Ba	97	84	46						
Ni	162	233	93						
Sc	10	<10	19						
CIPW - Norms									
Q	38.85	42.04	14.44	37.23	34.41	37.78	35.51	37.64	39.31
Or	9.08	3.91	2.31	1.94	2.44	7.1	11.05	1.81	9.16
Ab	30.86	43.58	34.15	47.64	40.2	38.57	31.63	36.19	29.71
An	11.11	4.78	24.48	7.25	13.67	7.34	11.32	8.43	10.6
C	1.6	1.4	0	0.52	0.67	2.6	1.9	3.46	2.04
Di	0	0	7.87	0	0	0	0	0	0
Ap	0.22	0.07	0.27	0.24	0.24	0.25	0.25	0.24	0.24
Il	1.03	0.42	1.52	0.58	0.98	0.59	0.59	0.97	0.69
Ot	0	0	0	0	0	0	0	0	0
Hpr	7.3	3.84	14.99	4.6	7.38	5.76	7.75	11.26	8.27
A / CNK = $Al_2O_3 / CaO + Na_2O + K_2O$ Molecular ratios									
A/CNK	1.13	1.14	0.82	1.02	1.03	1.15	1.13	1.3	1.15

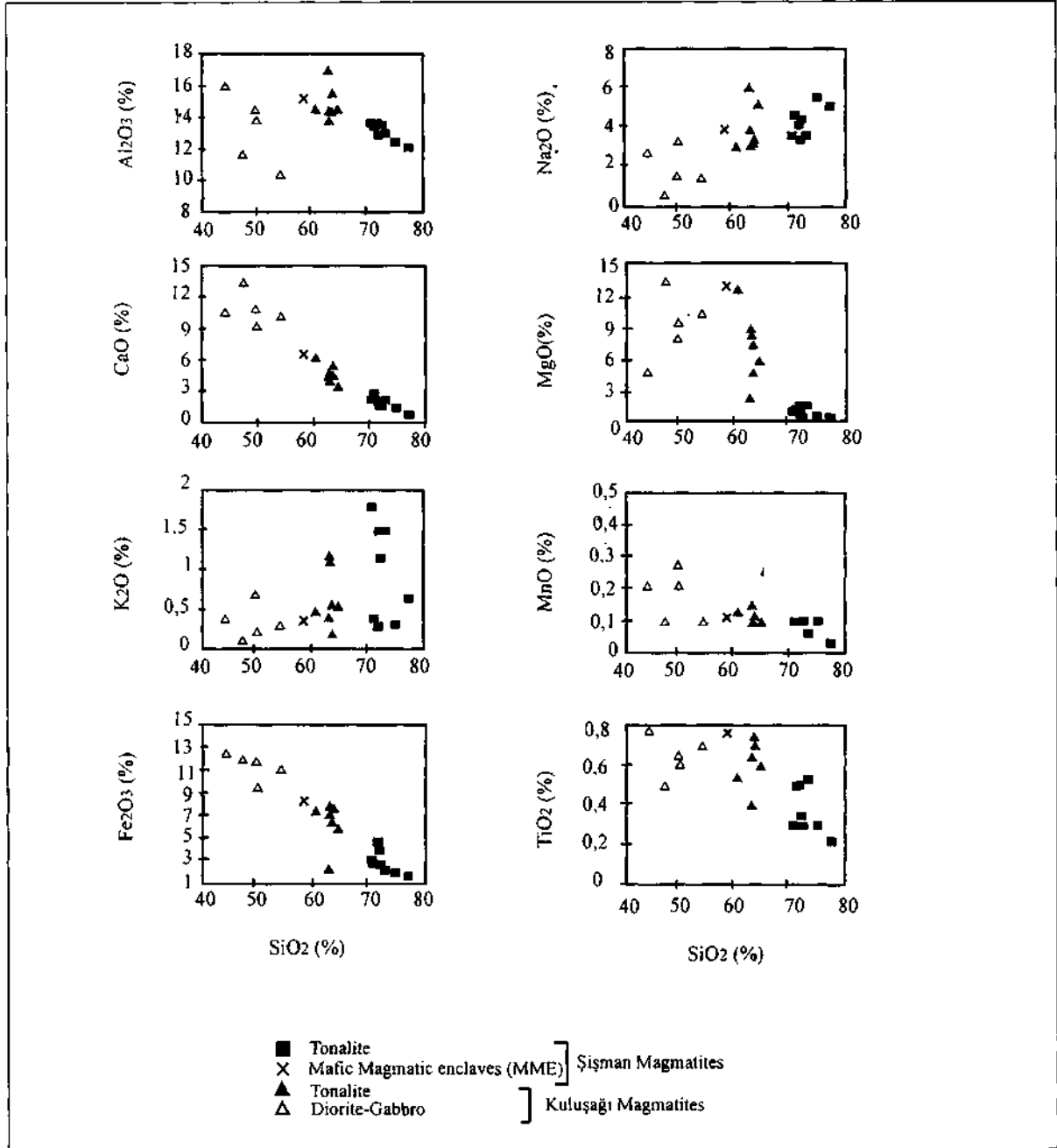


Fig. 8- Variation diagrams of major oxides of Şişman and Kuluşağı magmatites.

with increasing SiO_2 contents, while there is a weak negative correlation in SiO_2 - K_2O variation diagram of Şişman magmatites. There is no significant correlation in MnO - SiO_2 variation diagram (Fig. 8).

SiO_2 values in rock samples of Kuluşağı mag-

matites are ranges from 44.16 to 64.48% while those in Şişman magmatites are changes from 71 to 77.28%. This difference SiO_2 values cause two different clusters to occur in Marker diagrams (Figs. 8 and 9).

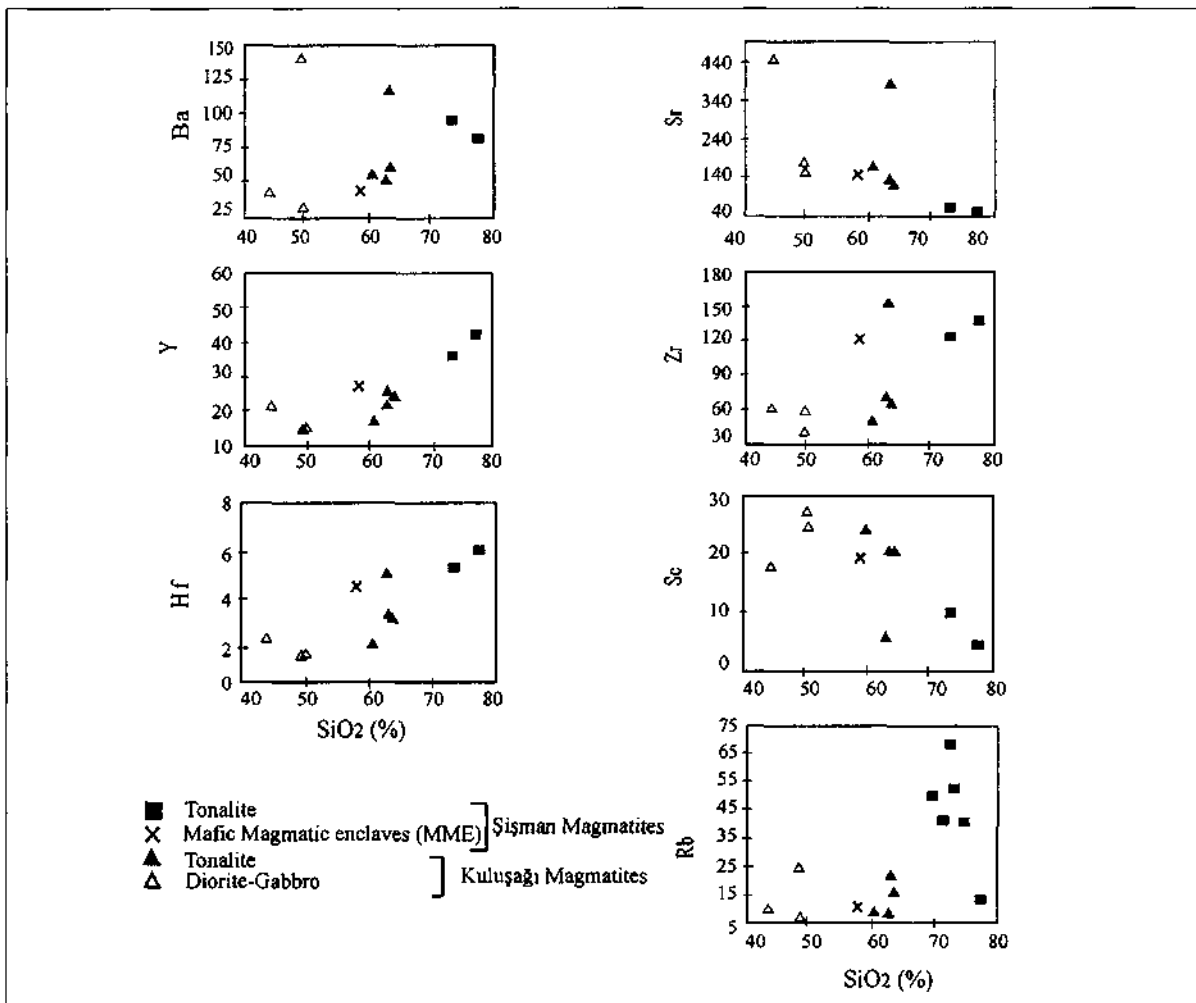


Fig. 9- Variation diagrams of trace elements of Şişman and Kuluşağı magmatites.

Examination of variations of trace elements in rock samples from Şişman and Kuluşağı magmatites reveals that Sc, Y, Zr and Hf contents increase with increasing SiO_2 values while Sr content decreases.

Concentrations of Ba, Rb and Sr, which are known as large ions, are consistent with those of CaO and K_2O . As known, Ba and Rb are retained in K-bearing minerals, while Sr in Ca-bearing minerals (particularly plagioclase). Like CaO, Sr contents are also decreased with respect to increase of SiO_2 concentrations. Observed different correlations in K_2O contents of Şişman and Kuluşağı magmatites

are also detected for Ba and Rb contents. Ba and Rb contents of Kuluşağı magmatites increase with increasing SiO_2 concentrations, while they are decreased in samples from Şişman Magmatites (Fig. 9).

Among high-charged cations, Zr has a concentration ranges from 55 to 74, ppm in Kuluşağı magmatites (except for sample HD-24), while 125 to 139 ppm in Şişman magmatites. Hf, Th, U and Nb also results groupings similar to that of Zr.

Concentration of Y changes from 16.4 to 25 ppm in Kuluşağı magmatites, while it is from 37 to 42.9 ppm in Şişman magmatites.

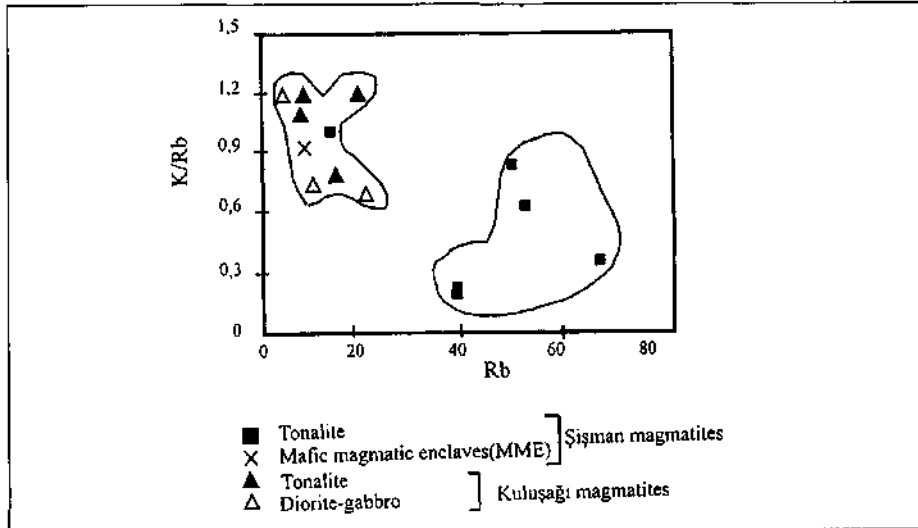


Fig. 10- K/Rb-Rb variation diagram of rock samples from Şişman and Kuluşağı magmatites.

A linear trend is expected in K/Rb-Rb variation diagrams for rock types formed as a result of solidification of a homogeneous magma (Jakes and White, 1970). Whereas, Şişman and Kuluşağı magmatites tend to show different correlations on K/Rb-Rb variation diagrams (Fig. 10). Petrogenetic and trace element studies indicate that these two magmatites are of same magma origin but formed in different stages.

Rock samples from Yüksekova complex plot in

sub-alkaline field on alkali-silica diagram (Fig. 11). In AFM diagram used, for determining sub-magma type, diorite and gabbros of Kuluşağı magmatites plot in tholeiitic field while tonalitic rocks plot on the boundary between tholeiitic and calc-alkaline (Fig. 12). Rocks of Şişman magmatites are located in calc-alkaline field. In A-B diagram of Debon and Le Fort (1982), rock samples of Kuluşağı magmatites show a negative slope in IV and V sectors of meta-aluminous area. As shown in the same diagram, such a trend has a similar extend with main calcemic (CAFEM) trend (Fig. 13).

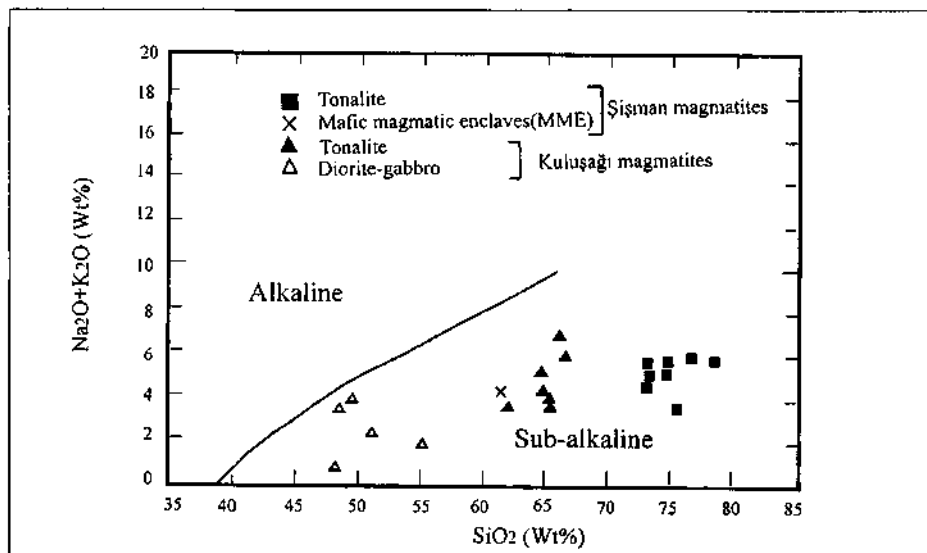


Fig. 11- Position of rock samples from Şişman and Kuluşağı magmatites on total alkali-silica diagram (Irvine and Baragar, 1971).

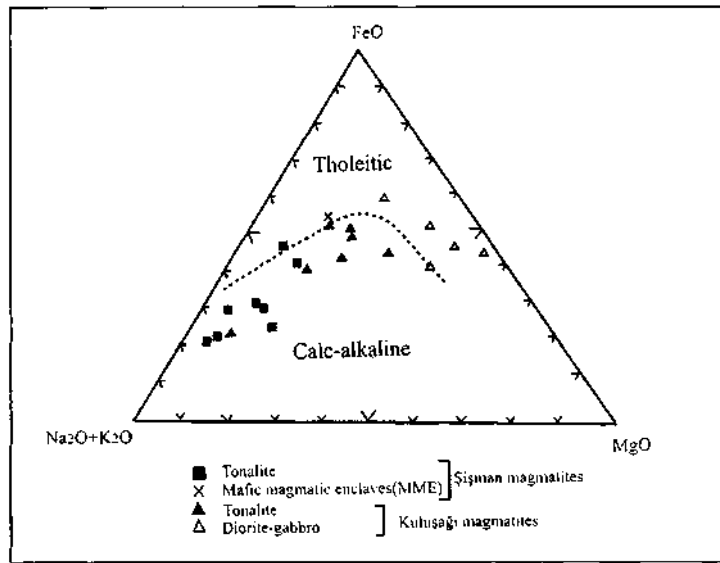


Fig. 12- Position of rocks samples from Şişman and Kuluşağı magmatites on AFM triangular diagram (Irvine and Baragar, 1971).

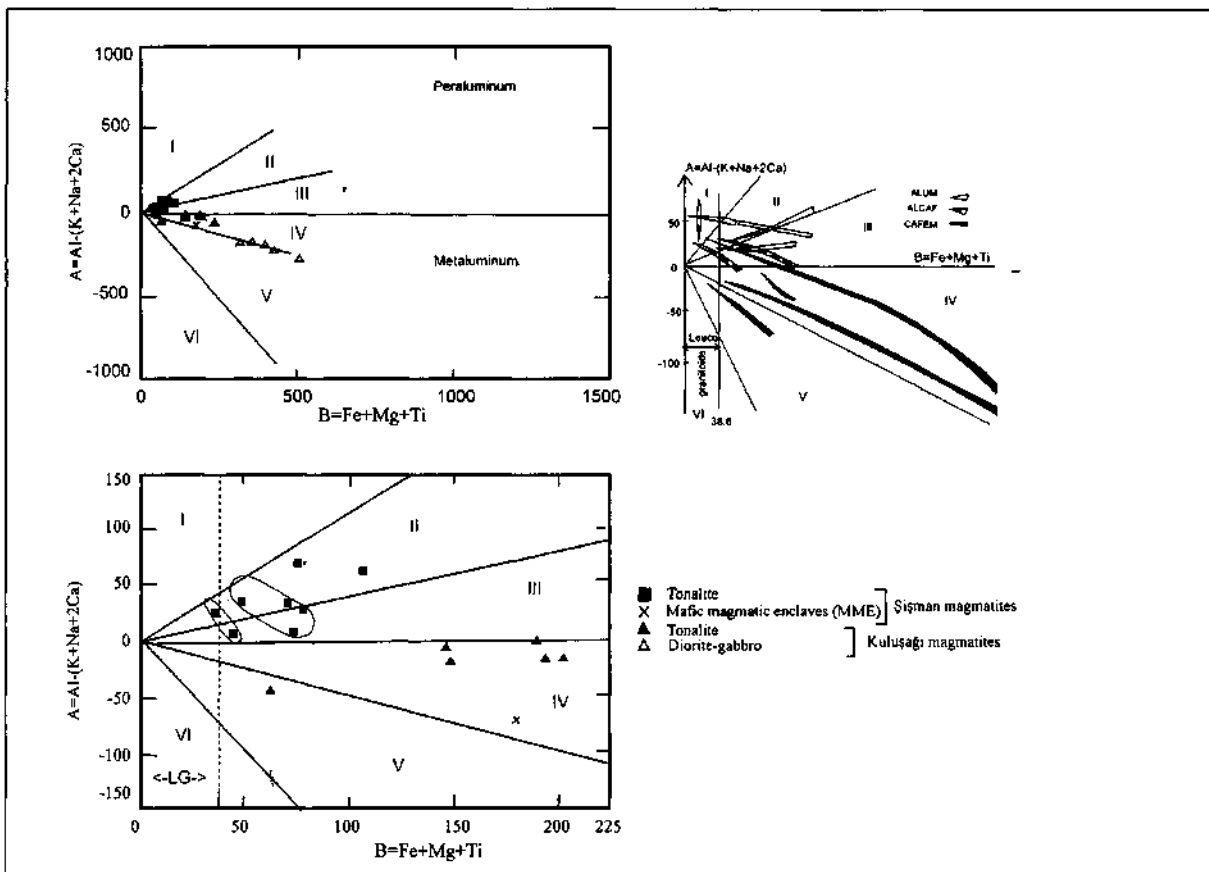


Fig. 13- Distribution of rock samples from Şişman and Kuluşağı magmatites on A-B characteristic mineral (Debon and Le Fort, 1983)

Table 4- Comparison of described features of Şişman and Kuluşağı magmatites to I-S type granitoid classification (Chappel and White, 1974).

Kuluşağı and Şişman magmatites	I-TYPE	S-TYPE
A large SiO ₂ range Composition changes from granodiorite to gabbro	A large SiO ₂ range Composition changes from granite to diorite	SiO ₂ range is limited Composition is not changeable. (In general, leucocratic monzogranites are dominant)
It has volcanic equivalents (Kapıkaya volcanites)	It is found with its volcanic equivalents	No volcanic equivalent
Dark colored minerals are hornblende and biotite	Dark colored minerals: hornblende for mafic types and bitotite for felsic. types	No hornblende. Biotite and muscovite are dominant
Magnetite is more common than ilmenite	Magnetite is dominant ore mineral	Ilmenite is dominant ore mineral
Secondary minerals are sphene and apatite	Orthite, sphene, needle-like apatite are secondary minerals	Monazite, cordierite, garnet, andaluKızmehmet Mahallesi, sillimanite and coarse apatite are secondary minerals
Enclave in tonalite is diorite	Enclaves are hornblende-bearing diorite	Enclaves are of meta sedimentary rock character
Element variation diagrams are generally regular	Element variation diagrams are regular. They are linear or close to linear.	Element variation diagrams are not regular
Na ₂ O is >3.2%-felsic (8 tonalite samples from Şişman magmatites and 2 granodiorite samples from Kuluşağı magmatites)	Na ₂ O in felsic types is >3.2% while Na ₂ O in mafic types is >2.2%	Na ₂ O is <3.2% in rocks with about 5% K ₂ O content while Na ₂ O is <2.2% in rocks with about 2% K ₂ O content
Mol (Al ₂ O ₃) / ((CaO)+(Na ₂ O)+(K ₂ O)) is >1.1 for Şişman magmatites while Mol(Al ₂ O ₃)/((CaO)+(Na ₂ O)+(K ₂ O)) is <1.1 for Kuluşağı magmatites	Mol (Al ₂ O ₃) / ((CaO)+(Na ₂ O)+(K ₂ O)) <1.1	Mol (Al ₂ O ₃)/((CaO)+(Na ₂ O)+(K ₂ O)) is >1.1%
CIPW-normative corundum s 0.52 3.46% in Şişman magmatites while it yields no value in Kuluşağı magmatites	CIPW-normative diopside or <1% normative corundum	CIPW-normative corundum >1%

In A-B diagram of Debon and Le Fort (1982), tonalites of Şişman magmatites show two different negative slopes in II and III sectors of peraluminous area and yield similar trends with main trends of aluminofelsic (CAFEM) assemblages (Fig. 13). This assemblage is derived from a hybrid source formed by mixing of mantle and sialic materials. On the basis of criteria suggested by Chappel and White (1974), except for the findings that Şişman magmatites are peraluminous and contain corundum normatively, all other features of these magmatites are in accordance with I type granitoids. As shown from Table 4, intrusive rocks of Yüksekova complex

completely resemble to I type granitoids, excluding differences of Şişman magmatites.

Based on Shand index (Maniar and Piccoli, 1983) computed using major oxide data, Kuluşağı magmatites have a metaaluminous character, while Şişman magmatites are in peraluminous character (Fig. 14). This feature is consistent with the results of A-B diagram of Debon and Le Fort (1982).

GEOCHEMISTRY OF RARE EARTH ELEMENTS (REE)

Data on rare earth elements of rock samples from Şişman and Kuluşağı magmatites were normalized on the basis of chondrite values described

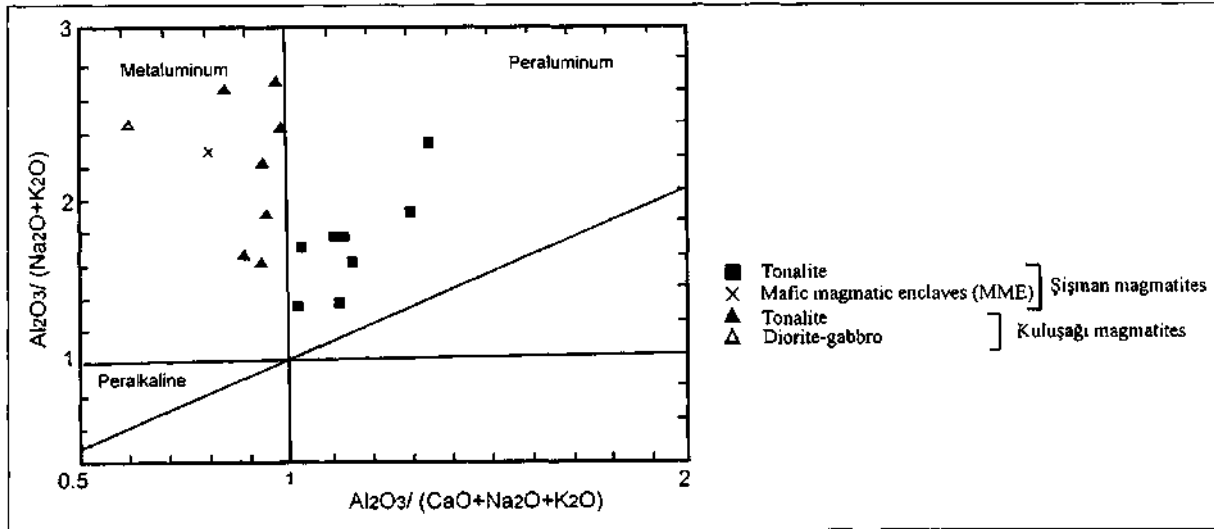


Fig. 14- Position of rock samples from Şişman and Kuluşağı magmatites on Shand index diagram (Maniar and Piccoli, 1983).

by Evensen et al., (1978) (Table 5). Enrichment coefficient of La $((La/Sm)_{CN})$, which is one of light rare earth elements, with respect to that of Sm, which is one of intermediate rare earth elements, and enrichment coefficient of La $((La/Yb)_{CN})$ with respect to that of Yb, which is one of heavy rare earth elements, were examined separately for each rock group of Şişman and Kuluşağı magmatites (Table 6). As shown in Table 6, Kuluşağı mag-

matites are less enriched in heavy rare earth elements in comparison to Şişman magmatites. If they were products of fractional crystallization, gabbroic and dioritic rocks of Kuluşağı magmatites would consume heavy rare earth elements and would be more enriched than Şişman magmatites. This difference between such rock groups is also shown in distribution diagram of normalized rare earth elements (Fig. 15).

Table 5- Normalized values (Evensen et al., 1978) of rare earth element (RRE) contents of rock samples from Şişman and Kuluşağı magmatites.

K U L U Ş A Ğ I M A G I	SAMPLES	La	Ce	Pr	Nd	Sm	Eu	Gd	Tb	Dy	Er	Tm	Yb	Lu	Ho
		KS1-P28	12.2	12	1.25	11.8	11.6	8.7	11.2	15	12.7	13.9	13.6	14.4	13.3
	KS2-P18	15.9	15.9	1.6	14.9	15.9	12.2	14.0	19	16.6	18.6	17.5	18.5	17.3	17
	HD-24	130.8	109.8	7.24	48.9	26.9	14.3	19.6	21	15.9	16.3	16.0	16.7	15.7	15
	KS1-P3	24.9	17.5	1.79	16.7	17	14.1	16.0	21	17.5	19.9	19.5	19.5	18.5	18
	HD-27	44.5	41	3.45	27.7	20.5	15.8	17.2	20	16.0	16.2	14.4	14.9	13.7	15
	HD-50	34.7	30.7	2.41	19.2	14.9	12	12.9	15	12.0	12.3	11.7	11.8	11.0	11
	HD-51	29.8	30.4	2.32	19.2	14.8	12.5	12.1	15	12.1	11.8	10.9	11.0	1.2	11
	KS4-24	20.8	23.5	2.35	22.8	22	12.4	20.6	28	23.8	27.7	27.3	29.0	28.3	24
	HD-180	17.1	22.4	2.1	19.9	19.4	14.9	17.2	22	18.2	20.5	19.9	21.1	2.0	18
	HD-106	22.4	26	2.57	25.1	27.4	11	27.2	36	33.1	38.9	38.6	40.5	39.7	34

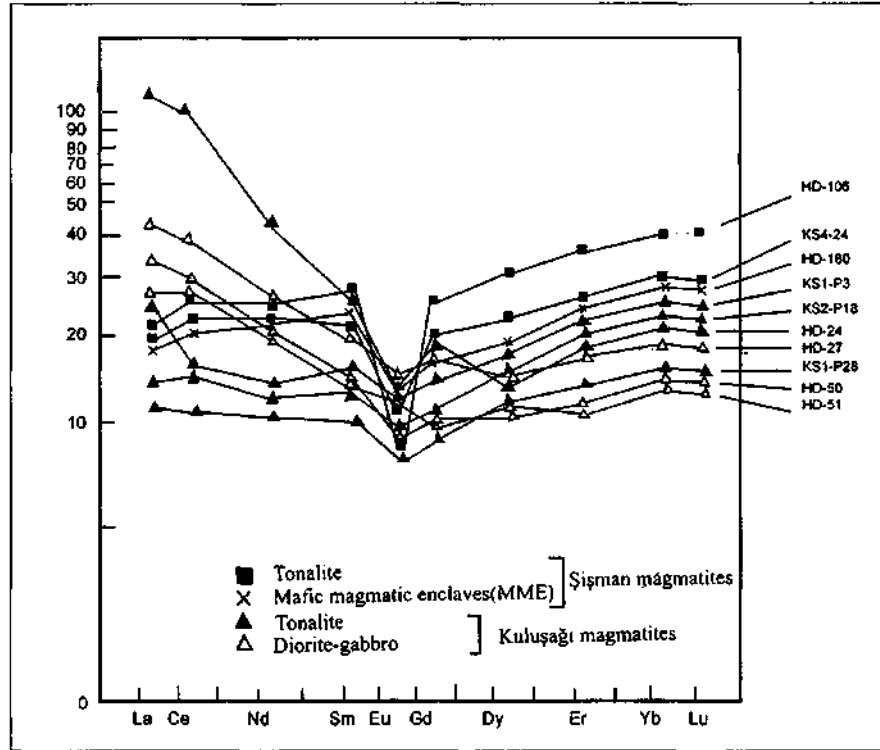


Fig. 15- Distribution of chondrite-normalized values of NTE contents of şişman and Kuluşağı magmatites.

Table 6- $(La/Sm)_{CN}$ and $(La/Yb)_{CN}$ values of rock samples from Şişman and Kuluşağı magmatites.

	Sample No	Rock name	$(La/Sm)_{CN}$	Average	$(La/Yb)_{CN}$	Average
K U L U Ş A Ğ I M A Ğ	KS1-P28	Tonalite	1.05	1.02	0.85	0.85
	KS2-P18		1		0.85	
	HD-24		4.86		7.83	
	KS1-P3	Gabbro-Diorite	1.46	1.98	1.28	2.49
HD-27	2.17		2.99			
HD-50	2.32		2.99			
HD-51	2		2.70			
Ş İ Ş M A N M A Ğ	KS4-24	Tonalite	0.94	0.88	0.71	0.63
	HD-106		0.82		0.55	
	HD-180	MME (mafic magmatic enclave)	0.88		0.81	

The fact that curves drawn for rock groups of Şişman and Kuluşağı magmatites are consistent with each other but not internally consistent indicates that Şişman and Kuluşağı magmatites belong to different formation stages.

RELATION BETWEEN MINERALIZATION AND ALTERATION

DISTRIBUTION OF MINERALIZATION

East-west extending Kızme Mehmet site copper mineralization is observed along two parallel structural lines with a length of about 6 km. and a width of 1 km. The one in north begins from eastern part of Kızme Mehmet site and extends towards Mişmiş hill. The one in south extends from the Taşlı hill ridge at east to Ziyaret hill - Harabe hill ridges at west. These lines belong to old fractures and are filled with acidic dikes of Harabe hill magmatites. In connection with N60°E and N60°W trending tension fractures, these lines give rise to formation of large ore and alteration packets (Fig. 16).

MINERALIZATION TYPES

Based on mode of occurrence observed within the magmatic suite, mineralization in the study area may be categorized into three main groups; namely vein type, coating in fracture and fissures, and disseminated type mineralizations. Mineralization

types and relation between ore minerals and alteration are summarized in Table 7.

Vein type mineralizations

Iron mineralizations.- Black colored iron mineralizations are generally observed as veins on the boundary between tonalites of Şişman magmatites and dacites of Harabe hill magmatites. They are well exposed around Harabe hill. They have a thickness of 5 cm. to 50 cm. and an extension of 10 m. to 100 m. Dominant strike and dips of iron veins are N80°E/35°NW and N10°W/35°SW.

In this mineralization, macroscopically observed ore minerals are hematite, magnetite, and lesser amounts of malachite. Chloritization and silicification are detected as the main alteration types in massive magnetite veins.

Mineralizations in association with barite vein. - Barite vein which is exposed only 400 m. southeast of Taşlı hill in the study area has a position of N70°E/45°NW. This vein with a thickness of 0.5 to 2 m. continues 100 m. Stockwork zones, that are cut by quartz veins and consist of galena, pyrite and chalcopyrite minerals with a thickness of 1.5 m. are found at lower and upper parts of barite veins within andesites which are subjected to epidote-chlorite-carbonate alteration.

Table 7- Mineralization types of ore minerals and their distribution in alteration assemblages.

Ore Mineral	Alteration Type			Mineralization Type	
	Potassic	Propylitic	Phyllitic	Disseminated	Veinlet/Vein
Pyrrhotite	X	X		X	
Magnetite	X	X		X	X
Rutile		X	X		
Pyrite	X	X	X		X
Chalcopyrite	X	X	X		X
Sphalerite		X			X
Bornit		X			X
Galena		X			X

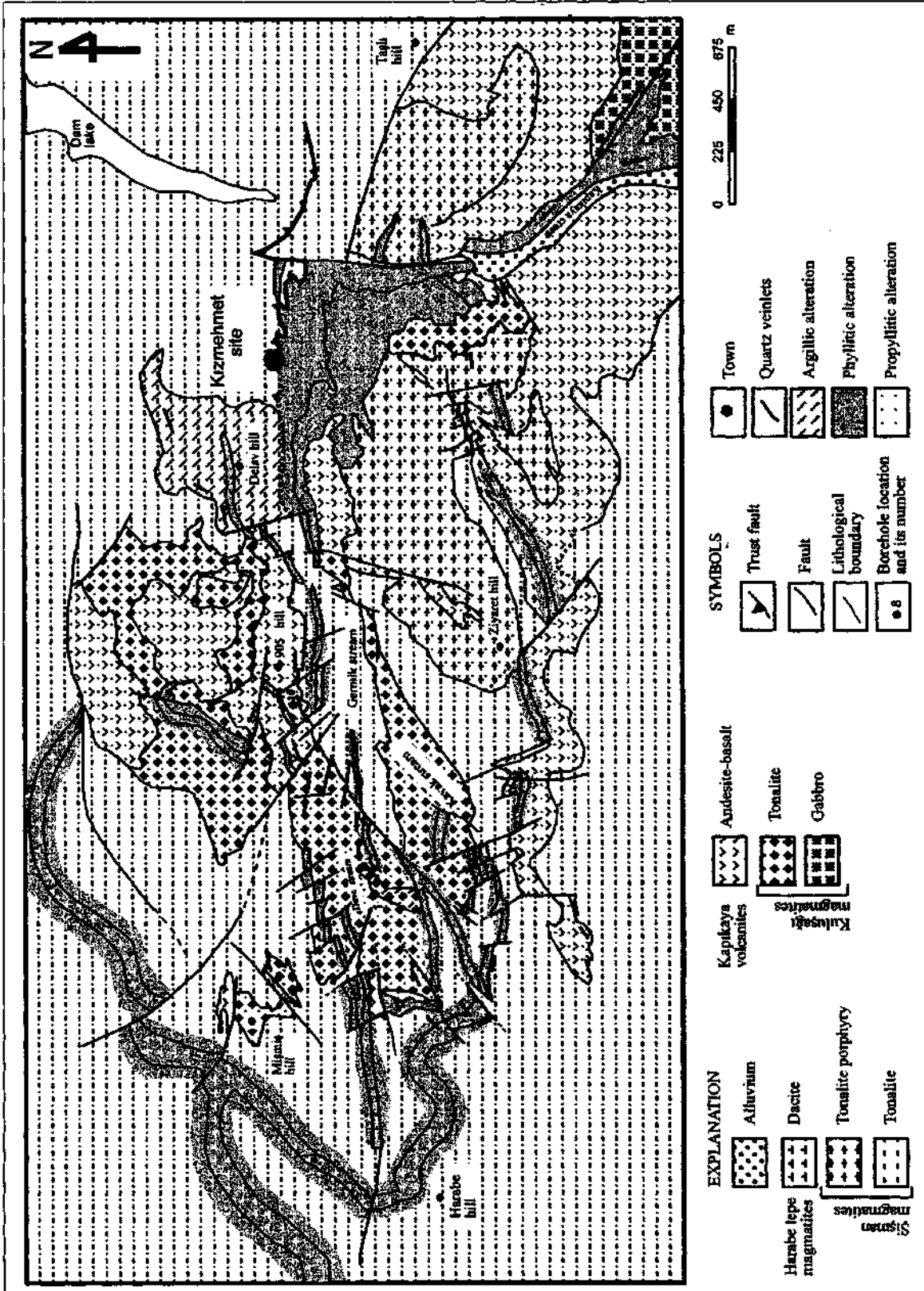


Fig. 16- Structure and lithology map of Kizme Mehmet site.

Mineralizations in association with quartz-carbonate vein and veinlets.- Quartz and carbonate veins are observed together with propylitic alteration locating between Ziyaret hill, Taşlı hill and Deve hill. Their thickness changes from a few cm. to 1 m. The dominant strike and dip of quartz and carbonate veins in N60°E/65°NW. In addition, capillary quartz and carbonate veinlets in intense propylitic and sericitic belts show a stockwork appearance.

Chalcopyrite, magnetite, hematite and bornite are observed in quartz and carbonate vein/veinlets within the propylitic zone, while Chalcopyrite and pyrite are absent in quartz and carbonate vein/veinlets of phyllitic zone.

Coating type mineralization in fissure and fractures.- This type of mineralization is detected variously trending fissure and fractures of the rocks. The main minerals of coating type mineralization, that is widely exposed in all units of the study area, are pyrite and Chalcopyrite. These minerals are completely altered on the surface, If coating type mineralization is existed in propylitic zone, chloritization is very intense at the contact with country rock. If it is found in phyllitic zone, secondary quartz and an intense sericitization are observed at the contact.

Disseminated type mineralization.- Disseminated type mineralization in chlorite-epidote zone is composed of fine grained Chalcopyrite, pyrite, magnetite, and a lesser amount of pyrrhotite, while that in quartz-sericite alteration zone consists of pyrite and Chalcopyrite. Ore minerals of biotite-quartz zone are disseminated magnetite, pyrite, pyrrhotite and a lesser amount of Chalcopyrite.

MINERALOGY, STRUCTURE AND TEXTURE OF MINERALIZATION

Main ore minerals of Kizmehmet site pyrite-copper mineralization are pyrite, Chalcopyrite and magnetite. In addition to these minerals, pyrrhotite, galena, sphalerite, bornite, rutile-anatase and ilmenite were determined as the accessory minerals. Moreover, secondary limonite, hematite, maroasite, chalcocite and covellite were also observed.

Due to mineralogic relations explained below, mode of occurrence was determined from older to younger as follows: (I) pyrrhotite, magnetite, rutile and ilmenite, (II) pyrite, (III) Chalcopyrite and sphalerite, (IV) bornite and (V) galena.

Pyrrhotite.- Disseminated pyrrhotite is found in propylitic and potassic alteration zones. In general, pyrrhotite with euhedral and subhedral forms is found in pyrite as inclusions and in some cases, it occurs on the boundary with Chalcopyrite.

Magnetite.- Magnetite is existed in veins and also it disseminates in propylitic and potassic alteration zones. Magnetites in massive veins are subhedral and euhedral and changed to hematite in places. Magnetites in propylitic and potassic zones are observed in two types. First is euhedral, coarse grained magnetites and the second is anhedral magnetites which are formed by oxidation of iron originated during alteration of the mafic minerals to chlorite and decomposition of them along the cleavages.

While first type of magnetites change to hematite, second type of magnetites do not show any sign of decomposition. Magnetites have an intermediate reflection strength and brown and grayish colors.

Rutile.- Rutile is commonly observed in phyllitic zone and it has a needle-like shape.

Ilmenite.- Under microscope, ilmenite appears in pink-brown and gray-white colors. It has a certain reflection pleochroism and anisotropy.

Pyrite.- Pyrite often observed together with Chalcopyrite, is commonly found in three types of mineralization. It is detected in all types of determined alterations in the study field.

Pyrites in rock samples in which oxidation is intensely observed are partly or completely changed to limonite. Due to cataclasis effect, pyrites gain a brecciated appearance and are changed to limonite along fracture and fissures. In addition, fracture and fissures of pyrites, that are undergone to a cataclasis, are filled with chalcopyrite in places.

Inclusions detected in pyrite are pyrrhotite, magnetite and rutile. Distribution of inclusions in pyrite crystals is irregular. Pyrite itself is observed as inclusions in chalcopyrite and galena.

Scanning-Electron Microscope (SEM) studies performed on element content of pyrite yielded 46% Fe and 53% S.

Chalcopyrite. - In general, chalcopyrite is found as anhedral grains. Scanning Electron Microscope (SEM) studies performed on element contents of chalcopyrite yielded 34.5% Cu, 31.66% Fe and 33.82% S.

In addition, as a result of SEM studies, unknown mineral inclusions of 5 micron in size with two different compositions were determined in chalcopyrite. Elemental composition of one of these inclusions is 33.71% Co, 29.21% Mg, 27.28% S, 6.33% Fe and 3.46% Cu, while second inclusion has a composition of 25.45% Cu, 0.01% Al, 14.4% Ca, 25.49% Fe and 34.90% S.

It was observed that chalcopyrite was changed to malachite and limonite in oxidation zone, while it was altered to chalcosite and covellite in cementation zone. SEM quantitative point analysis conducted on covellites yield a composition of 69.50% Cu, 18.89% Fe, 9.65% S and 1.96% Si. SEM quantitative point analysis conducted on chalcosites yield a

composition of 79.17% Cu, 18.34% Fe, 1.19% S and 1.31% Si.

Sphalerite. - Sphalerite With anhedral grains contain chalcopyrite and pyrite inclusions.

Bornite. - Bornite is seldom detected in quartz veins within the propylitic zone. Bornites of anhedral grains are associated with chalcopyrite and hematite and contain chalcopyrite inclusions in places.

Galena. - Galena is generally found with pyrite and sphalerite and they contain pyrite inclusions in some places. Galena in association with sphalerite is observed in sutures.

Marcasite. - Marcasite is detected as anhedral grains or bar-like shapes. It is generally developed in association with sphalerite, chalcopyrite and galena.

RELATION OF ALTERATION TO MINERALIZATION

Radial dikes of dacitic composition of the Harabe hill magmatites and granodiorite porphyries at depth (cut in drill holes) are rocks which facilitate Kızmehtmet site copper mineralization (Fig. 17).

It is observed that units of Harabe hill magmatites and surrounding rocks are subjected to phyllitic alteration. Phyllitic belt is cut by quartz

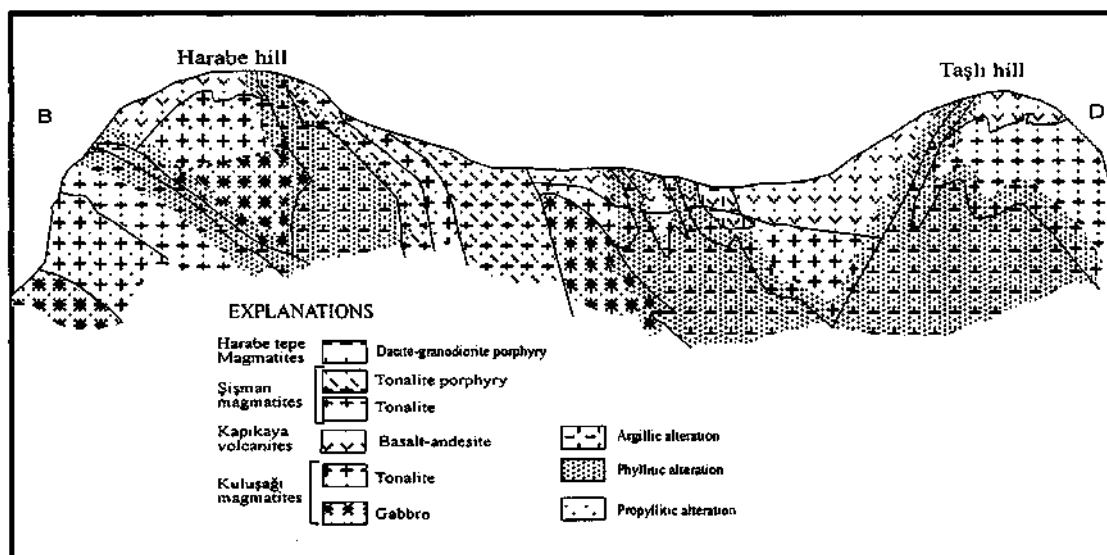


Fig. 17- A schematic section showing relation among rock assemblages within the Yüksekova complex (no scale).

veins which contains pyrite-chalcopyrite zone of 1 cm to 0.5 m thicknesses. Cu, Pb, Zn, As and Ag contents of rock samples collected from these Kız Mehmet site are 1.07%, 80 ppm, 296 ppm, 56 ppm and 3.3 ppm, respectively (Tüfekçi and Dumanlılar, 1994).

Consistent phyllitic alteration in dacites of Harabe hill magmatites is surrounded by propylitic alteration, that is widely exposed in the area. Between these two halos, argillic alteration is observed in south of Kız Mehmet site and in Kavak stream. Quartz, carbonate and barite veins associated with pyrite, magnetite, chalcopyrite and galena minerals are present in N70E/45°NW propylitic zone. Average Cu, Pb, Zn, As and Ag element concentrations of samples collected from this zone are 0.015%, 0.7%, <0.1%, <0.4% and 2.5 ppm (Tüfekçi and Dumanlılar, 1994). In comparison with phyllitic hole, Cu concentrations are decreased, while Pb values are increased.

Coating type sulfite mineralization and ore-bearing quartz capillary vein as well as disseminated pyrite are observed on intensely altered at the 905 hill and in the area between Kavak and Deve stream. Cu concentrations in this area changes from 0.04% to 4.44% in the studied samples (Tüfekçi and Dumanlılar, 1994).

Like on the surface, well developed phyllitic alteration zones in drill zones are also detected around dacite and granodiorites of Harabe hill magmatites.

A potassic alteration and a copper anomaly were determined at depths between 0 and 50 m in KS-5 well drilled along Kapıkaya creek.

Although no Au anomaly was found at the surface within Kız Mehmet site copper mineralization, gold concentrations of 0.14-2.62 ppm were determined at depths between 80 and 130 meters in KS-3 well. In addition, a gold concentration of 1 ppm was also detected at depths between 97 and 100 m in KS-7 well. Chemically determined gold in samples was not clearly seen during polished section determination. During limited SEM studies conducted on these samples no visible gold grain was

observed. Also propylitic alteration is dominant alteration type in levels where gold concentrations are chemically determined, which is surrounded by phyllitic alteration. However, the presence of Cl, P and S determined in these samples by SEM studies, indicates that magma is saturated with aqueous fluids and forms a suitable environment for gold transportation. Aydal (1989) and Aydal et al., (1992) who studied gold-bearing quartz veins in Hatay-Kisecik, stated that As, Zn, Cu, S and P_2O_5 concentrations are increased in gold-bearing hydrothermal vein contacts.

If any gold presence detected in porphyry copper mineralizations, it is generally found as disseminated grains in sulphite minerals or veins, and in quartz. Highest gold concentration is observed in potassic zone. In addition, small but high-grade gold-silver-chalcopyrite veins are found in propylitic belt, while gold disseminations raising due to highly acidic fluids are detected in the argillic zone (Sillitoe, 1981). Intrusive rocks of Yüksekova complex associated with Kız Mehmet site porphyry copper mineralization show some similarities to country rocks of similar mineralizations given in the literature. Porphyry Cu-Mo or Cu-Au deposits are generally a part of ore zoning of main arc granitoids (Sillitoe, 1981).

Granitoids hosting porphyry copper enrichments are generally classified as I type granitoids (Chappel and White, 1974). As known, this type of granitoids are originated from areas very close to magma and are closely associated with subduction processes (Sawking, 1984). Composition of intrusives related to porphyry copper mineralizations is from diorite to granite. Intrusives in porphyry copper mineralization areas generally cut each other and are settled as multi-phase intrusions (Erler, 1981).

The difference of gold-bearing porphyry copper deposits from other Cu-Mo systems may be explained as follows: (a) Known gold-rich porphyry copper deposits are poor in Mo, (b) 80% of deposits are rich in hydrothermal magnetite and (c) They may be found in volcano-plutonic island arc and continental margins (Sillitoe, 1981). These features

are consistent with those of Kızme Mehmet copper mineralization.

RESULTS

Results of geologic, petrographic and geochemical studies conducted in the study area may be summarized as follows:

Three main units were differentiated around İspendere. Jurassic-Lower Cretaceous İspendere ophiolite is located at south of the study area and it has a tectonic contact with Upper Cretaceous aged Yüksekova complex. At north, Yüksekova complex is unconformably covered by Eocene aged Kirkgeçit formation.

Yüksekova complex, which is related to mineralization around Kızme Mehmet site was differentiated as Kuluşağı magmatites (gabbro, quartz diorite and tonalite), Kapıkaya volcanites (andesitic and basaltic volcanic rocks), Şişman magmatites (tonalite and tonalite porphyry) and Harabe hill magmatites (dacite and granodiorite), and all were mapped.

Based on total alkaline-silica and AFM diagrams for Kuluşağı and Şişman magmatites, gabbro and quartz diorite type rocks are product of a tholeiitic character, while other rock groups are product of a calc-alkaline type magma. According to Debon and Le Fort (1982) and based on Shand index criteria, Kuluşağı magmatites exhibit a cafemic (CAFEM) assemblage character in which Metaaluminous type mantle material is dominated, while Şişman magmatites exhibit an aluminocafemic assemblage type in which sialic origin of peraluminum character is dominated.

Harker diagrams constructed on the basis of rare earth elements and trace element geochemistry, indicate that Kuluşağı and Şişman magmatites are formed at different stages by subduction processes, and it is also approved by petrogenetic and tectonogenetic data. Based on these data, Kuluşağı and Şişman magmatites are I type volcanic arc granitoids (VAG) of a calc-alkaline character (except for the character that $(Al_2O_3)/(CaO)+(Na_2O)+(K_2O)$ ratio of Şişman magmatites is $>1,1$).

Mineralization is related to Harabe hill magmatites and it is observed within these magmatites or rocks having contact with them (Kuluşağı magmatites, Kapıkaya volcanites and Şişman magmatites). Mineralization is detected as disseminated grains in quartz-carbonate veins and fracture-fissures, while as coating within the rock.

Main ore minerals in the order of abundances are pyrite, chalcoprite, and magnetite. In addition to these minerals, pyrrhotite, sphalerite, bornite, galena, rutile-anatase, ilmenite and gold-silver (chemically) were also determined. Moreover, limonite, hematite, marcasite, chalcocite and covellite were observed as secondary alteration products.

Ore paragenesis in the order of occurrence, from older to younger was determined as follows: (I) pyrrhotite, magnetite and rutile, (II) pyrite, (III) chalcoprite and sphalerite, (IV) bornite and (V) galena.

Four different alteration types are recognized in association with mineralization. Alteration types described are potassic, propylitic, phyllitic and argillic. Mineralization is generally associated with quartz veinlets and sulfite coatings in phyllitic and propylitic alterations.

On the basis of geometric features, mineral paragenesis and alteration types determined in Kızme Mehmet site pyrite-copper mineralization, mineralization can be thought of a porphyry or stockwork pyrite-copper type mineralization.

Kızme Mehmet site copper mineralization is similar to pyrite-copper mineralizations in the literature by means of origin and tectonic setting and is found in multistage I type granitic rocks associated with volcanic island arc granitoids.

ACKNOWLEDGEMENTS

This study is a part of GAP Mineral Exploration Project conducted by Department of Mineral Research of General Directorate of MTA. Authors thank to senior geologist M. Şahin Tüfekçi and other project staff, for their contributions in the field and during the preparation of the manuscript.

Manuscript received March 2. 1999

REFERENCES

- Ashley, P. M., Billington, W. G., Graham, R.L. and Neale, R.C., 1978, Geology of the Coalstoun Porphyry Copper Prospect, Southeast Queensland, Australia: *Econ. Geol.* Vol. 73, pp. 945-965.
- Asutay, H.J., 1985, Baskil (Elazığ) çevresinin jeolojik ve petrografik incelenmesi: A.Ü. Fen Bilimleri Enst. Doktora Tezi, (unpublished), 156 s, Ankara.
- , 1986, Baskil (Elazığ) çevresinin jeolojisi ve Baskil magmatitlerinin petrolojisi. *MTA Bull.*, 107, 49-72, Ankara.
- Aydal, D., 1989, Doğan Ocak (Kisecik-Hatay) altın kuvars damarının mineralojik ve jeokimyasal olarak incelenmesi: *Selçuk Üniv. Mim. Müh. Fak. Derg.*, 4/2, 26-40.
- , Bülbül, M., and Kadioğlu, K., Y., 1992. Hatay altın yataklarının jeokimyasal olarak incelenmesi: *Türkiye Jeoloji Bült.*, C. 35., 49-59.
- Baykal, F., 1966, 1:500.000 ölçekli Türkiye Jeoloji Haritası, Sivas paftası, MTA publ., Ankara.
- Beyarslan, M., 1991, İspendere Ofiyolitinin petrografik özellikleri: F.Ü. Fen Bilimleri Enst, Yüksek Lisans Tezi, (unpublished), 57 p, Elazığ.
- Bilgöl, A.F., 1984, Geology of the Elazığ area in the Eastern Taurus region: In: O. Tekeli ve M.C. Göncüoğlu (eds), *Geology of the Taurus Belt int symp. Proceedings* 199-208.
- Chappel, B.W. and White, A.J.R., 1974, Two contrasting granite types: Expanded abstract, *Pacific Geology*, 8, 173-174.
- Debon, F. and Le Fort, P., 1982, A chemical mineralogical classification of common plutonic rocks and associations: *Transactions of the Royal Soc. Of Edinburg: Earth Sci.*, 73 p. 135-149.
- Dumanlılar, Ö., 1993, İspendere, (Malatya) civarı magmatitlerinin jeolojisi ve petrografisi. A.Ü Fen Bilimleri Enst, Yüksek Lisans Tezi, (unpublished), 62 p, Ankara.
- Erler, A., and Aral, H. 1981, Porfiri Bakır Yatakları: ODTÜ Müh. Fak. Yayl., No:67, Ankara.
- Evensen, N.M., Hamilton, P.J. and O'nions, R.K., 1978, Rare earth abundances in chondritic meteorites. *Geochim. Cosmochim. Acta*, 42, 1199-1212.
- Hempton, M. and Savcı, G., 1982, Elazığ Karmaşığının petrolojik ve yapısal özellikleri: *TJK Bült.*, 25. 2. 143-150.
- Irvine, T.N. and Baragar, W.R.A., 1971, A guide to the chemical classification of the common volcanic rocks: *Can. Jour. Earth Sci.*, 8, 523-548.
- Jakes, P. and White, J.R., 1970, K/Rb ratios of rocks from island arcs. *Geochim. Cosmochim. Acta*, 34. 849-856.
- Lowell, J.D. and Guilbert, J.M., 1970. Lateral and vertical alteration-mineralization zoning in porphyry ore deposits. *Econ. Geol.*, 65, 373-408.
- Maniar, P.D., and Piccoli, P.M., 1989, Tectonic Discrimination of Granitoids: *Geol. Soc. Of America Bull.*, v. 101, p. 635-643.
- Pearce, J.A., Harris, N.B.W and Tindle, A.G., 1984, Trace element discrimination diagrams for the tectonic interpretation of granitic rocks. *J. Petrology*, vol. 25, P 956-983.
- Perinçek, D., 1979, The Geology of Hazro-Korudağ-Çüngüş-Maden-Ergani-Hazar- Elazığ- Malatya Area: *Guide Book, Tür. Jeol. Kur. Bull.*. 33s.
- Poyraz, N., 1988, İspendere-Kömürhan (Malatya) Ofiyolitlerinin jeolojisi ve petrografisi. Doktora Tezi, G.Ü. Fen Bilimleri Enst., 151 s. (unpublished), Ankara.
- Sawkins, F. J., 1984. *Metal deposits in relation to plate tectonics.* Springer-Verlag Berlin Heidelberg. 325 s.
- Sillitoe, R.H., 1981, Ore deposits in Cordilleran and island-arc settings: *Ariz. Geol. Soc. Dig. Vol. XIV*, 49-70.
- , 1993, Gold deposits in Western passific island arcs: The magmatic connection: *IAEG weekend course 8-9 May, Tralee-Ireland.*
- Sirel, E., Metin, S. and Sözeri, B., 1975, Palu (KD Elazığ) denizel-Oligosen'nin stratigrafisi ve mikro paleontolojisi-Türkiye Jeol. Kur. Bült., C. 18, 175-80.
- Streckeisen, A., 1976, To each plutonic rock, its proper name. *Earth Sci. Rev.*, 12, 1-13.
- Turan, M., 1984, Baskil-Aydınlar (Elazığ) yöresinin stratigrafisi ve tektoniği: Doktora Tezi. FÜ Fen Bil. Enst., 180 s. (unpublished).
- , Aksoy, E. and Bingöl, F.A., 1995, Doğu Torosların jeodinamik evriminin Elazığ civarındaki

- özellikleri: FÜ Fen ve Müh. Bil. Bull., 7 (2), 177-199.
- Tüfekçi, M.S., Balçık, A., Ulutürk, Y., and Minas, M., 1979, Keban ve civarının molibden cevheri olanakları: TJM Kongresi Bült.-1.
- and Dumanlılar, Ö., 1994, Malatya-İspendere ve Elazığ-Baskil-Nazaruşacı arasında görülen cevherleşmelerin genel görünümü ve maden jeolojisi çalışma raporu: MTA Rep. No: 9739 (unpublished) Ankara.
- Yazgan, E., 1981, Dođu Toroslarda etkin bir Paleo-kita kenarı etüdü (Üst Kretase-Orta Eosen): HÜ Yerbilimleri, 7,83-104.
- and Asutay, H.J., Gültekin, M.C., Poyraz. N., Sirel, E. ve Yıldırım, H., 1987, Malatya güneydoğusunun jeolojisi ve Dođu Torosların jeodinamik evrimi MTA Rep. No: 2268.
- , and —————, 1981, Definition of Structural units located between Arabian platform and Munzur Mountains and their significance in the geodynamic evolution of the area 35 th Congr. Geol. Soc. Turkey, abstracts p. 44-45.
- , and Chessex, R., 1991, Geology and tectonic evolution of the Southeastern Taurides in the region of Malatya. Tür. Petrol Jeol. Der. Bult., 3. 11-42.

THE INDEX MINERALS AND MINERAL ASSEMBLAGES DETERMINED IN METAMORPHITES OF EVCİLER-ÇATKÖY (ÇAYIRALAN-YOZGAT) SEGMENT OF AKDAĞMADENİ MASSIF

M.Bahadır ŞAHİN* and Yavuz ERKAN**

ABSTRACT.- In the studied area, which is representing some part of metamorphic rocks of Akdağmadeni massif, some index minerals and mineral assemblages reflecting progressive regional dynamo-thermal metamorphism have been determined. In the metapelites belonging to the bottom levels of metamorphic rocks, the index minerals such as biotite, garnet, staurolite, kyanite, orthoclase and sillimanite and their assemblages have been determined; in the semi-pelitic rocks which take place above the metapelitic series we see index minerals such as plagioclase, calcite, diopside, hornblende, tremolite and their assemblages with the increasing carbonate in environment. In the metacarbonates that we see widely at the top most of metamorphic series, the mineral groups such as calcite, epidote, plagioclase, diopside and tremolite were found and they reflect metamorphism conditions. In the mineral assemblages originated from various amphibolites found almost in every lithology of metasedimentary sequence as intercalations and lenses, we see hornblende, plagioclase and garnet as index minerals. Looking at the experimental formation conditions of the mineral assemblages mentioned above, we could say that the metamorphic rocks of the studied area were formed under the progressive regional dynamo-thermal metamorphism conditions. It is pointed out by looking at the index minerals and mineral assemblages in metapelitic derivatives, metamorphism has occurred at 400-700 °C temperature and 3.5-6.5 kb pressure conditions progressively. The mineral assemblages found in semi-pelitic derivatives and metacarbonates also show a progressive metamorphism of 350-600 °C and medium-high grade. The mineral assemblage we see in the lithologies such as amphibolites reflects about 600 °C temperature and 6 kb pressure conditions.

INTRODUCTION

The metamorphic masses crapping out between Yozgat, Sivas, Kayseri, Niğde and Kırıkkale provinces in Central Anatolia are named as Central Anatolian massif (Ketin, 1983). The names central anatolian crystalline basement (Tolluoğlu, A.Ü. and Erkan, 1989) and Central Anatolian Complex (Erlar, A. and Bayhan, H., 1995) has also been used.

The Akdağmadeni massif (Fig. 1) is the largest of many independent metamorphic masses and located NE of the region. The massif is overlain by Mesozoic and Cenozoic units and is considered by many miners and geologists since 19th century because of its metallogenic potential. The mining and investigations, especially basic geologic investigations of ore deposits started towards the end of 1970's scientifically. The first observations founding these investigations were made by Pollak (1958) and Vache (1963). Investigators described the

metamorphic rock groups as quartzite, marble, micagneiss, mica schist, and mica quartzite. Pollak (1958) divided these rock groups into three series namely basement series, marble series and upper series. Vache (1963) explained that the basement rocks have been metamorphosed under mesokatazonal conditions and medium and upper series under epizonal conditions. But the later studies dealing metamorphism doesn't support this idea of Vache (1963).

Erkan (1980) depending on the field observations, mineral characteristics and the mineral assemblages found in very thick metasedimentary rocks such as calcsilicate gneiss, gneiss and amphibolite in east of Akdağmadeni, says that it is impossible to divide the regional metamorphic rocks of this region into upper and basement series. He also states it is not easy to say that, first a high-grade regional metamorphism and then a low-grade metamorphism were effective in the region. He re-

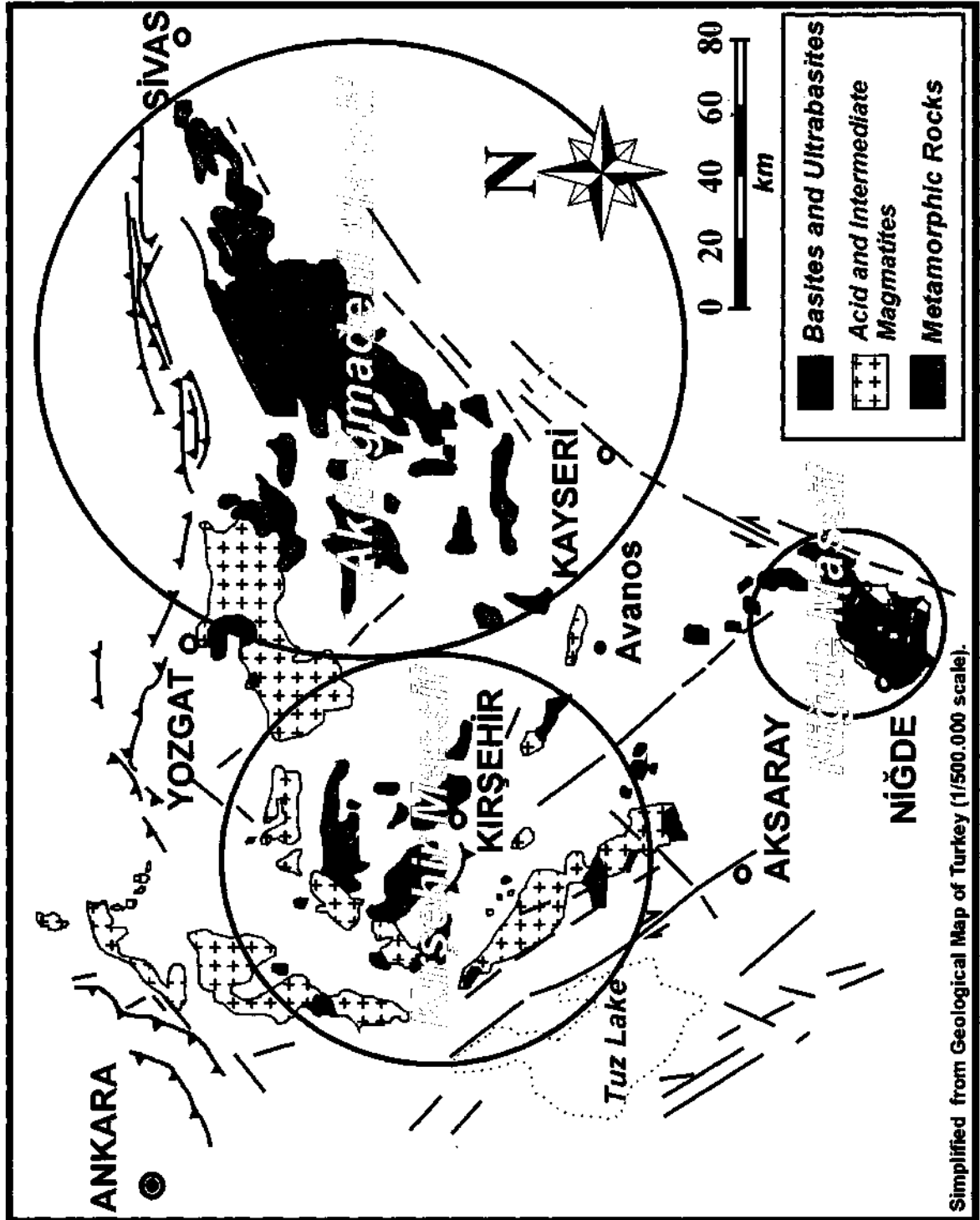


Fig. 1 - Metamorphic massifs of Central Anatolian crystalline complex.

cognized kyanite + staurolite and sillimanite + orthoclase paragenesis in the metamorphic rocks south of Akdağmadeni. However he says the mineral staurolite, which is very sensitive to change of temperature, and pressure conditions should change to chlorite-serisite aggregate or to chloritoid by a second low-grade metamorphism, but he couldn't observe any change in this mineral.

Özcan et al., (1980) carried out their studies in the northern part of central anatolian massif, between Akdağmadeni and Yıldızeli, and observed the sequence as augen gneiss, biotite-garnet gneiss, amphibolite, mica schist, marble, quartzite, calcsilicate marble and massif marble. They indicated staurolite + sillimanite + muscovite + biotite + garnet + quartz + tourmaline, kyanite + muscovite + quartz + sillimanite + biotite + oligoclase/andesine + quartz ± K-feldspar ± garnet ± muscovite, staurolite + kyanite + muscovite + biotite + labradorite + quartz, scapolite + diopside + hornblende + andesine + calcite (talc + phlogopite + orthoamphibolite + orthopyroxene + olivine + spinel in metaultramafites) mineral assemblages according to lithologic groups and metamorphic conditions (Özer and Göncüoğlu, 1982).

Dökmeci (1980) prepared a generalized lithostratigraphic section of the area around Akdağmadeni. The metamorphites named as Akdağ metamorphic group identified as Köklüdere formation (various gneiss and schist) and Özerözü formation (generally marbles).

Tülümen (1980) examined the petrographic and petrologic characteristics of metamorphic rocks, granites and scarns in his work in Akdağmadeni. Metamorphic rocks were differentiated to some facies according to their mineral paragenesis. These facies were established in a range from muscovite schist to almandine-biotite gneiss indicating rock names.

Sağıroğlu (1982) examined the metamorphic rocks and metamorphic conditions in his work dealing with lead-zinc deposits and their metasomatism near Akdağmadeni. He decided that the mafic metamorphites he defined as amphibolite and

amphibole gneiss according to their mineralogical compositions are magmatic origin.

Şahin (1991) in his work around Akdağmadeni-Başçatak, indicates that the metamorphites of sedimentary origin has been metamorphosed progressively under medium-high grade regional metamorphism conditions. It is revealed by some structural analyses that these rocks show superimposed fold geometry and undergone four different folding phases. In another work he stated that he didn't observe the interchange of sillimanite \leftrightarrow kyanite. He says this change only can be when the anatexis conditions are available therefore there were no temperature-pressure conditions for anatexis in the studied area (Şahin and Erkan, 1994).

Alpaslan (1993) studied the metamorphites around Yıldızeli, NE of Akdağmadeni massif. He named the metamorphites as Yıldızeli group and differentiated this group from bottom to top as Aşılık metamorphite containing metapelitic and migmatitic rocks, Fındıcak metamorphite containing calcsilicate and metapelitic rocks, Pelitlikaya quartzite Member containing quartzite and Kadıköy metacarbonate containing marbles. He claimed that the retrograde metamorphism has occurred during the uprising of Kırşehir block and he found the age of metamorphism as Santonian-Maestrichtian by K-Ar method.

After his studies at the east of Akdağmadeni Yılmaz et al., (1994) named the metamorphites as Akdağmadeni lithodem. They stated that this lithodem includes gneiss, amphibolite, schist, marble and quartzite and has been metamorphosed in high amphibolite facies.

The lithostratigraphic units of the studied area (Fig. 2), which is located between Çatköy and Evçiler villages, south of Akdağmadeni massif, are grouped bottom to top as metapelites, semi-metapelites, metacarbonates and metabasites (as lenses and intercalations in all these lithologic groups) (Şahin, 1999). The lithologies forming the mentioned lithostratigraphic units are mica-schist, mica-gneiss, sillimanite-mica-schist, garnet-staurolite-kyanite-mica-gneiss, quartz-muscovite-schist

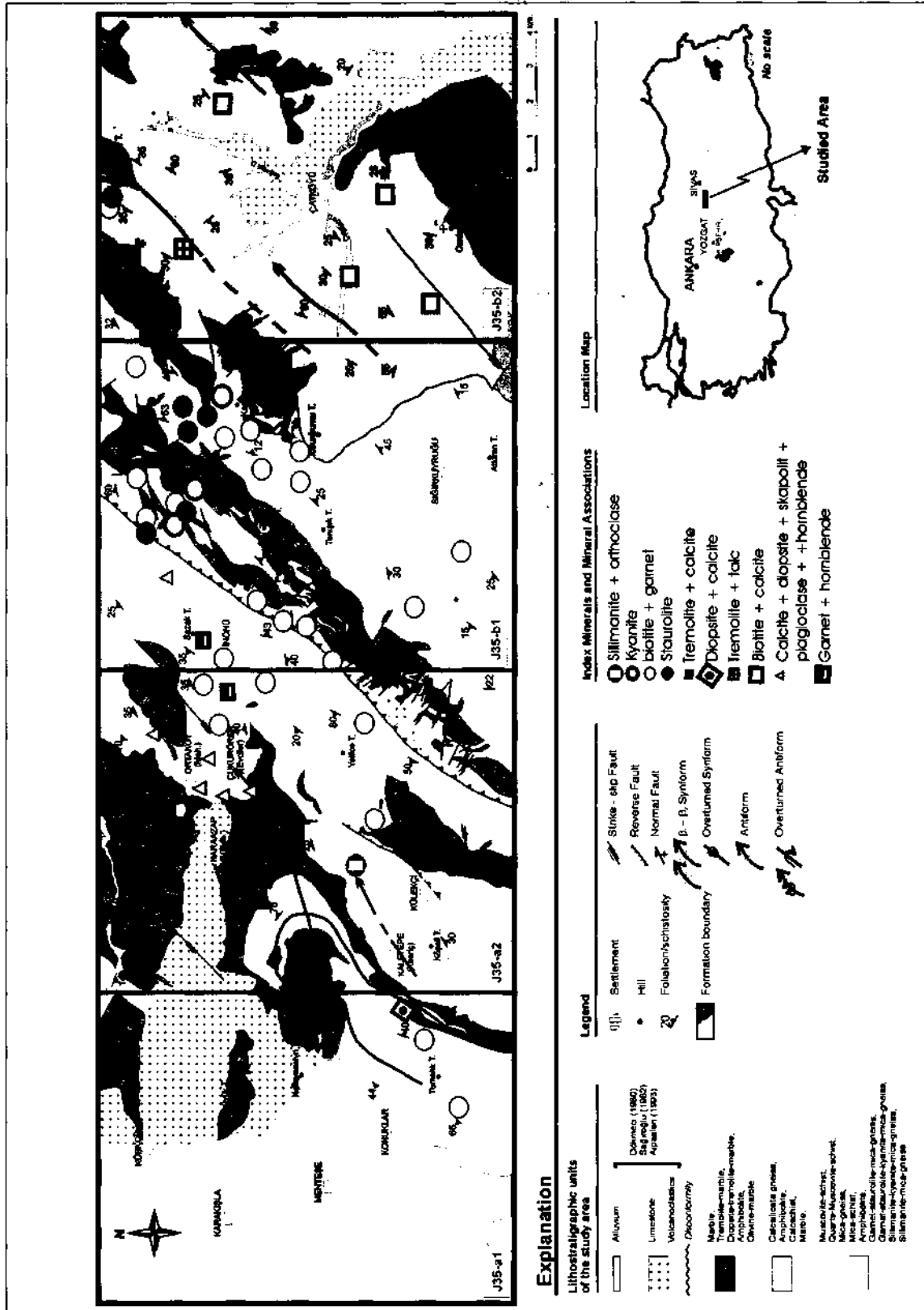


Fig. 2- Map of index minerals and mineral associations in Evçiler-Çatköy part of Akdağmadeni massif metamorphites.

forming metapelites, calcsilicate gneiss, calcschist forming semi-metapelites, epidote-marble, tremolite-diopside-marble, epidote-tremolite-marble, graphite-marble, monomineralic marbles forming metacarbonates and amphibolites forming metabasites (Şahin, 1999).

All of the investigations made on the metamorphic rocks of Akdağmadeni massif reveal that the metamorphites have a sedimentary origin with some basic intercalations. The bottom most units of this sequence of metasedimentary character consist of metapelites (various schist and gneisses). Semi-metapelites (calcsilicate-gneisses, calcschist and calcsilicate marbles), which formed by the increasing carbonate in environment, overlie this series (Fig. 3).

The upper most units consist of metacarbonates and in the border of passage from semi-metapelites to metacarbonates; sometimes a level, which is dominantly consisting quartzites of psammitic origin has been observed. The lithologies forming the metacarbonates of Akdağmadeni mas-

sif are marbles, tremolite-marbles, diopside-tremolite-marbles and olivine marbles.

INDEX MINERALS AND MINERAL ASSEMBLAGES

DEVELOPMENT AND ZONES OF METAMORPHISM

Some index minerals and mineral assemblages were determined in the metasedimentary units and in metabasites by some mineralogical and petrographic determinations. These are given in Table 1.

Some phase diagrams that obtained experimentally and literary are used to find the formation conditions and environments of index minerals and mineral paragenesis described in studied area and given in Table 1. The phase diagrams based on chemical composition and pressure (P) and temperature (T) parameters were interpreted for metamorphic derivatives of pelitic rocks, carbonates and basic rock groups severally.

Metapelites

When we consider the index minerals of

Table 1- "Index minerals and mineral assemblages of investigated area.

Unit	Lithology	Index Mineral	Mineral Association
Metapelite	Mica-gneiss Mica-schist	Kyanite Staurolite Garnet Biotite Muscovite Sillimanite	Biotite + muscovite Biotite + garnet Biotite + kyanite Biotite + staurolite Biotite + staurolite + kyanite Garnet + biotite + staurolite Garnet + biotite + staurolite + kyanite Sillimanite + biotite
Semi-metapelite Metacarbonate	Calcsilicatic gneiss Calcschist Marble	Calcite, diopside, scapolite, plagioclase, hornblende chlorite, tremolite, talc, biotite	Talc + tremolite + calcite Tremolite + calcite + quartz Plagioclase + calcite Diopside + calcite Plagioclase + calcite + diopside + scapolite + hornblende
Metabasite	Amphibolite	Plagioclase (andesine), hornblende (green), garnet, epidote	Plagioclase + hornblende + garnet + biotite + epidote

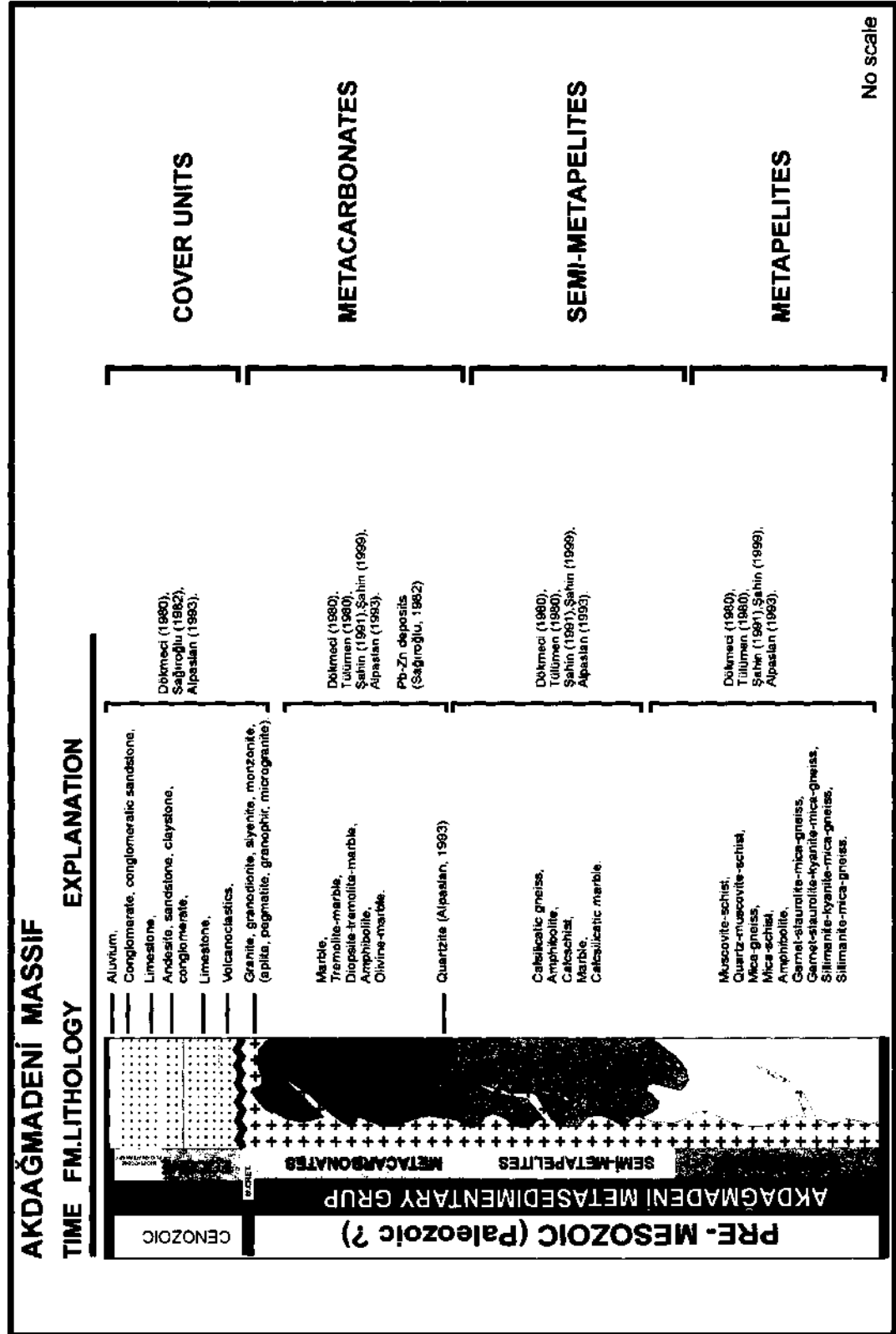


Fig. 3- Generalized lithostratigraphic section of Akdağmadeni massif (Şahin, 1999).

metapelites in the studied area; ASH system, based on SiO_2 , Al_2O_3 , H_2O and P-T parameters and giving formation conditions of kyanite and sillimanite which are the polymorphs of aluminum silicate; FASH system, reflecting formation conditions of staurolite and garnet (almandine) (FeO is added to parameters of chemical composition in this system); KNFASH system, in which the reactions involving mica taking place and in which K and Na of the chemical composition is interpreted and finally KFASH (AFM) system, in which the mineral assemblages appear dur-

ing progressive metamorphism in metapelitic rocks will be discussed on AFM projections.

Index mineral "kyanite" and ASH system.- When we consider the diagram (Fig. 4) called ASH system (Bucher and Frey, 1994) which shows the formation and inversion conditions of the minerals, that are polymorphs of aluminum silicates (andalusite, sillimanite and kyanite) as a function of temperature (T) and pressure (P), it has been seen that mineral kyanite is formed along "kyanite geotherm" at about 400 °C temperature and about 3.7

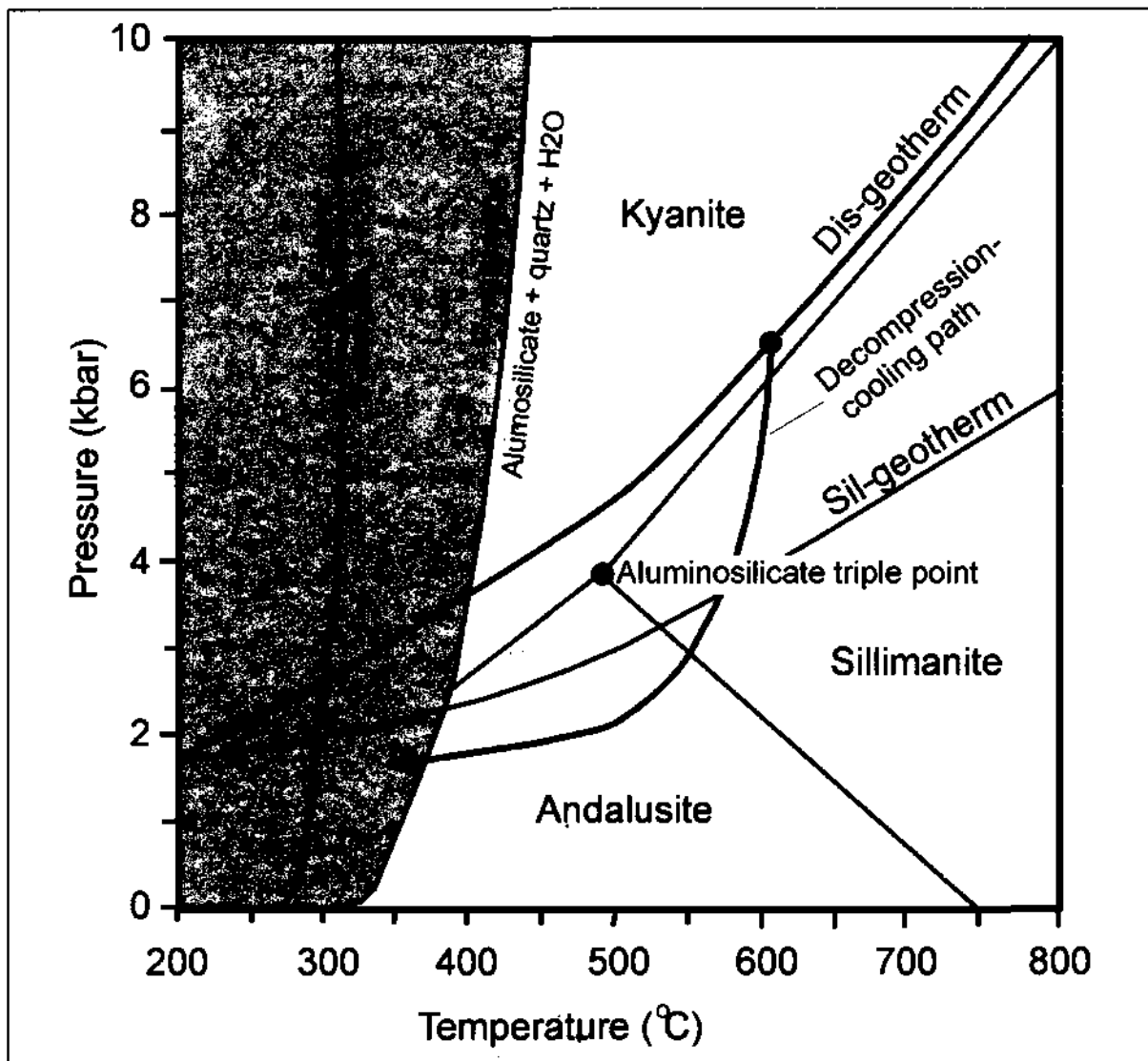


Fig. 4- Equilibria in the ASH system (Bucher and Frey, 1994).

Kb referring to this temperature after pyrophyllite.

In the samples taken from the studied area the mineral "kyanite" was identified in "biotite + kyanite", "biotite + staurolite + kyanite" and "garnet + biotite + staurolite + kyanite" assemblages. Therefore, the formation conditions and stability fields of the minerals biotite, garnet and staurolite that are forming assemblages together with kyanite should be examined on the related phase diagrams and finally the formation conditions and stability fields of the mineral assemblages should be explained. But when we look at the ASH diagram in figure 4 and the reactions (reaction 5) in ASH system (Table 2). It can be seen that the formation reaction of kyanite as "pyrophyllite=kyanite + 3 quartz + H₂O". Since we can't see the mineral pyrophyllite in the examined samples, the rocks that involving kyanite as diagnostic mineral and the other metapelites having similar compositions should be formed at conditions at least over the stability field of pyrophyllite.

Sillimanite that is another polymorph of aluminum silicate and formed in progressive metamorphism by the increasing temperature will be discussed after the minerals biotite, garnet and staurolite are examined.

Index minerals "staurolite+garnet" and FASH system.- The FASH system (Bucher and Frey, 1994) showing the formation conditions and stability fields of the minerals staurolite and garnet is eval-

uated by adding FeO component to ASH system.

When we look at the FASH system (Fig. 5) and "the reactions taking place in Table 3, we see that the mineral garnet (almandine) is formed at about •510 °C by the reaction (9) "chlorite + chloritoid + quartz". Staurolite is formed by the reaction (11) "chloritoid + kyanite" at the same temperature. The first appearance of the minerals staurolite and garnet (almandine) shows the transition from green schist facies (low pressure-low temperature) or from low-grade metamorphism to amphibolite facies (medium-high pressure, medium-temperature) or to medium grade metamorphism.

In the metapelites cropping out in the studied area, the minerals staurolite and garnet are found in "biotite + staurolite", "biotite + garnet", "biotite + staurolite + kyanite" and "biotite + garnet + staurolite + kyanite" assemblages. Therefore it will be reasonable to examine these two diagnostic minerals together with the other minerals that take place in mineral assemblages with them and than to come to a conclusion about the metamorphic conditions occurred.

Index minerals "biotite-muscovite" and KNFASH system.- The mica minerals that often found in metapelites of the investigated area biotite and muscovite. When we look at the phase diagram of KNFASH system (Fig. 6) which is formed by the addition of K and Na to FASH system and the reac-

Table 2- Reactions in the ASH system (Bucher and Frey, 1994).

Sillimanite (Sil), Kyanite (Ky), Andalusite (And)	Al ₂ SiO ₅
Quartz (Qtz)	SiO ₂
Pyrophyllite (Prl)	Al ₂ Si ₄ O ₁₀ (OH) ₂
Kaolinite (Kln)	Al ₂ Si ₄ O ₅ (OH) ₄
(1) And = Ky	
(2) And = Sil	
(3) Sil = Ky	
(4) Kln + 2 Qtz = Prl + H ₂ O	
(5) Prl = Ky + 3 Qtz + H ₂ O	
(6) Prl = And + 3Qtz + H ₂ O	

look at again to the previously examined FASH system (Fig. 5) and the reactions of this system (Table 3) it is observed that the minerals staurolite and garnet (almandine) assembling with biotite form "biotite + staurolite + garnet" paragenesis together with the biotite coming from the reaction (12) "chloritoid + quartz" at about 550 °C. The mineral chloritoid can't be observed in the studied area. This paragenesis observed NE of inonu village (J35-b1) is another data indicating the progressive character of metamorphism. The assemblage "staurolite + kyanite + biotite + garnet" observed in the same area refers to high temperature-high pressure range of medium grade metamorphism (amphibolite facies) and represents the disappearance temperature of staurolite (below 670°) and pressure conditions of about 5Kb.

The KNFASH system shown in figure 6 and the reaction (25) of the Table 4, indicate (with the presence of quartz) the upper most boundary of stability field of muscovite. Here "K-feldspar (orthoclase) + sillimanite" assemblage is formed by the reaction "muscovite + quartz". But aluminum silicate polymorph is accompanied by albite according to reaction (24). In the mineral assemblage formed by the reactions (24) and (25), aluminum silicate polymorph is accompanied by "K-feldspar + albite + quartz" assemblage. The "sillimanite + orthoclase + andesine + quartz" assemblage observed in sillimanite-mica gneiss sample taken from NE of Kaletepe Village shows the continuously increasing temperature. Here the completely disappearance of staurolite and the appearance of "sillimanite (or kyanite) + K-feldspar + andesine + quartz" assem-

Table 3- Reactions in the FASH system (Bucher and Frey, 1994).

Chlorite (Chl)	$\text{Fe}_5\text{Al}_2\text{Si}_3\text{O}_{10}(\text{OH})_8$
Chloritoid (Cld)	$\text{FeAl}_2\text{SiO}_6(\text{OH})_2$
Staurolit (St)	$\text{Fe}_4\text{Al}_{18}\text{Si}_{7.5}\text{O}_{44}(\text{OH})_4$
Almandine (Alm)	$\text{Fe}_3\text{Al}_2\text{Si}_3\text{O}_{12}$
Hercynite (Hc)	FeAl_2O_4
Magnetit (Mag)	FeFe_2O_4
Hematite (Hem)	Fe_2O_3
(7)	$\text{Chl} + 4 \text{Prl} = 5 \text{Cld} + 4\text{Qtz} + \text{H}_2\text{O}$
(8)	$\text{Chl} + 4\text{Hem} = \text{Cld} + 4\text{Mag} + 2 \text{Qtz} + 3\text{H}_2\text{O}$
(9)	$\text{Chl} + \text{Cld} + 2 \text{Qtz} = 2\text{Alm} + 5 \text{H}_2\text{O}$
(10)	$3\text{Chl} = 3\text{Alm} + 2 \text{Mag} + 12\text{H}_2\text{O} (+\text{QFM})$
(11)	$8 \text{Cld} + 10 \text{Ky} = 2\text{St} + 3 \text{Qtz} + 4 \text{H}_2\text{O}$
(12)	$23\text{Cld} + 7\text{Qtz} = 2\text{St} + 5 \text{Alm} + 19\text{H}_2\text{O}$
(13)	$75\text{St} + 312 \text{Qtz} = 100 \text{Alm} + 575 \text{Ky} + 150\text{H}_2\text{O}$
(14)	$3\text{Cld} + 2 \text{Qtz} = \text{Alm} + 2 \text{Ky} + 3 \text{H}_2\text{O}$
(15)	$3 \text{Cld} + 2 \text{Qtz} = \text{Alm} + 2 \text{And} + 3 \text{H}_2\text{O}$
(16)	$8\text{Cld} + 10\text{And} = 2\text{St} + 3 \text{Qtz} + 4 \text{H}_2\text{O}$
(17)	$75\text{St} + 312 \text{Qtz} = 100\text{Alm} + 575\text{Sil} + 150\text{H}_2\text{O}$
(18)	$75\text{St} + 312 \text{Qtz} = 100 \text{Alm} + 575\text{And} + 150\text{H}_2\text{O}$
	Decomposition of staurolite in qtz-free in rocks
(19)	$2\text{St} = \text{Alm} + 12\text{Sil} + 5\text{Hc} + 4\text{H}_2\text{O}$
(20)	$2\text{St} = \text{Alm} + 12\text{And} + 5\text{Hc} + 4\text{H}_2\text{O}$

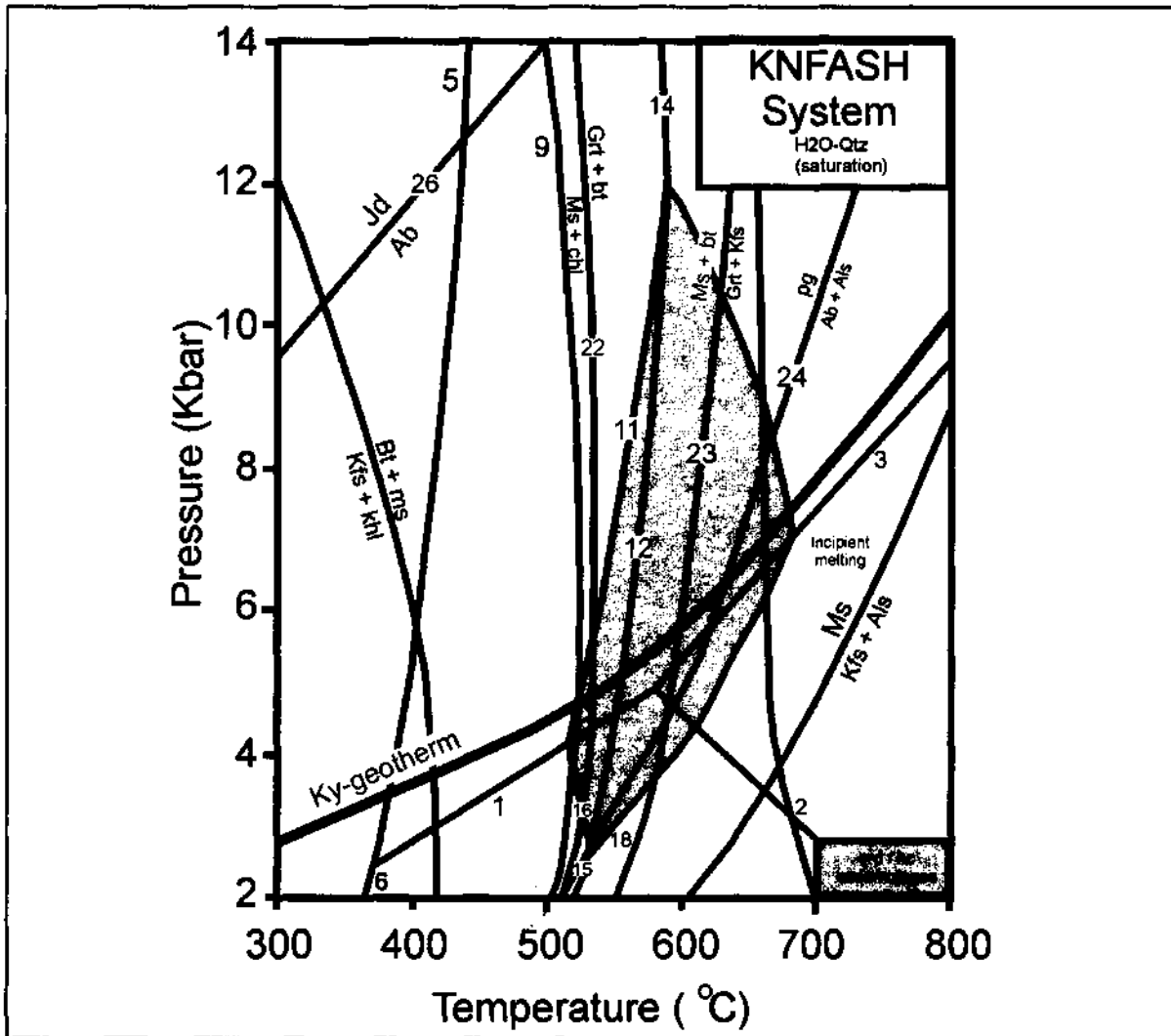


Fig. 6- Equilibrium in KNFASH system and mica reactions (Bucher and Frey, 1994).

blage show the high temperature metamorphism reaching to melting (above 700 °C).

According to the index minerals, mineral assemblages and phase diagrams mentioned above, it can be said that the related metamorphism conditions change by the physical and chemical parameters of environment with respect to time and space. It will be convenient to show the appearance and formation conditions of the diagnostic minerals and mineral assemblage in metapelites of the studied area on AFM diagrams according to their progressive formation order (Fig. 7).

The minerals and mineral assemblages observed in metapelites cropping out in the studies area and stating the progressive development of regional metamorphism in AFM diagrams of figure (7), follow the progressive formation order taking place in (Fig.8).

Semi-metapelites and metacarbonates

The index minerals taking place in the mineralogical composition of the marbles that considered as metacarbonates, calcsilicatic gneisses and calcschist and defined as semi-metapelites cropping out in the studied area will be discussed by

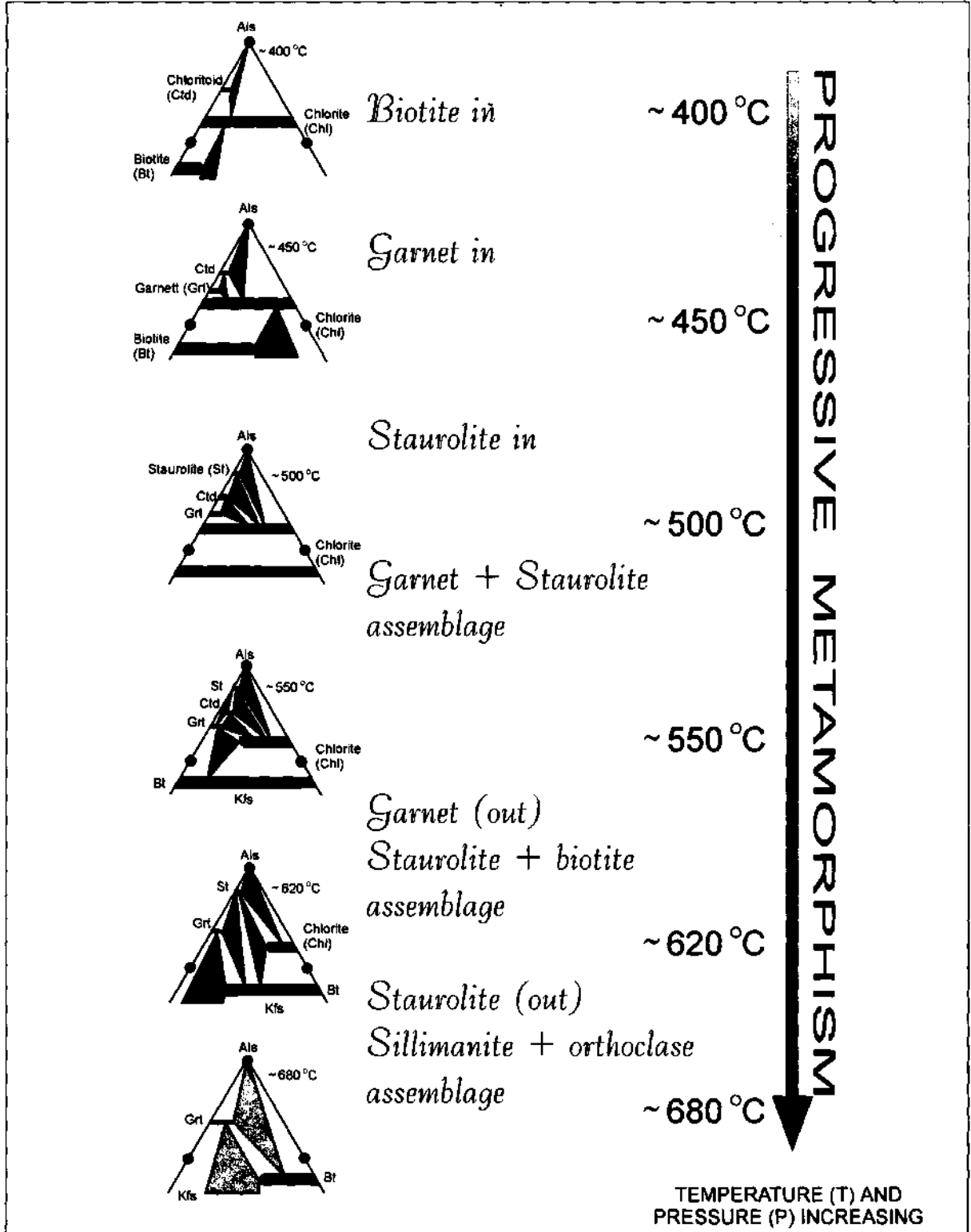


Fig. 7- Progressive metamorphism of metapelites in the investigated area (AFM diagrams, Bucher and Frey, 1994).

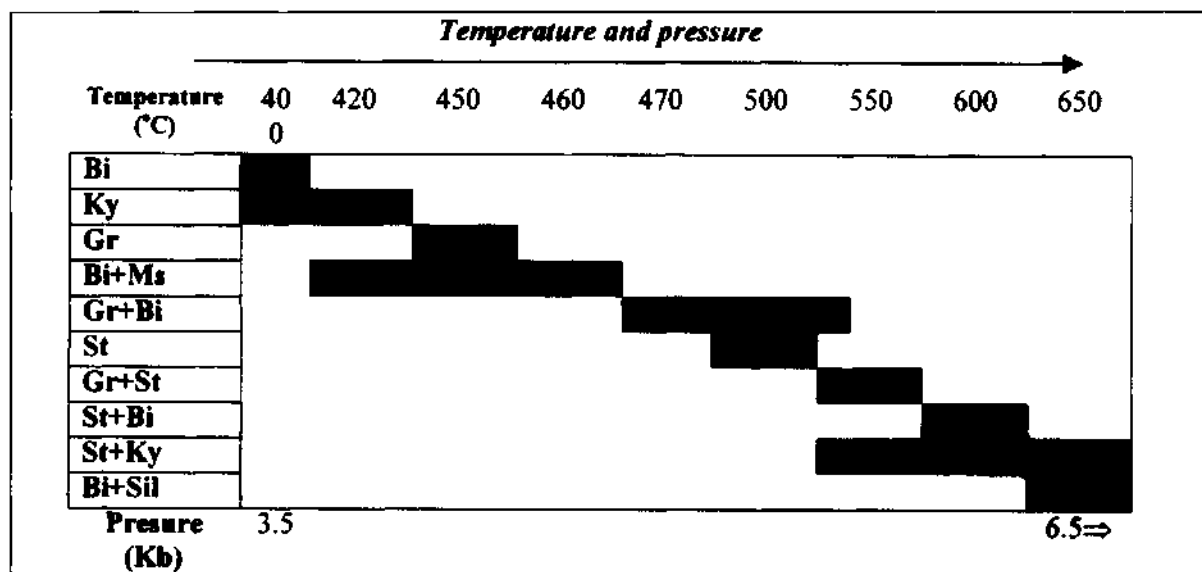


Fig. 8- Index minerals and mineral associations of metapelites in the investigated area.

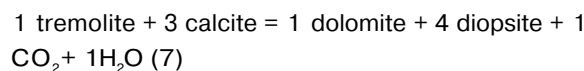
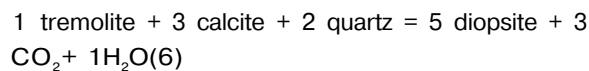
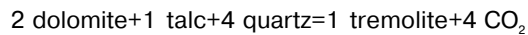
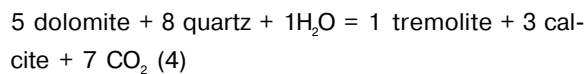
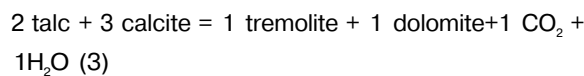
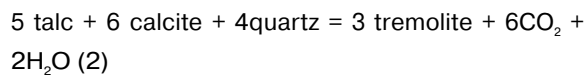
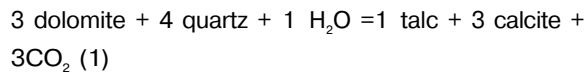
Table 4- Important reactions in the KNFASH system (Bucher and Frey, 1994).

Biotite (Bt)	$\text{KFe}_3\text{AlSi}_3\text{P}_{10}(\text{OH})_2$
Muscovite (Ms)	$\text{KAl}_3\text{Si}_3\text{O}_{10}(\text{OH})_2$
Paragonite (Pa)	$\text{NaAl}_3\text{Si}_3\text{O}_{10}(\text{OH})_2$
K-feldspar (Kfs)	KAISi_3O_8
Albite (Ab)	$\text{NaAlSi}_3\text{O}_8$
Jadeite (Jd)	$\text{NaAlSi}_2\text{O}_6$
Garnet (Grt)	
Aluminium silicate (Als)	
(21)	$3\text{Chl} + 8\text{Kfs} = 5\text{Bt} + 3\text{Ms} + 9\text{Qtz} + 4\text{H}_2\text{O}$
(22)	$\text{Ms} + 3\text{Chl} + 3\text{Qtz} = 4\text{Alm} + \text{Bt} + 12\text{H}_2\text{O}$
(23)	$\text{Ms} + \text{Bt} + 3\text{Qtz} = \text{Alm} + 2\text{Kfs} + 2\text{H}_2\text{O}$
(24)	$\text{Pa} + \text{Qtz} = \text{Ab} + \text{Als} + \text{H}_2\text{O}$
(25)	$\text{Ms} + \text{Qtz} = \text{Kfs} + \text{Als} + \text{H}_2\text{O}$
(26)	$\text{Jd} + \text{Qtz} = \text{Ab}$
	Discontinuous reaction in the KNFASH system
(27)	$\text{Ctd} = \text{St} + \text{Grt} + \text{Chl}$
(28)	$\text{Grt} + \text{Chl} = \text{St} + \text{Bt}$
(29)	$\text{St} + \text{Chl} = \text{Bt} + \text{Als}$
(30)	$\text{St} = \text{Grt} + \text{Bt} + \text{Als}$
(31)	$\text{St} + \text{Bt} = \text{Grt} + \text{Als}$
(32)	$\text{St} + \text{Chl} = \text{Als} + \text{Grt}$
(33)	$\text{Grt} + \text{Chl} = \text{Bt} + \text{Als}$

using the phase diagrams derived from experimental work and then will be studied petrologically.

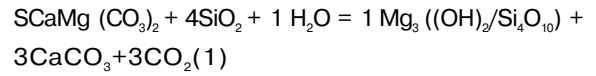
The diagnostic minerals observed in the calc-silicatic gneisses, calcschist and marbles of the studied area and forming the base of petrologic interpretation are calcite, plagioclase, diopside, scapolite, hornblende, chlorite, tremolite, talc and biotite and the assemblages of these minerals. These minerals are accompanied by quartz, titanite, apatite and epidote in many samples.

In this section first of all, the formation of talc, tremolite and diopside that are the index minerals of carbonate rocks of the studied area and having CaO-MgO-SiO₂ major components will be discussed. The resulting mineral parageneses also will be discussed. As a result of the experimental works carried by Turner (1968), Metz and Trommsdorff (1968); the below reactions involving quartz, dolomite, calcite talc and diopside were identified (Winkler, 1976).



When we consider the figure 7 which is first prepared by Metz and Trommsdorff (1968) and Later updated by Metz (1970) and Metz and Puhan (1970, 1971), it has been seen first that "talc+calcite" paragenesis appears over 400 °C temperature and low pressure conditions with the entrance of

dolomite and quartz to the reaction as below.



The investigation and observations done by Steck (1969), Puhan and Hoffer (1973) in Damara Belt, Africa and by Trommsdorff (1972) in Alps reveal that the first product of regional metamorphism is talc. The mineral talc is observed in calcschist derivatives and in "talc + tremolite + calcite" assemblage of semi-metapelitic derivatives taken from SE of Sıraalan hill (J35-b2).

The stability conditions of "talc + tremolite + calcite" assemblage which is represented by the reaction (2) of equilibrium diagram shown in (Fig. 9), change with respect to X_{CO₂} amount in fluid phase. But even if the amount of X_{CO₂} changes between 0.2 and 0.8 und Pf=1 Kbar and Pf=5 Kbar, the formation temperature of this assemblage remains between 490 °C and 600 °C. Since we don't know the total fluid phase pressure and the amount X_{CO₂} it could not be possible to give an exact value for the formation temperature of this mineral assemblage.

In addition to "tremolite+calcite+quartz" assemblage which occurred by the rising temperature in the tremolite-marbles of metacarbonates cropping out near Sıraalan hill (J35-b2) east of studied area, the presence of the diopside in the marbles indicates the rising of temperature up to 540 °C. Figure 9 shows that the formation of this paragenesis is also related to total fluid phase pressure and the amount of X_{CO₂}. The formation temperature of this reaction (6) giving diopside is higher than the formation temperature of reaction (2) giving talc. This situation shows that the stable mineral assemblage over 540 °C temperature is "diopside+tremolite+calcite+quartz". The presence of diopside in calcschists and absence of forsterite indicates that, the temperature can't be over 600°-700°C.

The "calcite+plagioclase" assemblage observed in the carbonated and semi-carbonated rocks of studied area also reflects the conditions of metamorphism. In the investigations carried out by Wenk

(1962) in Switzerland Alps. It is stated that the anorthite content of plagioclase taking place in "calcite + plagioclase" assemblage is increasing due to the increase in temperature increase during progressive metamorphism. The "calcite + plagioclase" assemblage found in the calcsilicatic gneiss and calcschist of the studied area represents medium grade metamorphism conditions. The typical mineral assemblage of calcsilicatic gneisses cropping out in Ortaköy, Çukurören and Sazak hill (J35-a2) is "plagioclase + diopside + scapolite + calcite + hornblende" (green). The presence of scapolite in this assemblage is interpreted as the indication of a medium-high grade metamorphism.

The minerals and mineral assemblages observed in carbonate and semi-carbonate lithologies show a progressive regional metamorphism as they are in the metapelitic derivatives. We observe the talc \rightarrow tremolite \rightarrow diopside sequence which is formed at 450°-600°C temperature and 4-5 Kbar pressure according to total fluid pressure (Pf) and amount of X_{CO_2} and we can't observe forsterite and wollastonite minerals. Therefore a medium-high grade metamorphism is expected.

Metabasites

The index minerals of the amphibolites, those are called metabasites and found in metapelitic

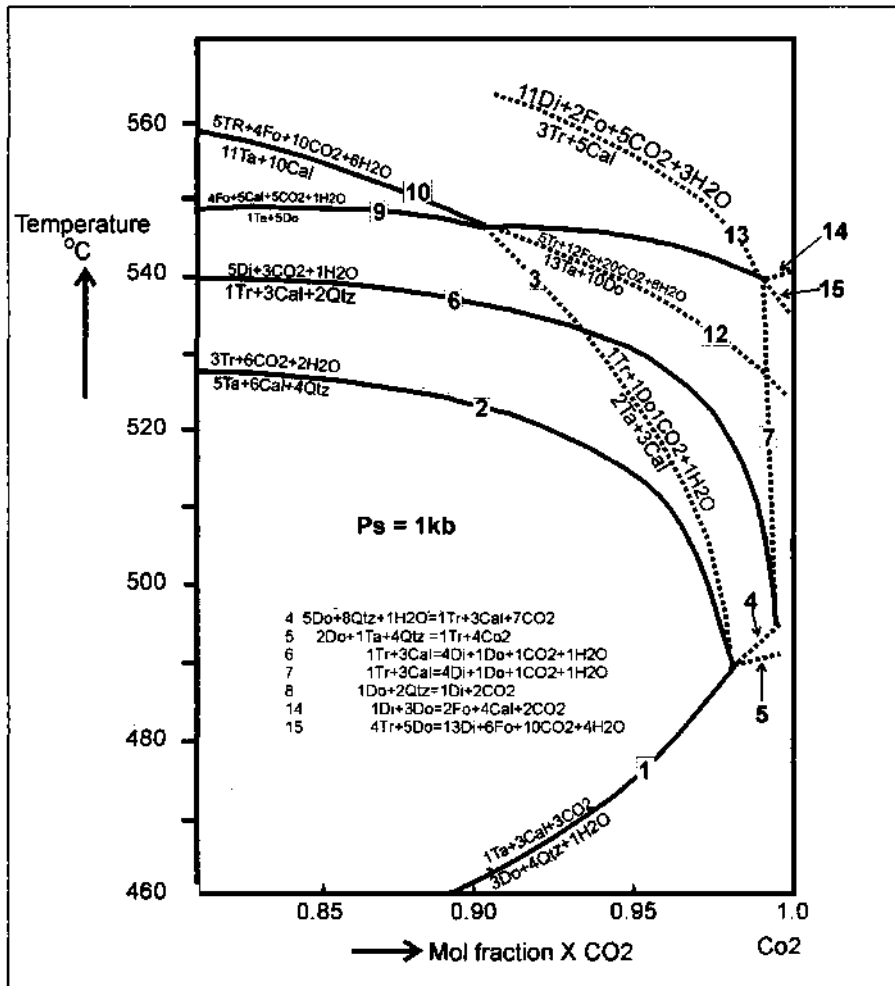


Fig. 9- Isobaric T-X_{CO2} diagram (Winkler, 1976)

units as lenses and intercalations, are plagioclase, hornblende, garnet and epidote. Apatite, titanite, quartz, biotite and opaque minerals sometimes accompany these minerals.

When we consider at their geological setting beside their mineralogical composition; it has been seen that they don't have a lithostratigraphic regularity like other metasedimentary units and they occur as irregular Lenses from a few meters to tens of meters in almost every lithological unit. In fact these findings show magmatic origin. The chemical analyses made by Sağıroğlu (1982) also show that the amphibolite group rocks of the massif are magmatic in origin. On his study the Niggli values has been evaluated and put on the diagrams prepared by Leake (1964). He stated that these values are in the field of "basic magmatic rocks" (Sağıroğlu, 1982).

The index minerals of the amphibolite samples

taken from the studied area those reflecting conditions of metamorphism are plagioclase (especially andesine in composition), green colored hornblende and accompanying garnet, biotite and epidote. They form the assemblage "plagioclase (andesine) + hornblende ± garnet ± biotite ± epidote. We can't see chlorite that normally accompanies "plagioclase + hornblende" assemblage at the starting conditions of amphibolite facies up to about 550°C temperature. We also can't see diopside that appears normally when it is reached to 650°C temperature and only garnet could be observed. When we consider at the above mentioned information above and the ACF diagram (Fig. 10) prepared by Bucher and Frey (1994), we can conclude that the amphibolites of the studied area are the products of a metamorphism taken place at about 600°C temperature and 6 Kb pressure.

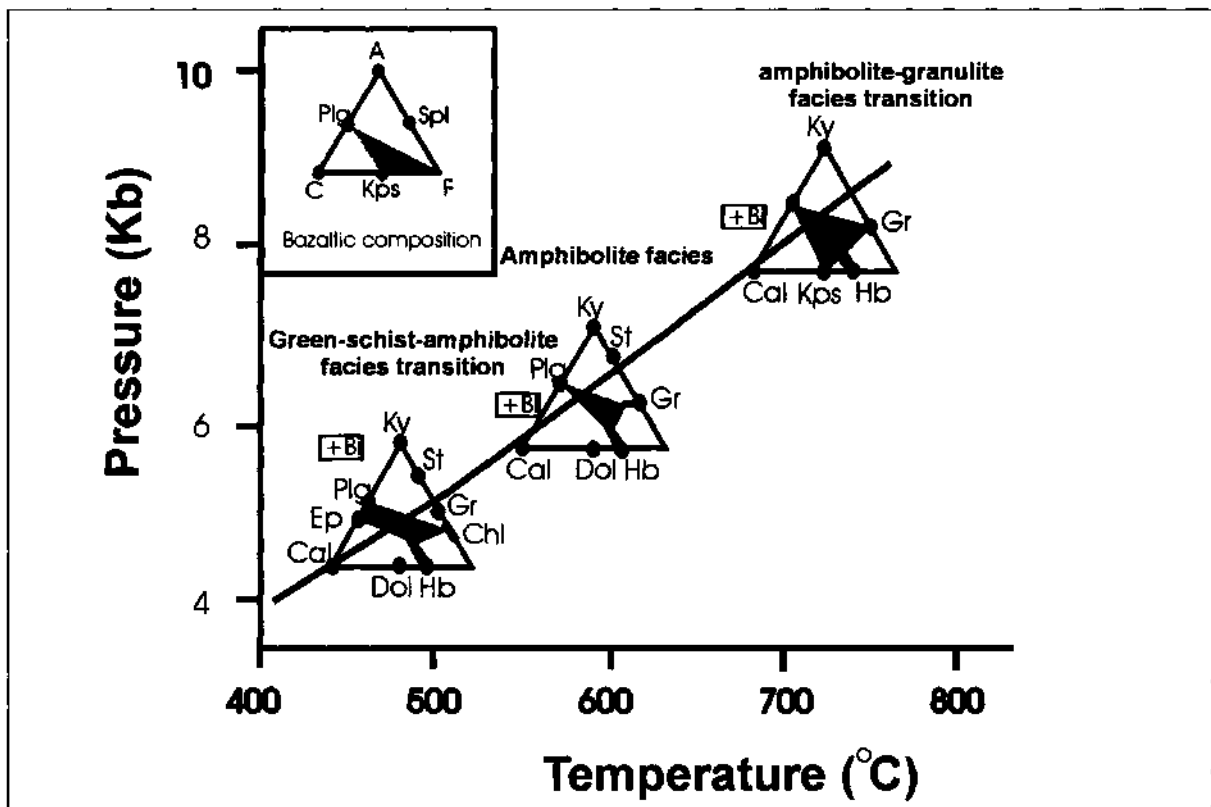


Fig. 10- Metamorphism of the mafic rocks (ACF diagram, Bucher and Frey, 1994).

CONCLUSION

When we consider the petrologic determinations of the mineral assemblages (Fig. 2) found in studied area, it is seen that the metamorphic rocks of the studied area have been metamorphosed progressively by a regional dynamo-thermal metamorphism. The minerals and mineral assemblages such as "biotite, garnet, kyanite, biotite + muscovite, biotite + garnet, staurolite, garnet + staurolite, biotite + staurolite, staurolite + kyanite, biotite + sillimanite" found in metapelitic derivatives show that metamorphism has taken place at 400°C-700° temperature and 3.5-6.5 Kb pressure conditions progressively. The "talc + tremolite + calcite, diopside + calcite + tremolite + quartz, plagioclase + quartz, plagioclase + diopside + scapolite + calcite + hornblende" assemblages found in semi-metapelitic derivatives and in metacarbonates also show a progressive metamorphism and represent a medium-high grade metamorphism at 350-600°C. The "plagioclase (andesine) + hornblende (green) ± garnet ± biotite ± epidote" assemblage found in lithologies like amphibolites reflect about 600 °C temperature and 6 Kbar pressure conditions. All the petrologic results obtained support each other regarding the type and character of metamorphism.

Manuscript received 14 Şubat 2000

REFERENCES

- Apaşlan, M., 1993, Yıldızeli yöresinin petrografik incelenmesi. Doktora Tezi., C.Ü., 359 s., (unpublished).
- Bucher, K. and Frey, M., 1994, Petrogenesis of metamorphic rocks. Springer-Verlag, Berlin, Heidelberg, 6 th. Ed., 317 p.
- Dökmeci, İ., 1980, Akdağmadeni yöresinin jeolojisi: MTA Rep.No: 6953., (unpublished), Ankara.
- Erkan, Y., 1980, Orta Anadolu Masifi'nin kuzeydoğusunda (Akdağmadeni-Yozgat) etkili olan bölgesel metamorfizmanın incelenmesi: Türkiye Jeol. Kur. Bül., C. 23, 213-218
- Erlar, A. and Bayhan, H., 1995, Orta Anadolu granitoyitlerinin genel değerlendirilmesi ve sorunları. Yerbilimleri, 17, 49-67.
- Ketin, L., 1983, Türkiye jeolojisine genel bir bakış: İTÜ Kütüphanesi, Sayı.1259, 595 s.
- Leake, B.E., 1964, The chemical distinction between ortho and para-amfibolites. Journal of Petrology, 5, 238-244.
- Metz, P., 1970, Experimental investigation of the metamorphism of silicious dolomites: II. Conditions of diopside formation. Contribution Mineral. Petrol., 28, 221-250.
- and Trommsdorff, V., 1968, On phase equilibria in metamorphosed silicious dolomites. Contr. Mineral. Petrol., 18, 305-309.
- and Puhan D., 1970, Experimented untersuchung der metamorphose von kieselig Dolomitschen Sedimenten I. Die Gleichgewichtstaden der Reaktion "3 dolomit + 4 quarz + 1H₂O = 1 talk + 3 calcit + 3 CO₂ für Gesamtgasdrucke von 1000. 3000 and 500 Bar. Contr Mineral. Petrol., 26, 302-314.
- and —————, 1971, Korrektur zur Arbeit. Experimentelle Untersuchung der Metamorphose von Kieselig Dolomitschen Sedimenten I. Die Gleichgewichtstaden der Reaktion "3 dolomit + 4 quarz + 1H₂O + 1 talk + 3 calcit + 3 CO₂ für Gesamtgasdrucke von 1000. 3000 and 5000 Bar. Contr. Mineral. Petrol., 31, 169-170.
- Özcan, A.; Erkan, A.; Keskin, E.; Oral, A.; Sümengen, M. and Tekeli, O., 1980, Kuzey Anadolu Fayı-Kırşehir Masifi arasının temel jeolojisi. MTA Rep.No. 1604., (unpublished), Ankara.
- Özer, S. and Göncüoğlu, M.C., 1982, Orta Anadolu Masifi doğusunda (Akdağmadeni-Yıldızeli) ilginç metamorfik parajenezler: MTA Bull., 95/96. s. 173-174.
- Pollak, A., 1958, 1957, Yılında Akdağmadeni-Yıldızeli sahasında yapılan prospeksiyon hakkında Rapor: MTA Rep. No 2321., (unpublished), Ankara.
- Puhan, D. and Hoffer, E., 1973, Phase relations of talc and tremolite in metamorphic calcite-dolomite sediments in the southern porition of the Damara Belt (SW Africa). Contr. Mineral..Petrol.. 40. 207-214.
- Sağıroğlu, A., 1982, Contact metasomatism and ore deposition of lead-zinc deposits of Akdağmadeni. Yozgat, Turkey: Londra Üniversitesi Ph.D. Thesis., 324 p., (unpublished).
- Steck, A., 1969, Kaledonische Metamorphose. NE-Gronland, Habilitationsschrift. Basel.

- Şahin, M. B., 1991, Başçatak köyü (Akdağmadeni-Yozgat) doğusunun jeolojik ve petrografik özelliklerinin incelenmesi: HÜ Fen Bilimleri Enst., Yüksek Mühendislik Tezi, 68 s., (unpublished).
- , 1999, Akdağmadeni Masifi Metamorfileri, Evciler-Çatköy kesiminin mineralojik ve petrolojik özelliklerinin incelenmesi. HÜ Fen Bilimleri Enstitüsü, Doktora Tezi. 105 s., (unpublished).
- and Erkan, Y., 1994, Petrological features of the metamorphics of the Yukarıçulhalı-Başçatak segment of the Akdağmadeni Massif. Buletin of MTA 116, 39-46.
- Tolluoğlu, A.Ü and Erkan, Y., 1989, Regional progressive metamorphism in the Central Anatolian Crystalline Basement, NW Kırşehir Massif, Turkey. M.E.T.U. Journal of Pure and Applied Sci., 22/3, 19-41.
- Trommsdorff, V., 1972. Change in T-X During metamorphism of silicious dolomitic rocks of the Central Alps. Schweiz. Mineral. Petrog. Mitt., 52, 567-571.
- Turner, F.J., 1968, Metamorphic petrology. McGraw-Hill Book Comp., New York.
- Tülümen, E., 1980, Akdağmadeni (Yozgat) yöresinde petrografik ve metalojenik incelemeler: Doktora Tezi. KTÜ Yerbilimleri Fakültesi, 157 s., (unpublished).
- Vache, K., 1963, Akdağmadeni kontakt yatakları ve bunların Orta Anadolu kristalinine karşı olan jeolojik çerçevesi: MTA Bull., 60, 22-36.
- Wervk, C., 1962, Plagioclase als indexmineral in den Zentralalpen. Miner. Petrog. Mitt., 42, 139-107.
- Winkler, H.G.F., 1976, Petrogenesis of metamorphic rocks. 4th Ed., Springer Verlag, New York, 334 p.
- Yılmaz, A., Uysal, Ş., Yusufoglu, H., Ağan, A., İnal, A., Aydın, N., Bedi, Y., Havzoğlu, T., Gog, D., inal, E., and Erkan, E.N., 1994, Akdağ Masifi (Sivas) dolayının jeolojik incelemesi: MTA Rep. No. 9721.. (unpublished), Ankara.